# Design and Evaluation of a Variable Resistance Orthotic Knee Joint

Andrew Herbert-Copley

Thesis submitted to the faculty of graduate and postdoctoral studies
in partial fulfillment of the requirements for the degree of

**MASTER OF APPLIED SCIENCE**

in Biomedical Engineering

Ottawa-Carleton Institute for Biomedical Engineering
University of Ottawa
Ottawa, Ontario

April 2015

# Abstract

Knee-ankle-foot orthoses (KAFOs) are full leg braces for individuals with knee extensor weakness, designed to support the person during weight bearing activities by preventing knee flexion. KAFOs typically result in an unnatural gait pattern and are primarily used for level ground walking. A novel variable resistance orthotic knee joint was designed and evaluated to address these limitations. This low profile design fits beneath normal clothing. Mechanical and biomechanical testing demonstrated that the design resisted knee motion during stance phase, released the knee joint without restricting the knee's range of movement, and provided flexion resistance during stair descent. Design modifications and related testing procedures were developed to further improve joint performance and to validate the design prior to testing on individuals with knee extensor weakness.

# Table of Contents

# List of Figures

# List of Tables

# Definitions

| | |
|---|---|
| Abduction | Movement of a limb away from the midline, in the frontal plane |
| Adduction | Movement of a limb towards the midline, in the frontal plane |
| Anterior | To the front of the body |
| Cadence | Number of steps in a given time, usually one minute |
| Centre of mass | The point within a rigid body object at which it can be assumed that the mass of the object is concentrated |
| Circumduction | Circular or cone-like movement of a body segment |
| Concentric Contraction | Muscle contraction in which the muscle gets shorter as it develops |
| Distal | Away from the rest of the body |
| Dorsal | Posterior surface |
| Dorsiflexion | Movement of the foot towards the knee |
| Eccentric contraction | Muscle contraction in which the external force overpowers the muscle so that it gets longer |
| Extension | Movement of a body segment causing an increase in the angle at the joint |
| External moment | Moment applied from outside the body |
| Flexion | Movement of a body segment causing a decrease in the angle at the joint |
| Gait cycle | Cycle of walking |
| Force platform | Common piece of gait analysis equipment, for measuring ground reaction force |
| Frontal plane | Divides a body part into front and back portions (also referred to as coronal plane) |
| Ground reaction force | Upward force applied by the ground to the foot, in response to the downward force applied by the foot to the ground |
| Internal moment | Moment generated by muscles and/or ligaments |
| Internal rotation | Rotation of limb about its long axis, the anterior surface moving medially |
| Kinematics | Movement of joints or body segments |
| Kinetics | Forces and moments that produce movement |
| Lateral | Away from the midline of the body |

| | |
|---|---|
| Medial | Towards the midline of the body |
| Orthosis | External support for some part of the body; also known as a brace |
| Plantarflexion | Movement of the foot away from the knee |
| Posterior: | To the back of the body |
| Prosthetic limb | Artificial limb |
| Proximal | Towards the rest of the body |
| Power | Rate at which work is done or energy is expended |
| Sagittal plane | Divides part of the body intro right and left portions |
| Stance | Phase of gait cycle when foot is in contact with the support surface |
| Step | Advancement of a single foot |
| Stride | Advancement of both feet (one step by each side) |
| Swing | Phase of gait cycle when foot is not in contact with the support surface |
| Transtibial amputation | Amputation of a leg between the knee and ankle joints |
| Transverse plane | Divides a body part into upper and lower portions |

# Abbreviations

| | |
|---|---|
| AFO | Ankle-foot orthosis |
| CMM | Coordinate measuring machine |
| CSCO | Compliant stance control orthosis |
| DoF | Degrees of freedom |
| FBD | Free body diagram |
| GRF | Ground reaction force |
| I.D. | Inner diameter |
| KAFO | Knee-ankle-foot orthosis |
| O.D. | Outer diameter |
| OWS | Ottawalk-Speed |
| OWVS | Ottawalk-Variable Speed |
| PCB | Printed circuit board |
| ROM | Range of motion |
| RPM | Rotations per minute |
| RPS | Rotations per second |
| RTL | Rehabilitation Technology Lab |
| SCKAFO | Stance-control knee-ankle-foot orthosis |
| SPL | Swing phase lock |
| TF | Transfemoral |
| TOHRC | The Ottawa Hospital Rehabilitation Centre |

# Acknowledgments

First of all, I would like to thank my two supervisors Dr. Edward Lemaire & Dr. Natalie Baddour for all of their guidance, support, and encouragement throughout my research. Thank you to Natural Sciences and Engineering Research Council of Canada for funding this research.

A thank you goes out to the following individuals:

*Staff of Chas A. Blatchford & Son Limited*
Chris Duke
Jawaad Bhatti
Saeed Zahedi

*Staff of The Ottawa Hospital Rehabilitation Centre*
Louis Goudreau
Tony Zandbelt
Ted Radstake
Joao Tomas

*Students of Dr. Lemaire and Dr. Baddour*
Andrew Smith
Emily Sinitski
Nicole Capela
Salomon Gonzalez Rivera

Finally, thank you to my family and friends.

# Chapter 1: Introduction

## 1.1 Introduction

During locomotion, the knee provides shock absorption, maintains stability during stance, and contributes to limb progression during swing. The knee extensor muscles resist knee flexion during stance, absorb forces due to body weight, and facilitate limb progression. When an external knee flexion moment acts on the knee, the knee extensor muscle group generates an opposing extension moment. If the knee extensors are not sufficiently strong, the knee will collapse due to the external knee flexion moment and the person will fall [1], [2].

Muscular weakness can result from peripheral neurological diseases (e.g., poliomyelitis), muscular diseases (e.g., Duchenne muscular dystrophy), central neurological diseases (e.g., multiple sclerosis), spinal cord injury, osteoarthritis, or severe injury [2]–[6]. Knee extensor weakness consequences can range from abnormal gait patterns to complete instability [3], [7]. Even if the extensor muscles are only slightly weakened, walking with an abnormal gait pattern is highly energy consuming and can cause soft tissue damage [2].

Knee-ankle-foot orthoses (KAFOs) are full leg braces designed for individuals with knee extensor weakness. Conventional KAFO designs can lock the knee in an extended position, which keeps the individual stable throughout stance. However, the resulting stiff-legged gait is an unnatural gait pattern that is inefficient for the user and can lead to soft tissue injury [2], [7], [8]. Stance control KAFOs (SCKAFOs) support the leg during weight bearing and permit free knee motion during swing phase. If the SCKAFO user has sufficient hip muscle strength for forward progression, SCKAFOs improve mobility compared to fixed knee KAFOs and provide many clinical benefits [7]. The most functionally advanced SCKAFOs are microprocessor controlled and provide more reliable mode switching. Microprocessor controlled SCKAFOs can be designed with multiple settings that allow the user to more easily negotiate different types of terrain.

In this thesis, the mechanical and hydraulic systems of a variable resistance orthotic knee joint were designed, based on the Ottawalk-Speed (OWS) [9] developed at the Ottawa Hospital Rehabilitation Centre and a variable flow hydraulic valve adapted from a commercial prosthetic ankle designed by Endolite Prosthetics and Orthotics Products (Chas A. Blatchford & Son Limited, Basingstoke, UK). The new knee joint, known as the Ottawalk-Variable Speed (OWVS), provides variable knee flexion resistance to improve level ground walking and stair descent. A manual, electronic control method was implemented to switch between valve settings, enabling valve and preliminary biomechanical tests.

## 1.2 Rationale

Individuals with knee extensor weakness need a KAFO to support the knee during stance, particularly when the knee experiences an external flexion moment. Studies have shown that SCKAFOs allow for a more natural gait pattern than conventional KAFOs due to knee joint release during swing, thereby enhancing mobility and walking [7], [10]. SCKAFOs that are currently available on the market use mechanical or microprocessor control. Mechanical devices have the advantage of not requiring external power and are generally smaller, more aesthetically pleasing, and less expensive. Microprocessor controlled orthoses have more reliable switching between modes and the ability to sense various terrains. An issue with many orthotic devices is that they require a fully extended knee to engage the locking mechanism, which may not be possible for all individuals with knee extensor weakness. Such individuals may not have the muscle strength and/or control to fully extend their knee consistently, and the orthosis will not catch an individual who stumbles and lands on a flexed knee. Other prominent issues that determine if an orthosis will be accepted by the user are device weight, size, and noise [7]. Ideally an SCKAFO should be made with minimal dimensions so that the device can be worn underneath pants, making the brace more aesthetically pleasing. Another issue is that SCKAFOs are expensive. Individuals with disabilities have reported that cost was a major reason for their unmet assistive device needs [11].

Currently the most versatile orthosis available is the Otto Bock C-Brace, which uses a linear hydraulic actuator to control knee flexion. The C-Brace's hydraulic actuator system has many advantages, primarily the ability to provide in-stance dampening, allowing the user to walk with a more natural gait pattern. The C-Brace also has control modes for walking on ramps, stairs, uneven ground, or to sit naturally. Unfortunately, this orthosis is very bulky, and the joint unit on the lateral side is too large to fit beneath clothing.

In contrast to the C-Brace, the Ottawa Hospital Rehabilitation Centre's (TOHRC) OWS SCKAFO design uses a linear actuator to stop knee motion once a certain knee angular velocity threshold has been passed. For the current project, a new SCKAFO knee joint was designed via a partnership between TOHRC and Endolite Prosthetics and Orthotics Products (Chas A. Blatchford & Son Limited, Basingstoke, UK), based on the OWS joint and a variable flow hydraulic valve that has been used in Endolite's Elan prosthetic ankle. This design enables varying knee flexion resistance, thus allowing individuals with knee extensor weakness to negotiate various terrains, specifically level ground, stairs and stand-sit motions.

## 1.3 Objectives

The goal of this thesis was to design, develop, and evaluate a new variable resistance orthotic knee joint for individuals with knee extensor muscular weakness. The project's objectives were to:

1. Design a variable resistance hydraulic orthotic knee joint that addresses current SCKAFO device limitations. Specifically, the orthosis should:
    a. Lock knee joint during stance, and release the knee joint during swing for level ground walking;
    b. Provide resistance to knee joint flexion during stair descent; and,
    c. Have minimal dimensions to reduce overall size and weight of the orthotic joint.
2. Manufacture a variable resistance joint prototype.
3. Mechanically test the joint to determine knee joint flexion resistance at each setting, knee joint extension resistance, and valve reaction time when switching between settings.
4. Biomechanically evaluate the new joint during:
    a. Level walking – The joint should lock the knee joint during stance (at any knee angle) and allow free knee motion during swing.
    b. Stair descent – The orthotic joint should resist knee flexion to lower the body's centre of mass smoothly to the following step.
    c. Stand-to-sit – Resist knee flexion to lower the body smoothly to a seat.

## 1.4 Contributions of the thesis

A mechanical and hydraulic system was designed and evaluated for a novel microprocessor controlled SCKAFO. This design uses a variable flow hydraulic valve to control knee flexion by varying the flow from a linear hydraulic cylinder. The new orthotic knee joint allows individuals with knee extensor weakness to walk on level ground with a more natural gait pattern, descend stairs smoothly, and sit in a controlled manner. This design is low profile, so the orthosis will fit beneath normal clothing.

## 1.5 Thesis outline

This thesis is divided into six chapters. Chapter 2 is a literature review of knee joint function during locomotion, focusing on the knee extensor muscles during level ground walking and stair descent, and the causes and effects of knee extensor weakness. Orthotic solutions for individuals with knee extensor weakness are then reviewed, and product reviews of current KAFO and SCKAFO designs are presented. Chapter 3 summarizes the design and development process used to create the orthotic knee joint. This chapter includes the design's specification, criteria, calculations, tests, and methods used to arrive at the final design. Chapter 4 presents the results of mechanical tests performed on the joint. Chapter 5 presents results of biomechanical tests. Chapter 6 presents a thesis summary and outlines future work for the OWVS.

# Chapter 2: Literature Review

This chapter reviews the literature on knee joint function, knee extensor weakness, and Knee-Ankle-Foot Orthoses (KAFOs) to demonstrate the requirements for a variable resistance Stance Control Knee-Ankle-Foot Orthosis (SCKAFO). Section 2.1 provides an overview of knee joint function during locomotion, focusing on level ground walking and stair descent, for both able-bodied individuals and individuals with knee extensor weakness. Section 2.2 outlines the causes and effects of knee extensor weakness on gait. Section 2.3 discusses orthotic options for dealing with knee extensor weakness and a design review of existing KAFO devices, outlining the orthotic mechanics and design advantages and disadvantages. Section 2.4 provides a summary of the main conclusions and implications of the literature review.

## 2.1 Knee joint function during locomotion

The knee is the largest synovial joint in the body, connecting the lower limb (shank) to the upper limb (thigh). Knee movement is primarily in the sagittal plane (Figure 2.1 is a diagram of the anatomical planes). Fourteen muscles control the knee during gait, and can be divided into extensor and flexor groups. Knee extensor muscles decelerate knee flexion during stance and contribute to limb progression during swing. During the swing phase, the knee extensor muscles also contribute to limb progression [1].

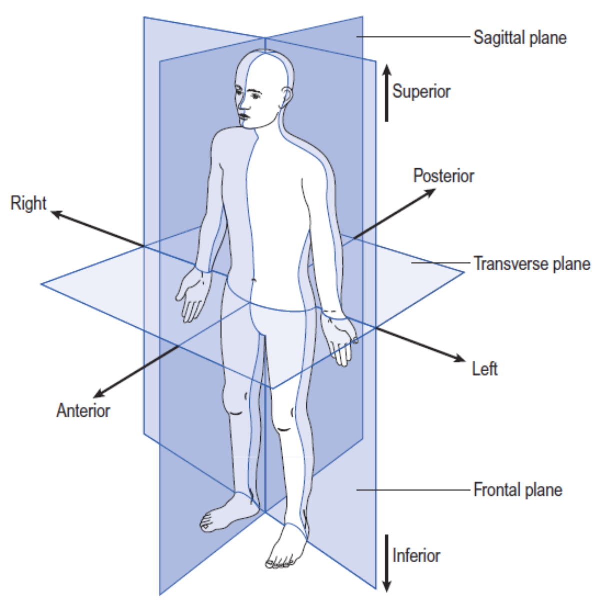


Figure 2.1: Diagram showing the three anatomical planes (sagittal plane, frontal/coronal plane, and transverse/horizontal plane) and the six fundamental directions (right, left, anterior, posterior, superior and inferior) [12].

### 2.1.1 Normal level ground walking

2.1.1.1 Gait cycle

The gait cycle is composed of two phases, stance and swing (Figure 2.2). Stance phase is when the limb is in contact with the ground (foot contact with ground until foot leaves the ground). Stance sub-phases are initial contact, loading response, mid stance, and terminal stance. Swing phase is when the limb is in the air (foot off until foot contacts the ground again). Swing sub-phases include pre-swing, initial swing, mid swing, and terminal swing [1].

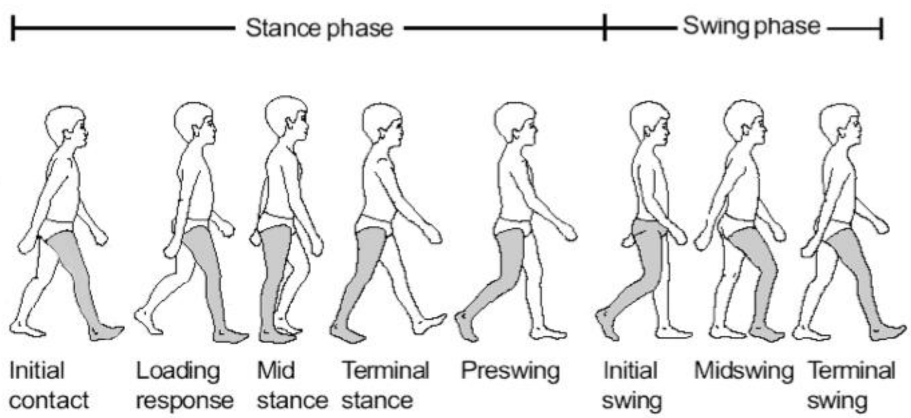


Figure 2.2: Phases and sub-phases of the gait cycle (adapted from [13]).

The gait cycle can also be divided into three tasks: weight acceptance, single limb support, and swing limb advancement. Weight acceptance is the first task of stance phase, and is comprised of initial contact and loading response. Weight acceptance includes shock absorption when the foot contacts the floor, limb stability, and preservation of forward limb progression. Single limb support is the second task and involves mid stance and terminal stance sub-phases, where body weight is supported and the opposite limb is in the air. Swing limb advancement is when the limb is lifted in the air and prepares for the next stance phase. Pre-swing, initial swing, mid swing, and terminal swing sub-phases are part of the limb advancement task [1]. Table 2.1 defines each gait cycle sub-phases.

2.1.1.2 Knee function during walking

During stance phase, the knee provides limb stability during weight bearing and prepares the limb for swing phase. The ground reaction force (GRF) vector with respect to the knee joint centre determines the external moment's direction. When the GRF vector is anterior to the knee joint centre of rotation, an external extension moment acts on the knee and a GRF vector posterior to the knee joint centre of rotation produces an external flexion moment at the knee (Figure 2.3) [2].

Table 2.1: Gait cycle sub-phases [1].

| **Phase** | **Task** | **Sub-phase** | **% gait cycle** | **Description** | **Function** |
|---|---|---|---|---|---|
| Stance | Weight acceptance | Initial contact | 0-2 | Foot contact with ground, knee is extended | Stable weight bearing |
| | | Loading response | 2-12 | Active knee flexion (20˚ flexion) | Shock absorption, stability, anterior knee joint movement |
| | Single limb support | Mid stance | 12-31 | Active knee extension (15˚ flexion) | Stable weight bearing, advance femur over tibia |
| | | Terminal stance | 31-50 | Active maximum knee extension (5˚ flexion) | Stable weight bearing, femur advances over tibia to max knee extension |
| | Swing limb advancement | Pre-swing | 50-62 | Passive knee flexion (40˚ flexion) | Knee prepares for swing phase and toe clearance |
| Swing | | Initial swing | 62-75 | Active knee flexion (60˚ flexion) | Knee flexes to advance limb and foot clearance |
| | | Mid swing | 75-87 | Passive knee extension | Knee extends passively (hip flexor moment) to advance limb |
| | | Terminal swing | 87-100 | Active knee extension | Knee extends to prepare for stance phase |

Figure 2.4 illustrates GRF vectors during stance phase (initial contact to pre-swing). When an external extension moment acts on the knee, the knee is in a stable state. When an external flexion moment acts on the knee, the joint is in an unstable position and an extension moment is required to oppose flexion and maintain stability, or the knee will collapse. This extension moment is generated by the knee extensor muscles (quadriceps), which are the dominant muscle group at the knee. During stance phase for a normal gait cycle, the quadriceps create an extension moment about the knee to decelerate joint flexion due to external flexion moments.

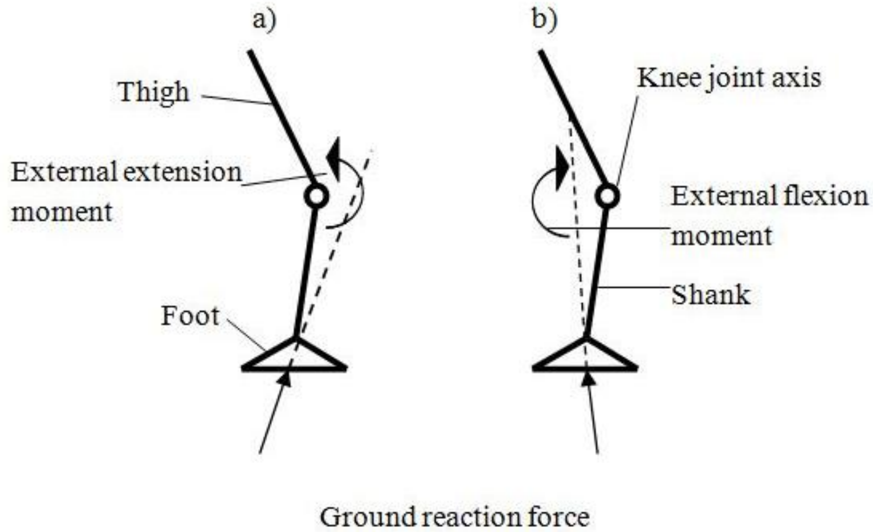


Figure 2.3: External moments acting at the knee: a) external extension moment when the GRF vector is anterior to the knee joint axis, b) external flexion moment when the GRF vector is posterior to the knee joint axis (adapted from [2]).

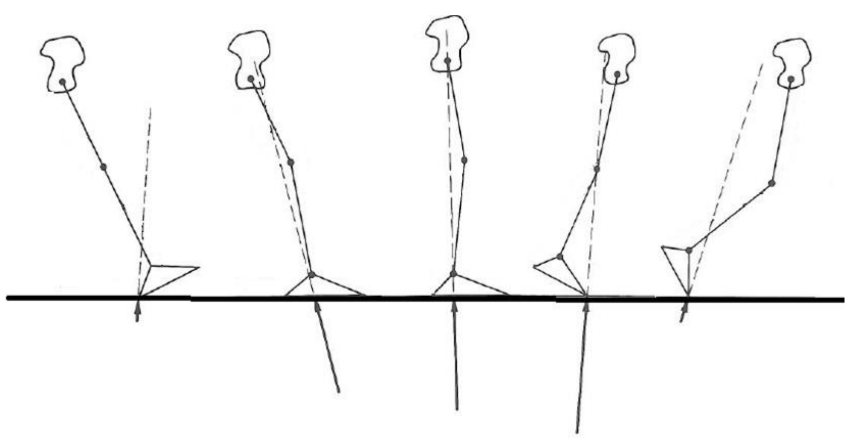

Figure 2.4: Ground reaction force vector magnitudes and directions for initial contact, loading response, mid stance, terminal stance, and pre-swing (adapted from [2]).

The GRF vector moves posterior to the knee joint axis during loading response, mid-stance, and pre-swing. As seen in Figure 2.4, the GRF magnitude between loading response and terminal stance is large and posterior to the knee joint axis, requiring substantial extension moments from the knee extensor muscles.

The knee joint flexes twice during a normal gait cycle. The first is during loading response and mid-stance, to absorb the impact from foot contact and advance the knee anteriorly. The second is during early swing phase, for foot clearance and following step preparation [1].

2.1.1.3 Knee kinematics during normal gait

The knee joint has a large range of motion (ROM) and moves in all three anatomical planes. Coronal plane motion (adduction/abduction) maintains vertical balance over the limb during single support and transverse plane rotation (internal rotation) accommodates for alignment changes. The knee joint's motion occurs in the sagittal plane (flexion/extension) for progression and advancement during swing and stance, as well as foot clearance [1].

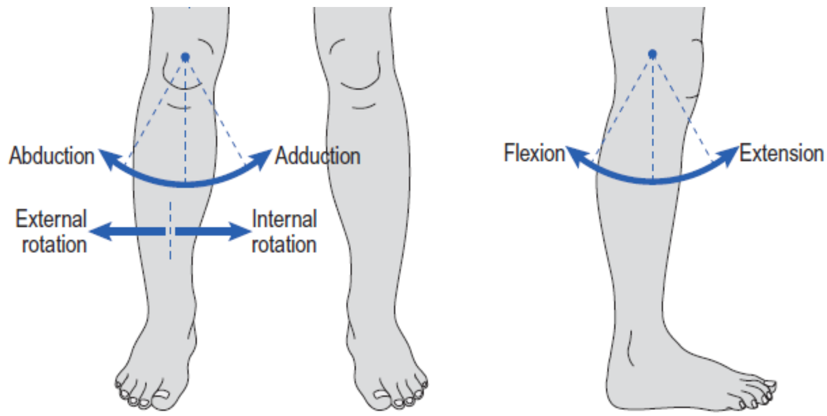


Figure 2.5: Movements about the knee joint [12].

Figure 2.6 shows the knee angle for able-bodied level ground natural cadence walking in the sagittal plane. The vertical line at 60 percent of the stride is the transition between the stance and swing phases of the gait cycle.

The knee ROM in the sagittal plane is approximately 0-70˚during the gait cycle, with two flexion movements (Figure 2.6). The first flexion peaks at approximately 20˚ during the transition between the loading response and mid stance, where the knee absorbs the impact from foot contact. The knee then extends to almost full extension (8˚) and then begins to flex again to prepare for the swing phase. Toe-off occurs at 60 percent of the stride cycle, at a knee angle of approximately 40˚. Flexion peaks at 70˚ in the initial swing phase and then extends to full extension for foot contact [1], [2], [14].

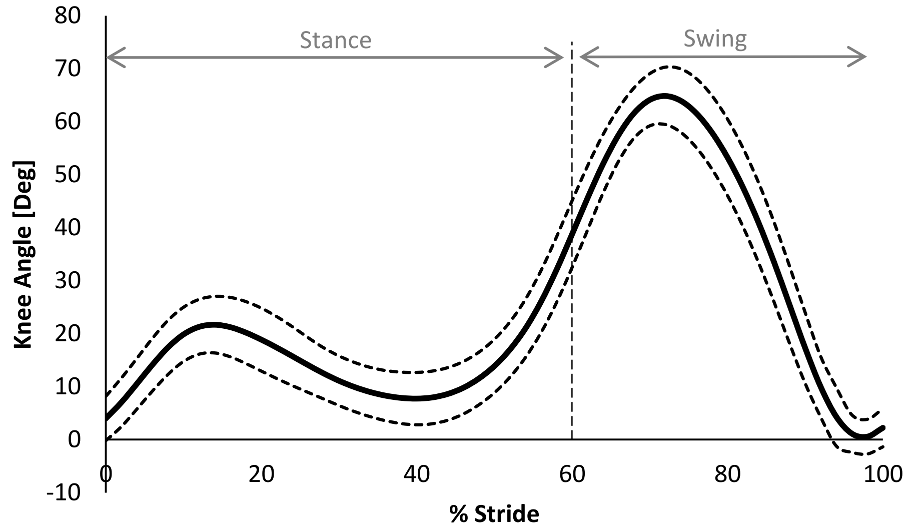


Figure 2.6: Knee angle for able-bodied, natural cadence, level ground walking with standard deviation shown with a dotted line (flexion is positive) (dataset from [14]).

Figure 2.7 shows knee angular velocity during normal cadence level ground walking for an able-bodied individual. During stance, angular velocity peaks at 150˚/s in flexion, but during swing phase, angular velocity peaks at 350˚/s in both flexion and extension.

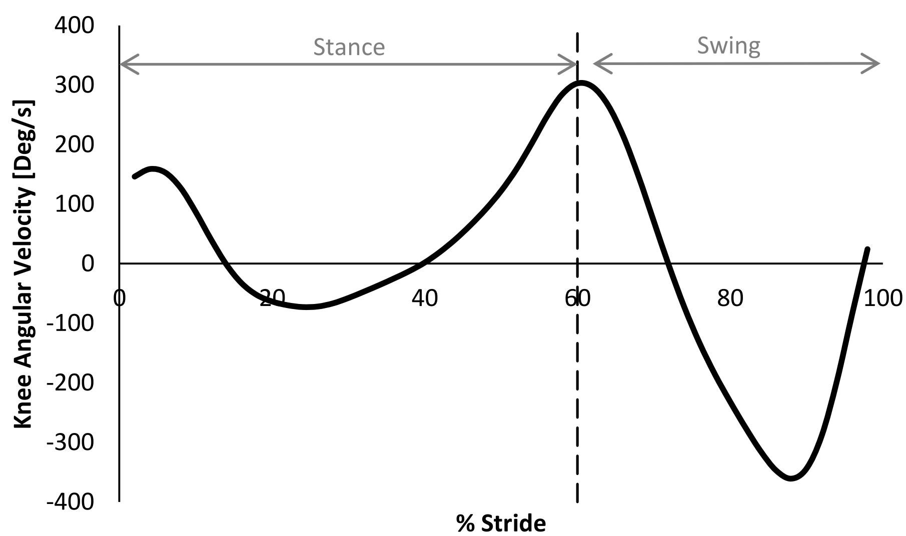


Figure 2.7: Knee joint angular velocity for able-bodied natural cadence level ground walking. Knee flexion is positive (dataset from [14]).

2.1.1.4 Knee joint kinetics for normal gait

Level ground natural cadence knee moment is shown in Figure 2.8. The largest external moment is an extension moment during loading response and mid-stance. The quadriceps muscles actively generate an extension moment to oppose the external flexion moment acting on the knee during the early stance, and to extend the knee during mid stance. This moment can be approximately 1.0 Nm/kg (mean plus standard deviation) [14]. During pre-swing, the quadriceps act eccentrically (lengthening under tension) to control knee flexion [15].

Knee joint power for natural cadence level ground walking is shown in Figure 2.9. A positive mechanical power indicates that the muscle is concentrically contracting (muscle shortening under tension) while a negative power indicates that eccentric muscles activity is absorbing energy [14], [15]. During swing phase, the knee muscles work to decelerate the shank and prepare the limb for knee extension, but the knee extensor muscles do not provide power to swing the leg forward. This energy comes from hip moments and from pendulum action at the knee joint [14], [16].

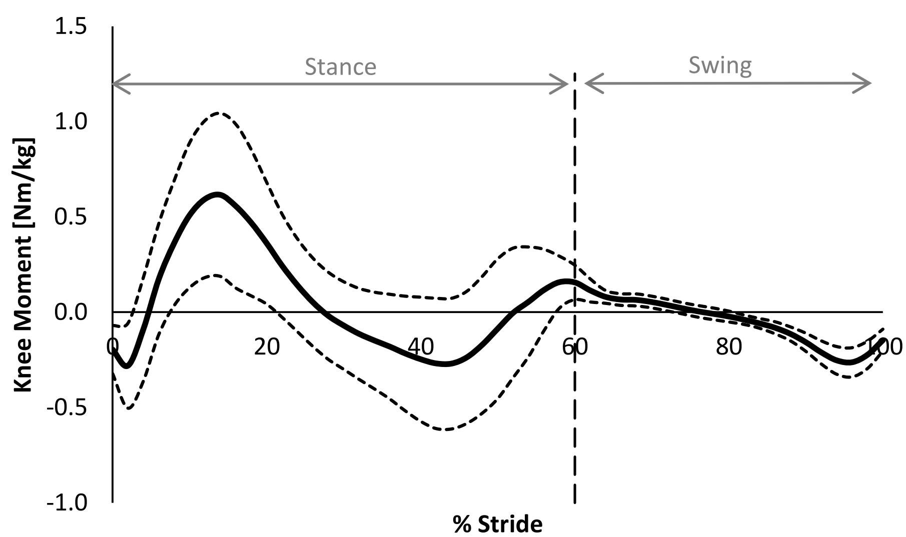


Figure 2.8: Knee joint moment normalized by bodyweight for able-bodied, natural cadence, level ground walking. Extension moment is positive (dataset from [14]).

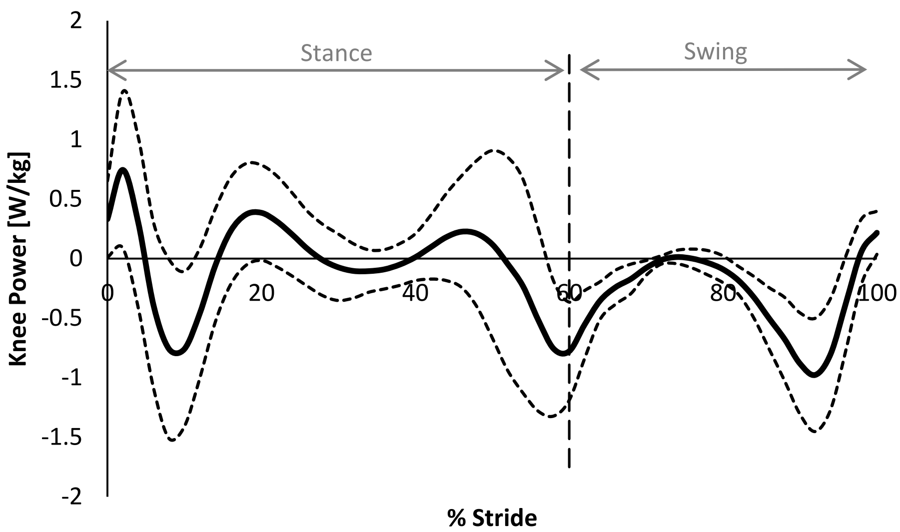


Figure 2.9: Knee joint power normalized to bodyweight for able-bodied, natural cadence, level ground walking. Positive powers indicate concentric contractions and negative powers indicate eccentric contractions (dataset from [14]).

## 2.1.2 Normal stair descent

### 2.1.2.1 Components of stair descent

The stepping cycle during stair descent can be divided into weight acceptance, single limb support, and swing limb advancement (Figure 2.10). The weight acceptance period occurs when the limb is rapidly loaded and forces from foot contact are absorbed. The single limb support phase controls body lowering to the following step. Swing limb advancement is responsible for foot clearance and opposite foot placement on the following step [1].

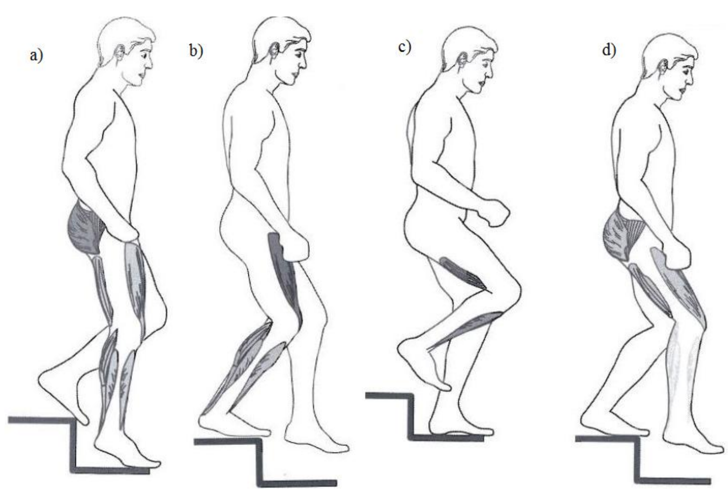


Figure 2.10: Periods of stair descent: a) weight acceptance, b) single limb support, c) early swing limb advancement, and d) late swing limb advancement (adapted from [1]).

2.1.2.2 Stair descent kinematics

Knee angle for normal stair descent at a typical step incline is shown in Figure 2.11. During stair descent, the knee is slightly flexed during weight acceptance. The knee joint flexes to absorb impact forces and then flexion increases during single limb support to lower the body to the following step. The ROM required for stair descent is larger than required for level ground walking, 90-100˚ during the early swing limb advancement phase [17]–[21].

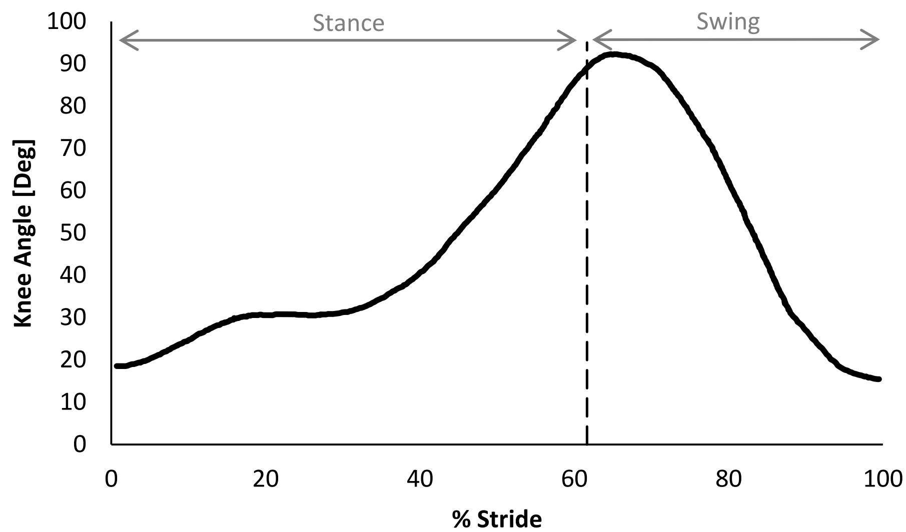


Figure 2.11: Knee joint angle for able-bodied stair descent for a typical step incline. Knee joint flexion is positive (reproduced from [17]).

2.1.2.3 Stair descent kinetics

The knee joint's role in stair descent is the same as level ground, but with larger external knee moments that place additional demands on the knee extensor muscles. The knee experiences two extension moment peaks during stair descent (Figure 2.12), the first during the mid stance, which is slightly smaller, and the second during terminal stance. Maximum knee extension moment during terminal stance has been reported as 1.4 Nm/kg [17]; 1.06±0.21 to 1.19±0.18 Nm/kg [22]; 0.91±0.29 Nm/kg for young adults and 0.83±0.17 Nm/kg for the elderly [20].

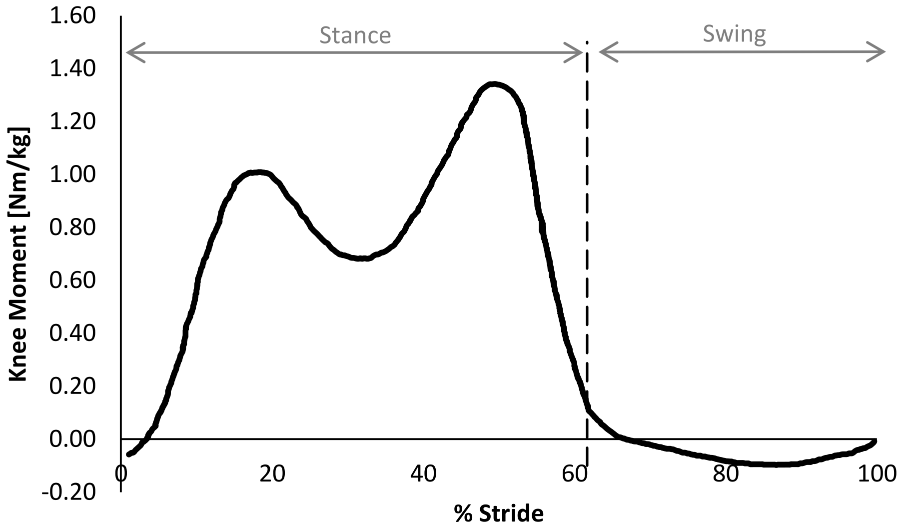


Figure 2.12: Knee joint moment for able-bodied stair descent for a typical step incline. Knee extension moment in positive (reproduced from [17]).

During stair descent, knee joint powers are mainly negative (eccentric), indicating that the muscles are working to control flexion (Figure 2.13). The maximum knee joint power absorption during stair descent occurs just before swing limb advancement, at the same time as the maximum joint extension moment (approximately -4.0 W/kg) [1], [17].

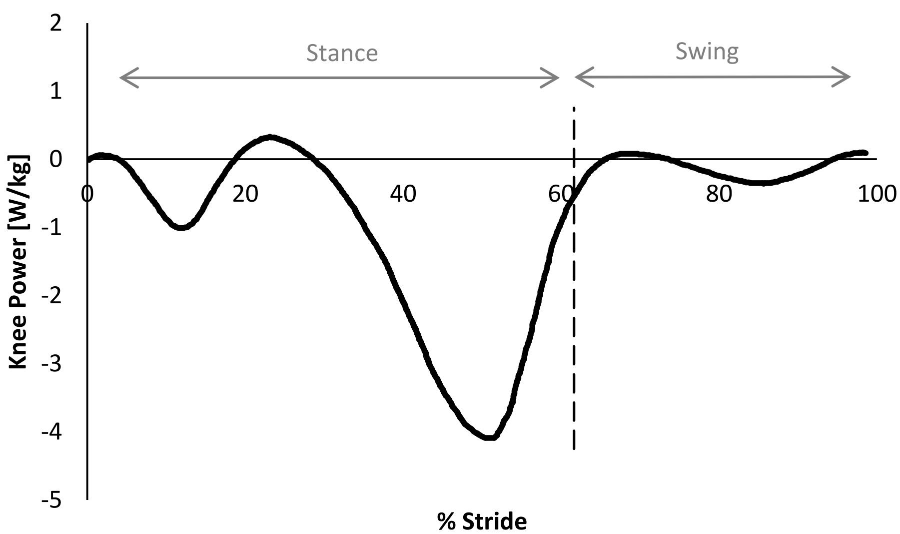


Figure 2.13: Knee joint power for able-bodied stair descent for a typical step incline. Positive powers indicate concentric contractions, negative powers indicate eccentric contractions (reproduced from [17]).

## 2.2 Knee extensor weakness

The knee extensor muscles maintain knee joint stability during stance phase. These muscles, primarily the quadriceps muscle group, resist knee flexion during the early stance to absorb shock and facilitate limb progression. If the knee extensors are not sufficiently strong, the knee will collapse due to the external knee flexion moment [1], [2].

Muscular weakness can result from peripheral neurological diseases (e.g., poliomyelitis), muscular diseases (e.g., Duchenne muscular dystrophy), central neurological diseases (e.g., multiple sclerosis), spinal cord injury, osteoarthritis, and severe injury [2]–[6]. The effects of knee extensor weakness can range from the individual having an abnormal gait pattern to complete instability [3], [7]. Even if the extensor muscles are only slightly weakened, walking with an abnormal gait pattern is highly energy consuming and can cause further soft tissue damage [2].

Limited statistics are available for individuals with knee extensor weakness since the condition can arise from many diseases or injuries. A study (2009) by the Reeve Foundation found that approximately 1.9 percent of Americans (~5,596,000 individuals) were living with some sort of paralysis [23]. In a Statistics Canada report (2012), approximately 1,971,750 individuals reported a mobility disability [24]. Furthermore, an American study (1997) found that approximately 989,000 individuals were using some type of knee orthosis [25].

### 2.2.1 Pathological gait

Individuals with knee extensor weakness can range from having a slightly unnatural gait pattern to complete instability while walking, depending on the severity of their condition. The knee extensor muscles are active in both stance and swing phases since these muscles control stance and the flexion rate during early stance. Individuals with knee extensor weakness are at risk of collapsing when an external knee flexion moment is acting on the knee joint (Figure 2.3 and Figure 2.4).

To avoid having the GRF vector pass behind the knee joint centre, certain techniques are adopted. In particular, people increase hip extensor muscle activity and anterior trunk flexion to shift the body centre of gravity forward. Long term effects of this strategy may include knee joint hyperextension since the joint is constantly being loaded to a fully extended position [2], [3]. Individuals will have trouble negotiating stair descent if they have moderate to severe knee extensor weakness, due to the large external knee flexion moments.

## 2.3 Orthotic management of knee extensor weakness

### 2.3.1 Ankle-foot-orthoses (AFO)

For less severe cases of knee extensor weakness, individuals can use a floor reaction ankle-foot-orthosis (AFO) (Figure 2.14). A floor reaction AFO resists ankle dorsiflexion, moving the GRF vector anterior to the knee joint axis and placing an external extension moment on the knee. By preventing dorsiflexion during the loading response and mid-stance, the GRF moves from behind the knee joint axis to the front, placing the knee in a stable position [2]. This helps individuals who adopt an anterior trunk bend technique.

Figure 2.14: Thermoplastic floor reaction AFO [26].

### 2.3.2 Knee-ankle-foot orthoses (KAFO)

While AFOs can be prescribed to people with mild knee extensor weakness, more severe cases require knee-ankle-foot orthoses (KAFOs) (Figure 2.15). KAFOs typically resist knee flexion with a three force design (Figure 2.16) [2]. The reaction forces F1 and F3 act in the anterior direction, on the shank and thigh respectively. The reaction force F2 acts at the knee in the posterior direction. This three force system prevents the knee joint from collapsing from an external knee flexion moment. Depending on the severity of the muscular weakness, different joints are required to prevent the knee from collapsing, ranging from offset-free motion joints to joints that remain locked during gait.

Figure 2.15: Thermoplastic KAFO [27].

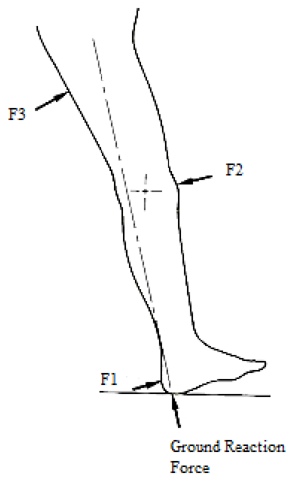



Figure 2.16: Forces required to prevent unwanted knee flexion (adapted from [2]).

Conventional KAFOs are generally made from custom moulded thermoplastic that conforms to the user’s leg, metal uprights, and hinged knee joints (Figure 2.17). The moulded thermoplastic design may also be referred to as a total surface bearing KAFO design. Conventional KAFOs can also be made using a metal and leather design, with metal uprights and leather straps to attach the orthosis to the leg. This design is less common because the moulded thermoplastic design distributes pressures more effectively and improves limb control. In addition, moulded thermoplastic KAFOs are lighter, more hygienic, and can be worn with different shoes. A disadvantage of the moulded thermoplastic style KAFOs is they do not accommodate for changes in volume as well as the leather strap systems [28].

Figure 2.17: Moulded thermoplastic and leather strap KAFO [28].

Conventional KAFO designs generally lock the knee in an extended position, which keeps the person stable throughout stance. However, the user must walk with a straight leg, resulting in unnatural gait patterns. Compensatory strategies may include circumduction of the braced limb, hip elevation of the braced limb, lateral sway, and/or increased contralateral ankle plantar flexion to clear the braced limb’s foot (vaulting) [2], [7], [8], [29].

Unnatural gait patterns are inefficient for the user and can lead to joint dysfunction and soft tissue damage, mainly at the hips and lower back due to long term gait compensation. This will cause the user pain and loss of motion. Walking with a locked-knee KAFO also limits the terrain the user can navigate, since toe clearance is more difficult to achieve. Stairs, ramps, curbs, and uneven ground terrains are much more difficult for users with these orthoses [8]. Due to these issues, the abandonment rate for conventional locked-knee KAFOs is very high (above 60 percent according to some sources) [6], [30], [31].

### 2.3.3 Stance control KAFO (SCKAFO)

Stance control KAFO (SCKAFO) support the leg during weight bearing and permit free knee motion during swing phase. If the SCKAFO user has sufficient hip muscle strength for forward progression, SCKAFOs improve mobility compared to fixed knee KAFOs [7].

There are many medical benefits of using a SCKAFO instead of a locked joint KAFO. Zacharais and Kannenberg analyzed the clinical benefits of stance control orthosis systems and found that SCKAFOs benefits could be grouped into three categories: general benefits, affected side benefits, and benefits for the sound side. General benefits include a more natural gait pattern, reduction of compensatory movements, lower energy consumption, greater walking speed, and overall higher patient satisfaction. The benefits for the affected (orthosis) side are greater knee ROM during swing, increased toe clearance, and reduced compensatory pelvic movements. The benefits for the sound side are reduction of ankle plantar flexion and compensatory pelvic movements during stance [10].

The primary issue for SCKAFO design is determining a method to control knee flexion during stance and release the knee joint during swing. A number of approaches have been developed for mechanical SCKAFOs. Weighted or spring loaded pawls can be used to lock the knee in extension at heel strike and unlock at toe off, based on leg position (Otto Bock Free Walk [32] (Figure 2.18), Becker UTX [33], Becker FullStride/SafetyStride/Stride4 (Figure 2.19), and Fillauer Swing Phase Lock 2 [34] (Figure 2.20)). This method is advantageous since a smaller joint can be used, resulting in an aesthetically pleasing, lightweight, and simpler orthosis. However, these orthoses do not lock while the knee joint is flexed, introducing uncertainty when negotiating terrains such as stairs, ramps, uneven ground, and obstacles such as curbs, as well as stumble recovery [35].

Another mechanical SCKAFO design uses the GRF to engage a locking mechanism. This method uses a hinged footplate or a foot stirrup in the ankle-foot section to transmit force through a pushrod to the joint’s locking mechanism (Horton Stance Control Orthosis [36] (Figure 2.21), Ottawalk belt-clamping experimental design [37] (Figure 2.22)). These orthoses can lock at any knee angle but are generally larger and require a mechanism at the foot to determine when the individual is in stance [35].

For individuals with knee extensor weakness but sufficient hip control, angular velocity based control can be used [35]. This design approach is based on knee angular velocity increasing during a stumble or fall, so the knee joint is designed to lock at a predetermined angular velocity, but allow for free motion at any angular velocity under this threshold [9]. The hydraulic implementation of this angular velocity approach is useful since the joint will lock in any position but only engage when the person's knee angular velocity reaches the threshold. These devices are only designed for individuals with sufficient hip strength since the SCKAFO does not resist flexion during stance, unless the threshold is reached. The Ottawalk rotary hydraulic [35] (Figure 2.23) and linear piston [9] designs use the angular velocity based approach.

#### 2.3.3.1 Otto Bock Free Walk/ Becker UTX

Free Walk / Becker UTX orthoses (Figure 2.18) are manufactured by two different companies but use the same ratchet and pawl design. The orthosis locks when the knee is fully extended (the spring-loaded pawl locks the knee in extended position). Knee joint release is triggered by 10˚ of dorsiflexion, which occurs just prior to toe off. The ankle joint is connected to a cable that disengages the spring-loaded pawl [7], [33], [38].

Figure 2.18: Otto Bock Free Walk [39].

The advantage of this design is its simplicity and aesthetics. The device is lightweight, low profile, can easily fit underneath clothing, and doesn't require an external power source. The primary disadvantage of this design is the SCKAFO requires a fully extended knee to engage the lock. If the limb is flexed during limb loading, then the leg will be unsupported. This could also be a problem if the individual were to stumble when the lock was not engaged and land with a bent knee. People with limited ankle ROM or who require a rigid AFO segment are contraindicated for this device [7].

#### 2.3.3.2 Becker FullStride, SafetyStride, and Stride4

The FullStride, SafetyStride, and Stride4 (Figure 2.19) are stance control orthotic knee joint systems from Becker Orthopedics. The mechanical joints all use a cabling system attached to the ankle joint that automatically unlocks the knee joint at the end of stance phase by releasing a spring loaded pawl, similar to the Otto Bock Free Walk and Becker UTX orthoses [33].

The FullStride uses a low-profile cable system that is attached to the ankle joint to trigger the release the knee joint lock. The knee joint is released at the end of stance phase, and the lock is reengaged once the knee is fully extended (similar design to Otto Bock Free Walk and Becker UTX) [33]. The SafteyStride uses a similar low-profile cable system attached to the ankle joint to unlock the knee joint at the end of stance phase, but the lock lever is reengaged during mid-swing to ensure joint stability prior to footstrike. When the lock lever is engaged to the teeth of a gear, the knee joint can extend, but flexion is not permited [40].


Figure 2.19: Becker FullStride, SafteyStride, Stride4 stance control orthotic knee joints [33].

The Stride4 (patent pending) also uses a low-profile cable system attached to the ankle joint to release the knee at the end of stance phase. The Stride4 uses a four bar linkage mechanism, so that joint rotation more closely mimics anatomical knee motion. The joint can switch between 3 modes: stance control (free knee motion during swing and locked knee during stance), locked knee joint, and free movement. In stance control mode, the joint uses a spring to assist with knee extension. The amount of knee extension required to reengage the knee joint lock can be adjusted to suit the individual [33].

These three joint designs are modular and can be easily changed on the same orthosis, and the patient can select the joint that meets their needs. None of these three requires external power and all are low-profile, aesthetically pleasing joints that could be worn beneath clothing. A disadvantage of these joints is that individuals must have sufficient ankle motion to generate the needed cable extension (minimum of 3-5˚ of ankle and/or forefoot movement [33]). The FullStride and Stride4 models also require a fully extended knee to engage the locking mechanism and stabilize the knee. The SafteyStride does not require a fully extended knee joint to engage the lock, but is the mechanism larger and heavier.

#### 2.3.3.3 Fillauer Swing Phase Lock 2

The Fillauer Swing Phase Lock 2 (SPL 2) is a gravity actuated locking joint (Figure 2.20). A weighted pawl falls into place and locks the joint when the knee is fully extended and the hip is flexed, so the thigh is anterior to the body. When the thigh moves posterior to the body and the leg is straight, the pawl disengages. These hip angles to engage/disengage the pawl are set by an orthotist. The SPL 2 can lock at 0˚ and 15˚ of knee flexion. The joint has four settings that are controlled by a remote push button switch: free motion, automatic lock/unlock, manual lock, and manual unlock [7], [34]. The SPL 2 must be used with a Swing Phase Control joint on the medial side that uses a spring and friction to regulate knee flexion during swing [34].

Figure 2.20: Fillauer SPL 2 joint mounted on standard KAFO uprights [41].

An advantage of the SPL 2 is that it can be sold as the joint alone and used with standard KAFO uprights. All stance control components are within the joint (i.e., the joint doesn't require parts elsewhere on the orthosis to control lock engagement). Also, the device also does not require external power. Disadvantages of this joint are that it requires full knee extension to lock the joint, and the orthosis is limited mainly to use on smooth level ground because thigh orientation determines the locking position [7].

#### 2.3.3.4 Horton Stance Control Orthosis

For the Horton Stance Control Orthosis, an eccentric cam is forced into a friction ring to lock the knee joint (Figure 2.21). A pushrod is connected to a thermoplastic stirrup that sits just below the orthosis ankle/foot section. When the heel contacts the ground, the stirrup is pushed upwards and the pushrod engages the cam and friction ring, locking knee motion. Due to the cam positioning, the cam will stay locked with knee flexion but the cam will disengage with an extension moment. The orthosis has three functional modes, controlled by a knob on the joint: automatic stance/swing, constant free knee motion, and constant locked knee extension [7], [36].

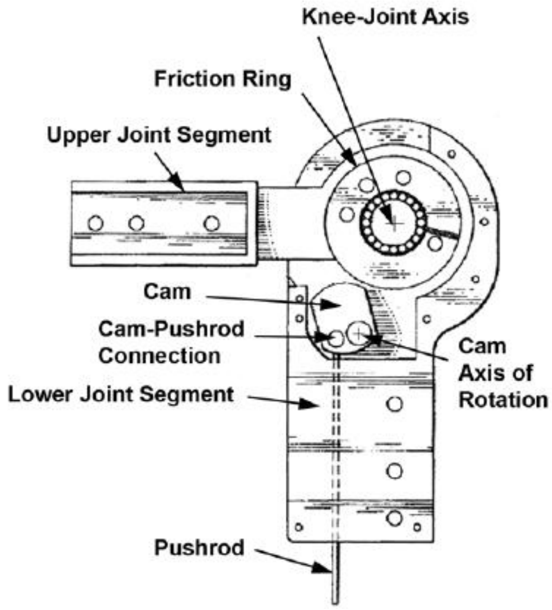


Figure 2.21: The Horton Stance Control Orthosis locking mechanism [7].

The Horton Stance Control Orthosis can lock at any knee angle, which is very important for individuals with severe knee extensor weakness. This allows the user to negotiate different types of terrain. The primary issue with the orthosis is its size. The orthosis is bulky and the ankle/foot section is large and heavy due to the stirrup section. The two-layer foot can result in debris becoming stuck between the layers, which will prevent the cam from moving into position. The boot’s size will also prevent users from wearing normal footwear [7].

2.3.3.5 Ottawalk Belt-Clamping Knee Joint

The Ottawalk Belt-Clamping Knee Joint was an experimental design developed by Yakimovich et al. in 2006 [37]. The design uses a tension belt that is attached to the upper and lower uprights of the KAFO and crosses the knee joint axis. During stance, the knee joint flexes and the belt tension increases and pushes against a lever to clamp the belt (Figure 2.22). The clamp is released when an extension moment occurs. The orthosis distinguishes between stance and swing modes using foot pressure or ankle angle connected to a pushrod [7], [37].

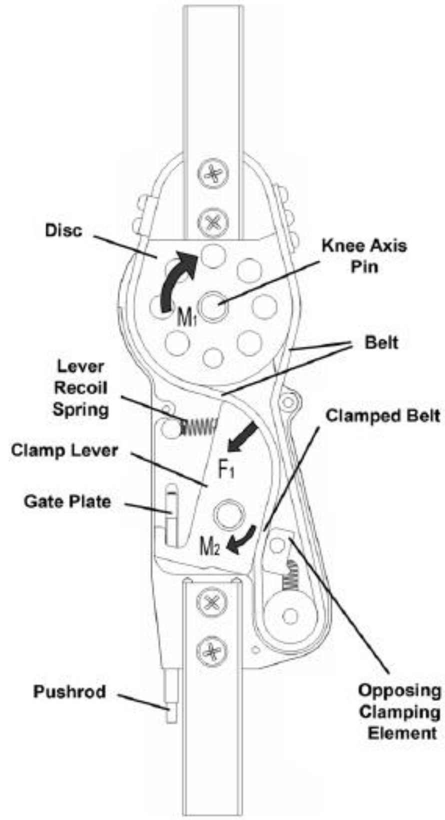


Figure 2.22: Ottawalk belt-clamping knee joint. $M_1$ is the knee moment (flexion moment shown), $M_2$ is the clamp lever moment, and $F_1$ is the belt force on the clamp lever [7].

This design has the advantage of being able to lock at any knee angle. The friction belt style joint could absorb some of the impact during initial loading [42]. Unfortunately, this joint is still quite bulky, and requires an extension moment to disengage the flexion lock.

2.3.3.6 Ottawalk-Speed Rotary hydraulic approach

The design uses a rotary piston with a flow-triggered one-way valve (Figure 2.23) to implement the angular velocity control approach. The rotary piston separates the flexion and extension chamber and, as the knee joint flexes, the flexion chamber volume decreases and the extension chamber increases. The hydraulic fluid is forced through the valve channel during flexion, where it passes a spring biased valve. If the drag force due to fluid velocity is larger than the spring force holding the valve open, the valve will shut, stopping flow and locking the joint. Because the valve is spring biased to stay open, the joint will always allow free extension [35].

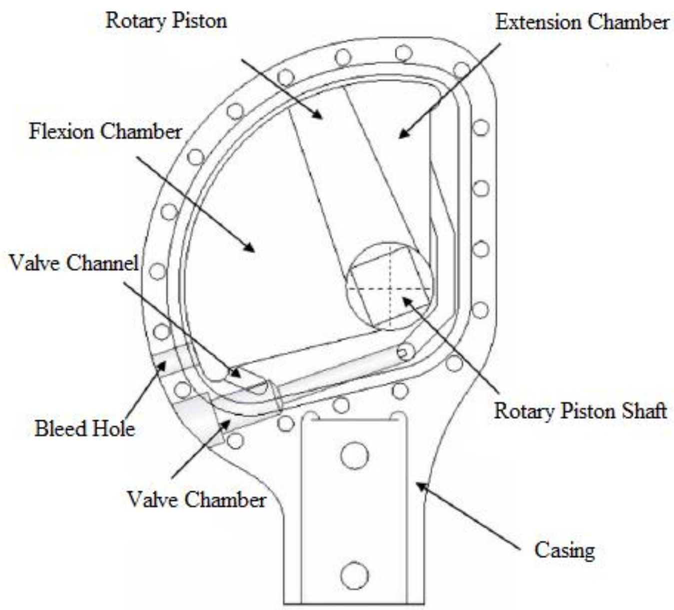


Figure 2.23: Ottawalk rotary hydraulic joint (adapted from [35]).

The angular velocity based approach benefits individuals who only require knee flexion resistance when a stumble or fall occurs. These joints are not designed to provide support throughout the stance phase, and should only be used with individuals with sufficient hip control. To support a 90 kg user, both lateral and medial joints are required, making the device bulky and heavy [9]. The knee flexion resistance engagement time was also insufficient (stopped knee flexion at 40˚ during leg collapse) [35].

2.3.3.7 Ottawalk-Speed Linear Piston hydraulic approach

This design (OWS-Speed) uses a similar concept as the rotary hydraulic approach but with a linear hydraulic piston that is able to accommodate higher pressures and reduced size. When the knee joint flexes, hydraulic fluid is pushed out of the cylinder and through a spring biased ball valve. Similar to the rotary design, if the ball's drag due to the fluid velocity is greater than the spring force opposing it, the joint will lock. Due to the spring bias, the flow can always enter the cylinder, allowing free extension [9].

This design improves weight and size compared the Ottawalk rotary hydraulic approach. This orthosis is meant for individuals with sufficient hip strength since the device does not support the user throughout stance, unless the threshold angular velocity is reached.

### 2.3.4 Microprocessor controlled KAFOs

Microprocessors are another method of controlling SCKAFOs. These orthoses rely on sensors to determine what the limb is doing and either lock, unlock, or apply resistance to the knee joint. The majority of these orthosis use pressure sensors, joint angle sensors, or strain gauges in the uprights to determine if the foot is in contact with the ground. Upon foot contact, the SCKAFO locks the knee during stance and releases the joint during swing. Microprocessor controlled KAFOs have the advantage of improved reliability of switching between modes and also have the ability to sense different walking terrain with the use of different sensors. The drawbacks to these joints are the fact that they require power, and need to be charged regularly. They also are more expensive than mechanical SCKAFOs.

2.3.4.1 Becker Orthopedic 9001 E-Knee

The Becker Orthopedic 9001 E-Knee [33] uses a magnetic one way dog clutch to control knee flexion during stance (Figure 2.24). The two ratchet plates are separated by a spring and one of the ratchet plates is attached to an electromagnetic coil. A pressure sensor at the foot can detect when the affected limb is weight bearing and when this is detected the electromagnetic coil is energized and the ratchet plates connect. The teeth on the ratchet plates only allow angular movement in one direction, allowing for knee extension [37], [43].

Figure 2.24: Becker Orthopedic 9001 E-Knee [33].

While the electromechanical ratchet design allows for reliable locking throughout stance and knee extension, the ratchet is loud and can be heard when the lock is engaged. The orthosis also has a finite number of locking positions due to the ratchet design, with up to 6˚ of knee flexion between each locked setting. Some users may not find this amount of knee motion acceptable prior to locking [7]. The Becker E-Knee is currently in a redesign phase and is not commercially available.

2.3.4.2 Otto Bock Sensor Walk

The Otto Bock Sensor Walk (Figure 2.25) [39] is the commercial version of the Dynamic Knee Brace Orthosis System designed by Kaufman *et al.* [29]. The design engages and disengages knee joint locking using a solenoid to control a wrap-spring clutch. The wrap spring clutch transmits torque to mating clutch hubs and when the knee flexes the spring tightens over the hub, stopping knee motion. Knee extension loosens the clutch spring. The clutch wrap spring can also be disengaged in flexion by the solenoid pulling back on the spring. Pressure sensors at the heel and forefoot are used to detect heel strike and toe off. A microprocessor interprets plantar pressure data and controls the solenoid [7], [29], [44].

Figure 2.25: Otto Bock Sensor Walk [39].

The Sensor Walk is a very strong SCKAFO and can be used by people who weigh up to 136 kg. The wrap spring clutch design does not require an extension moment to unlock the joint [38]. Issues with this SCKAFO are that the device is quite bulky and heavy, which can make the SCKAFO cosmetically unappealing. The Otto Bock Sensor Walk has recently been discontinued from the Otto Bock stance control orthosis line and replaced by the C-Brace [39], which is reviewed in Section 2.3.4.6.

2.3.4.3 Otto Bock E-Mag Active

The E-Mag Active (Figure 2.26) uses electromagnetic technology to lock the knee joint. A friction wedge, powered by an electromagnet, locks the knee in flexion during stance and requires the flexion load to be removed to unlock the joint during swing phase. Gyroscope and accelerometers on the KAFO's thigh portion are used to monitor the user's position in the gait cycle. The E-Mag Active is designed for locking while weight bearing and free knee motion during the swing phase. The orthosis will sense and remain locked if the patient is walking on varying terrains and elevations [11], [38].

Figure 2.26: Otto Bock E-Mag Active

Advantages of this SCKAFO are that the controls do not require ankle ROM, so the person can use the orthosis even if they do not have ankle control. The sensors controlling the joint are calibrated by an orthotist so that engagement and disengagement can be customized to the individual based on their gait patterns and recalibrated as the user's gait changes over time (i.e., if their condition worsens or improves) [11]. A disadvantage of this orthosis is that the user must be able to fully extend their knee to engage and disengage the locking mechanism.

#### 2.3.4.4 Cullell/Moreno-Actuator Design

A design approach by Moreno *et al.* [3] uses an actuator system to control the knee and ankle joint based on biomechanical data. This actuator design was adapted to a KAFO with a four-bar linkage knee joint that followed the knee's anatomical movement, simulating cruciate ligament movement (Figure 2.27). This SCKAFO uses two compression springs to control the knee joint. One compression spring, which has a larger elastic constant, absorbs impact from initial loading and stores this energy and help with energy return during terminal stance to extend the knee. The second spring is used for swing control by compressing during swing flexion, and helps with extension at terminal swing. The springs are selected based on the person's weight. A goniometer at the knee and two gyroscopes on the thigh and shank are used to determine where the limb is in the gait cycle, and a solenoid is used to switch between the two springs during stance and swing [3], [45].

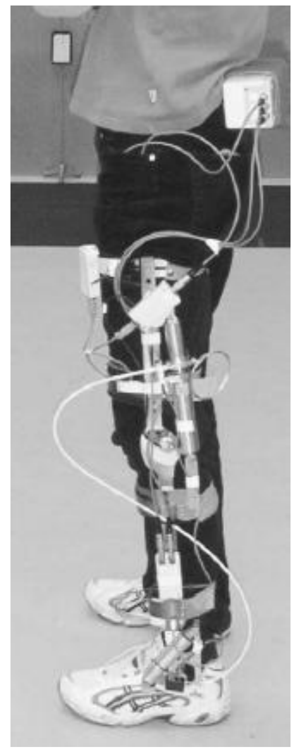

Figure 2.27**:** GAIT orthosis design by Moreno *et al.*[3].

The main advantage of this SCKAFO is its ability to assist with knee extension during both stance and swing phases. The device is currently not commercially available, and is quite large and bulky. The device is still in the design stage, but the assisted extension has shown to aid individuals walking with SCKAFOs [3], [35].

#### 2.3.4.5 Quasi-Passive Compliant Stance Control Orthosis

The quasi-passive compliant stance control orthosis (CSCO) [6] is an experimental design that incorporates a linear spring to compliantly support the knee joint during stance phase and allow free knee motion during swing. A pulley that wraps around the knee joint and pulls to compress a linear compression spring, converting linear stiffness to torsional stiffness. The joint has two stiffness modes with the engagement/disengagement of support spring. A worm gear drives a shaft that engages and disengages this spring. The CSCO used foot sensors to sense when the toe and or heel contact the ground. The support spring engages during weight acceptance and releases during terminal stance. During the swing phase, the controller monitors knee velocity, disengages the spring during the flexion portion of swing, and engages the spring during the extension portion [6].

The CSCO is not a commercial design, and further testing is needed to better understand the benefits of compliant support, since the orthosis has only been tested on able-bodied participants. In preliminary testing, kinematic patterns using the CSCO were similar to the Otto Bock Sensor Walk. The design is quite bulky and requires a large amount of external power [6].

#### 2.3.4.6 Otto Bock C-Brace

The Otto Bock C-Brace [39] is the only commercially available SCKAFO that provides in-stance dampening for knee joint flexion (Figure 2.28). A hydraulic actuator acts as a linear damper to control knee flexion. Two control valves (flexion and extension) adjust the damping by making throttle points larger or smaller for different fluid flow rates [46]. The orthosis uses two sets of sensors to control the joint, a knee angle sensor in the joint axis and a strain gauge on the shank's dorsal spring [39], [46].

The C-Brace senses the leg's position and adjusts knee resistance accordingly. Due to the hydraulic actuator design, the joint can apply varying amounts of knee flexion resistance, ranging from locked to free motion. This allows the user to walk with a more natural gait pattern since the knee is able to flex during stance, but can still maintain stability. The device can also be used on ramps, stairs, and even ground because it can sense the terrain. Knee flexion during stance also allows users to negotiate stairs, ramps, and sitting down. The C-Brace senses when a stumble occurs and provides knee joint stability at any knee angle.

Figure 2.28: Otto Bock C-Brace[39].

The C-Brace is currently the best commercially-available SCKAFO for walking on all types of terrain. The microprocessor has the ability to determine how the individual is moving and adjust accordingly. The main drawback with the C-Brace is its size, since the lateral unit is too large to fit beneath clothing. This orthosis must also be purchased as an entire unit because the dorsal spring part is instrumented with a strain gauge and a custom carbon fibre structure is needed to accommodate loading forces.

### 2.3.5 Orthosis summary

Table 2.2 provides a summary of the commercially available KAFO style orthoses. Sections 2.3.3 & 2.3.4 also reviewed experimental designs, but these are not available for purchase and many of the orthoses are still in the design and testing phases.

Table 2.2: Commercially available KAFO devices.

| Device/Model | Control Method | Advantages | Disadvantages | Cost |
|---|---|---|---|---|
| Conventional KAFO | Orthotic joints lock knee in an extended position | Inexpensive, simple, light | Knee cannot released for swing, adopt unnatural gait pattern | $3000 |
| Otto Bock Free Walk / Becker UTX | Ratchet pawl releases the knee at 10˚ dorsiflexion and re-engages the lock at full extension | Light, aesthetically pleasing, no external power required | Requires full extension to engage lock and sufficient ankle ROM | $4100 (complete orthosis) |
| Becker FullStride | Cable system attached to ankle joint releases spring loaded pawl at end of stance phase, and re-engages lock at full extension of the knee | Light, aesthetically pleasing, no external power | Requires full extension to engage lock and sufficient ankle ROM | $4200 (complete orthosis) |
| Becker SafetyStride | Cable system attached to ankle joint releases knee at end of stance phase, and an internal lever re-engages during swing phase to resist knee flexion but allow for knee extension | Does not require full knee extension to resist flexion | Requires sufficient ankle ROM. Bulkier joint than the Becker FullStride | $4400 (complete orthosis) |
| Becker Stride4 | Cable system attached to ankle joint releases the knee joint at the end of stance phase, and re-engages lock at full extension of the knee | Four-bar linkage mechanism that closely mimics anatomical knee motion | Requires full extension to engage lock and sufficient ankle ROM | $4500 (complete orthosis) |
| Fillauer Swing Phase Lock 2 | Gravity actuated ratchet and pawl, pawl falls in and out of locked position depending on thigh angle | Light, sold joint only, used with standard KAFO, no external power | Requires knee to be fully extended to engage the lock | $2900 (joint only) |
| Horton Stance Control Orthosis | Stirrup in foot section pushes a cam into a friction ring to lock the knee joint | Locks at any knee angle | Heavy, bulky, debris can get caught in foot/stirrup | $4000 (complete orthosis) |

| | | | | |
|---|---|---|---|---|
| Otto Bock Sensor Walk | Wrap spring clutch transmits torque to hubs that lock knee joint, foot pressure sensors verify stance, microprocessor controls solenoid to pull wrap spring clutch | Locks knee at any angle. Does not require extension moment to unlock knee | Bulky, low cosmetic appeal | $20,400 (Complete Orthosis) |
| Otto Bock E-Mag Active | Friction wedge and electromagnet locks the knee. Flexion load required to unlock. Accelerometers and gyroscope on the thigh detect limb position | Light, does not require sensors at foot/ankle, various knee extension angle settings | Knee to fully extended to lock, extension angle can be adjusted but must reach angle to lock, only locks in stance and releases in swing | $12,200 (Complete Orthosis) |
| Otto Bock C-Brace | Hydraulic linear dampener to control flexion, knee angle sensor and strain gauge on the dorsal spring sense limb movement and adjust joint stiffness | Variable resistive moments, apply resistance without locking the joint, allowing for multiple terrain | Expensive, bulky, cannot wear underneath pants | $70,000+ (complete orthosis) |

Section 2.3 discussed existing conventional KAFO, mechanical SCKAFO, and microprocessor controlled SCKAFO style orthosis. Advantages and disadvantages of each type of design as well as each individual orthosis were discussed. Microprocessor controlled orthosis are the leading technology because these orthoses can accurately sense and control knee flexion. A drawback of these designs is that they require external power to operate.

A SCKAFO engineering review article by Yakimovich *et al.*[7] discussed the technology and limitations of SCKAFOs currently on the market and in design-and-test phases. The two primary requirements for SCKAFOs are (i) to resist knee flexion but allow for free knee extension during stance and (ii) to permit free knee movement during swing. Yakimovich *et al.* also outline functional features that they found to be advantageous:

- Lock/resist knee joint flexion at any knee angle rather than just at full extension (ability to negotiate multiple terrains such as stairs and uneven ground as well as stumble recovery)
- Unlock knee at any knee or ankle angle to permit stair walking and sitting
- Permit controlled knee flexion during stance (for shock absorption)
- Smooth switching between swing and stance modes without requiring a knee extension moment to unload the joint
- Assisted knee extension during stance

After reviewing the orthoses, another area where SCKAFO design requires improvement is in size and aesthetics. While microprocessor controlled orthoses have improved functionality, many of these orthoses are bulky and cannot be worn beneath clothing.

## 2.4 Literature review summary

This literature review included knee joint function during locomotion, focusing on the knee extensor muscles during level ground walking and stair descent and the causes and effects of knee extensor weakness. Orthotic solutions for individuals with knee extensor weakness were then reviewed, and product reviews of current KAFO and SCKAFO designs were performed. The primary functions of these orthoses are to support the impaired limb during stance and allow for free knee motion during swing. From the literature review, it is clear that there are gaps in SCKAFO technology.

The most functionally advanced SCKAFOs are microprocessor controlled and provide increased switching reliability between modes. Some key features that are useful in SCKAFO design are: the ability to lock the joint without having to fully extend the knee joint, always allow for free knee extension, ability to apply various resistances to the knee joint to allow for locomotion on various terrains and shock absorption, and the ability to unlock the knee without requiring a knee extension moment. Different orthoses contain various aspects of these features, but many of these SCKAFOs are large and bulky, which is less appealing to the user. Currently, the most versatile orthosis available on the market is the Otto Bock C-Brace, but the main drawbacks of the orthosis are its size, that the orthosis has to be purchased as an entire unit, and that the device is expensive.

# Chapter 3: Design and Development

This chapter presents the design and development process that was used to create the variable resistance orthotic joint (OWVS). The rationale and objectives of the design are explained in Chapter 1. Section 3.1 and 3.2 review the design criteria and final design features of the OWVS. Section 3.3 discusses the mechanical hinge joint design including the geometry and force analyses. Section 3.4 explains the hydraulic circuit design and section 3.5 explains the hydraulic valve used in the design. Sections 3.6 and 3.7 discuss other components of the design and section 3.8 reviews the costs of manufacturing the prototype of the orthotic joint.

This thesis focuses on the mechanical and hydraulic design and evaluation aspects of the OWVS. While a simple control method was implemented to allow for mechanical and biomechanical testing, future work on an imbedded control system would be needed for a final product that engages appropriately at all times.

## 3.1 Functional design criteria

The OWVS must function as a SCKAFO for walking, supporting the knee during the stance phase and allowing uninhibited knee flexion and extension during the swing phase. From section 2.1.1, the knee joint's range of motion (ROM) is 0-70˚. The maximum knee angular velocity for level ground walking at a normal pace is approximately 300˚/s in flexion and 350˚/s in extension [1], [2], [14]. These angular velocities are for able-bodied individuals walking at a normal cadence, and individuals requiring a KAFO will likely walk at a slower cadence. Winter reported that the peak knee flexion angular velocity for slow cadence walking was approximately 285˚/s [14]. The maximum external extension moment during level ground, natural cadence walking occurs during early stance and can be as large as 1.0 Nm/kg (mean plus one standard deviation). Slow cadence walking generates a lower external knee extension moment (0.416 ± 0.342 Nm/kg) [1], [2], [14].

Research on the Otto Bock C-Leg (microprocessor controlled prosthetic knee) was analyzed because C-Leg's function will be similar to OWVS joint function [39]. During level ground walking, TF amputees land on the C-Leg with an extended knee and the knee remains extended until the end of stance phase. Due to the extended knee, the prosthetic limb experiences much lower peak knee flexion moments during early stance (0.14 ± 0.05 Nm/kg [47]).

For level ground walking, an ideal SCKAFO joint should resist a 1.0 Nm/kg flexion moment and maintain knee joint stability during stance. For swing phase, the joint should move freely to achieve uninhibited motion (approximately 300˚/s in flexion and 350˚/s in extension).

A variable resistance system should allow the user to negotiate terrains other than level ground. The joint should have settings for safely descending stairs and sitting down from a standing position. The knee flexes up to 100˚ during stair descent [17]–[21] and the maximum external knee flexion moment occurs during terminal stance. Knee flexion moments range from 0.80 to 1.40 Nm/kg for able-bodied individuals [17], [20], [22]. Stance times were analyzed to determine the support duration for stair descent (Table 3.1).

Table 3.1: Stance times for able-bodied stair descent.

| Source | Population | Stance Time [s] |
|---|---|---|
| Riener et al., 2002 [17] | Normal, 24° step incline | 0.75 |
| | Normal, 30° step incline | 0.73 |
| | Normal, 42° step incline | 0.73 |
| Novak and Brouwer, 2013 [48] | Normal adults | 0.97 |
| Novak and Brouwer, 2011 [22] | Young adults (18-55) | 0.70 |
| | Older adults (55+) | 0.74 |
| Protopapadaki *et al.*, 2007 [21] | Healthy young adults | 0.80 |
| Mian *et al.*, 2007 [19] | Young adults | 0.60 |
| | Older adults | 0.69 |

For people with no knee extensor strength, the joint should function like a microprocessor controlled TF prosthetic knee. Schmalz *et al.* reported that TF amputees descending stairs with the Otto Bock C-Leg experienced 65˚ of knee flexion and a maximum external flexion moment of 1.0 Nm/kg [49]. The OWVS resistance settings should support 50-100 kg individuals for 0.7 - 1.0 seconds during stance phase when descending stairs on the braced limb (65˚ of knee flexion).

Section 2.3 reviewed SCKAFOs and outlined several functional features that were found to be advantageous. In particular, the ability to lock the knee joint at any angle is very important for tripping and stumbling scenarios, where the individual might land with their leg in a flexed position. This is also useful for people who do not have sufficient limb strength to fully extend their leg during normal gait.

The OWVS must be able to disengage the locking mechanism at any knee angle, and not require an extension moment for the disengagement. The joint should also always allow for uninhibited knee joint extension. Since knee joint extension will not cause KAFO users to collapse, the joint should allow free knee extension at all times to enable more natural gait and to allow the user to more quickly extend their leg in a stumble scenario.

### 3.1.1 Structural design criteria

The main reasons for abandoning orthoses are weight, size, and bulkiness [50]–[52]. Orthotic joints should have minimal outer dimensions, without compromising strength. Reducing the joint and hydraulic system size would also help to reduce the total weight. Aesthetics are an important aspect of orthotic design. The device being designed should fit beneath a normal pair of loose pants.

The OWVS will be used on the lateral side of a KAFO, to reduce costs the joint should have the ability to be used with standard orthotic uprights and components. A modular design would allow users of different orthotic joints to easily switch to the OVWS. To ensure that the joint can be worn comfortably beneath standard clothing, the joint's medial-lateral profile should not exceed 30 mm (without the control board) and the joint should never protrude more than 50 mm off the lateral upright. For aesthetic and protective purposes, a low profile case should include device components and allow for control board mounting and batteries.

Weight is another important design aspect. Component weight should be minimized to keep the orthosis as light as possible, since KAFO users have knee extensor weakness and perhaps other co-morbidities. A heavier orthosis increases difficulty when lifting the leg and adds inertia to the limb that increases the likelihood of having an abnormal gait pattern. The joint's total weight should not exceed 560 g. The Ottawalk-Speed (OWS) joint currently weighs 278 g, and the new OVWS design should not increase the weight by more than 50%.

### 3.1.2 Control design criteria

Valve reaction time is an important design aspect. The reaction time should be as rapid as the weight acceptance task time in the gait cycle. Winter reported average natural cadence for level ground walking to be 105.3 steps/min (1.14 s cycle time) and average slow cadence to be 86.8 steps/min (1.38 s cycle time) [14]. The weight acceptance task time (Table 2.1) is approximately 0-12% [1] of the gait cycle, which would correspond to approximately 0.14 s for natural cadence walking and 0.17 s for slow cadence. The valve should be able to switch between the open and locked setting in less than 0.1 s.

### 3.1.3 Summary of design criteria

Table 3.2 summarizes the key design criteria for the OWVS orthotic knee joint.

Table 3.2: Summary of design criteria.

| Function | Criteria |
|---|---|
| User weight range | 50-100 kg |
| Total joint weight | <560 g |
| Maximum medial-lateral profile | 30 mm |
| Connection to orthosis | Modular design that can be used with standard orthotic components |
| Range of motion | 0 - 110˚ (fully extend limb and sit comfortably) |
| Function during stance | Lock and prevent knee joint flexion at any angle, allow knee joint extension |
| Function during swing | Free motion (uninhibited knee flexion and extension) |
| Function during stair walking | Resist knee flexion to lower body centre of mass smoothly. (support user for 0.7 - 1.0 seconds during the stance phase of stair descent) |
| Function during stand-to-sit | Resist knee flexion to lower body centre of mass smoothly |
| Freely permit maximum flexion angular velocity | > 325˚/s |
| Freely permit maximum extension angular velocity | > 350˚/s |
| Valve reaction time | <100 ms (0.1 s) switching between the open and locked settings |

## 3.2 Components

Figure 3.1 is an exploded view of the proposed orthotic joint with the main components labeled. Design and development is explained in the following sections.

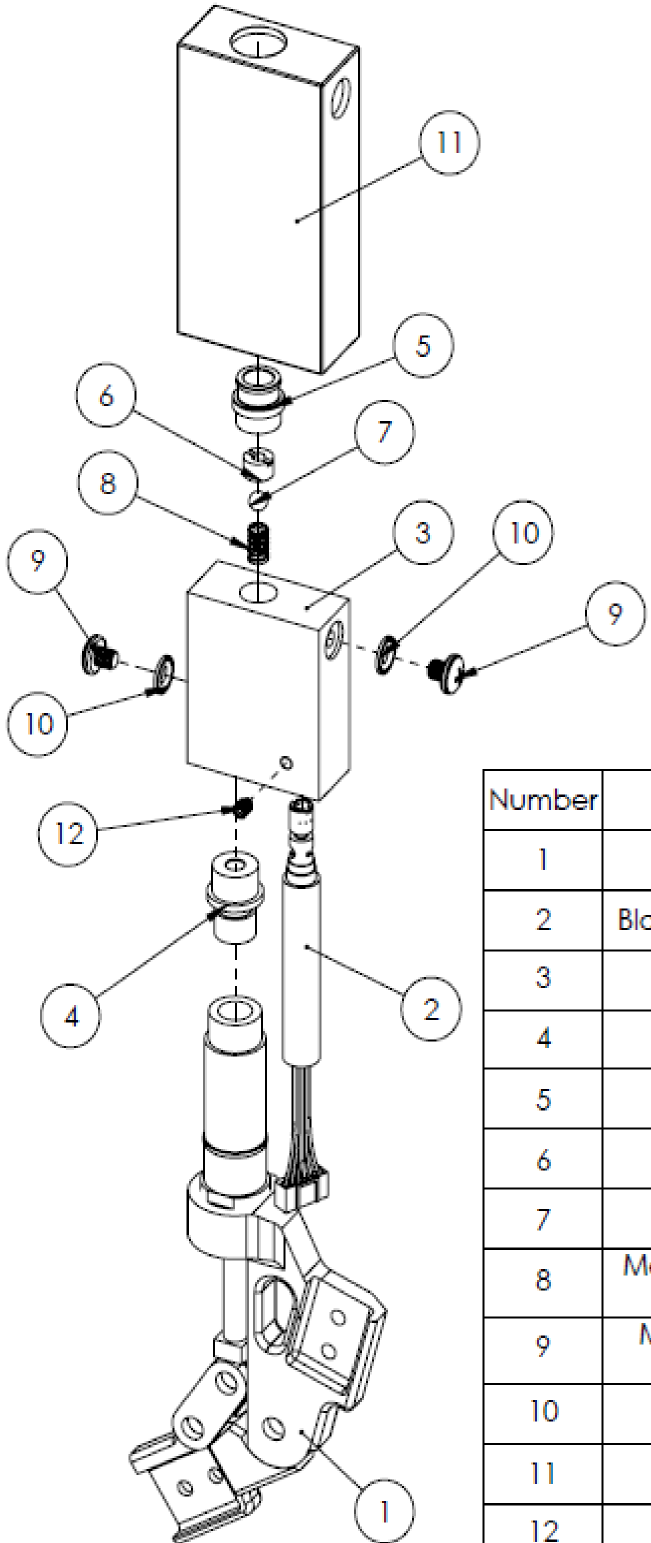


| Number | Part |
|---|---|
| 1 | OWS Joint |
| 2 | Blatchford Variable Resitance Valve |
| 3 | Hydraulic Circuit Block |
| 4 | Hydraulic Cylinder Adapter |
| 5 | Reservoir Connection |
| 6 | Check Valve Seat |
| 7 | 5 mm ∅ Ball |
| 8 | Metric Compression Spring (k = 0.33 lb/mm) |
| 9 | Metric Pan Head Philips Machine Screw (M5, 5 mm length) |
| 10 | Pressure Sealing M5 Washer |
| 11 | Case |
| 12 | Dog Point Set Screw (M4x0.7) |

Figure 3.1: Ottawalk-Variable Speed components.

## 3.3 Ottawalk-Speed joint

### 3.3.1 Original design

The OWVS was based on the OWS design by Lemaire *et al.* at TOHRC [9] (Figure 3.2). This single-axis joint mounts on the KAFO's lateral side. As the knee flexes, a connecting rod link pushes hydraulic fluid out of the hydraulic cylinder through the spring-biased one-way valve. The fluid flows past the ball valve into an external, expandable reservoir. If fluid velocity-induced drag on the ball is greater than the spring force opposing the drag, the ball blocks fluid flow to the reservoir and locks the joint. Flow can always enter the cylinder because of the spring bias, allowing free extension [9].

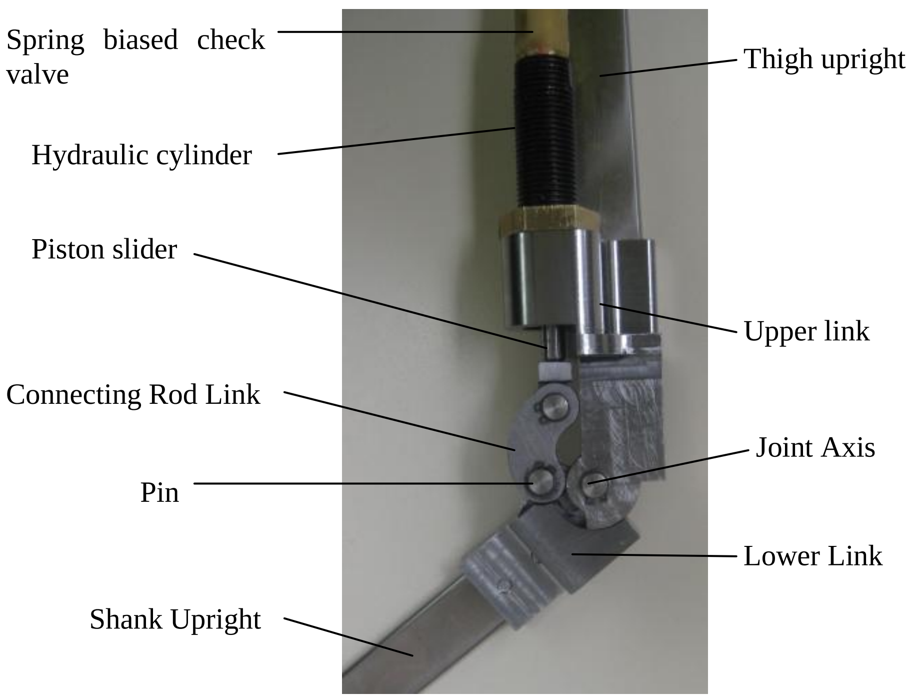


Figure 3.2: Original OWS SCKAFO joint design.

The upright connections and connecting rod link were made from 4140 grade steel and the valve was made of brass. A commercially available hydraulic cylinder was used in the design (Vektek mini threaded 20-0104-07; Vektek Inc; Emporia, Kansas) (Appendix B).

The orthotic joint had an average resistance to free-knee motion of 1.07 ± 0.24 Nm, which was considered negligible for human leg movement, and allowed for knee angular velocities over 300 deg/s. The theoretical maximum joint supportive moment was calculated as

150 Nm, and the joint successfully supported an average load of 144.6 ± 4.9 Nm over 20 knee collapse trials, with a maximum of 153.1 Nm [9].

The most recent OWS joint, developed by TOHRC, uses the same velocity based control technique, but the geometry and components have been improved (Figure 3.3). The main difference between designs is the hydraulic piston's angle. The original design had the hydraulic cylinder parallel with the thigh upright. However, placing cylinder at a 15˚ angle to the thigh upright facilitated the orthotist's job of adjusting thigh uprights and KAFO shell modifications during the fitting process. The joint redesign maintained a linear path for the slider. Other optimizations included increased strength, increasing ROM, and improved joint aesthetics.

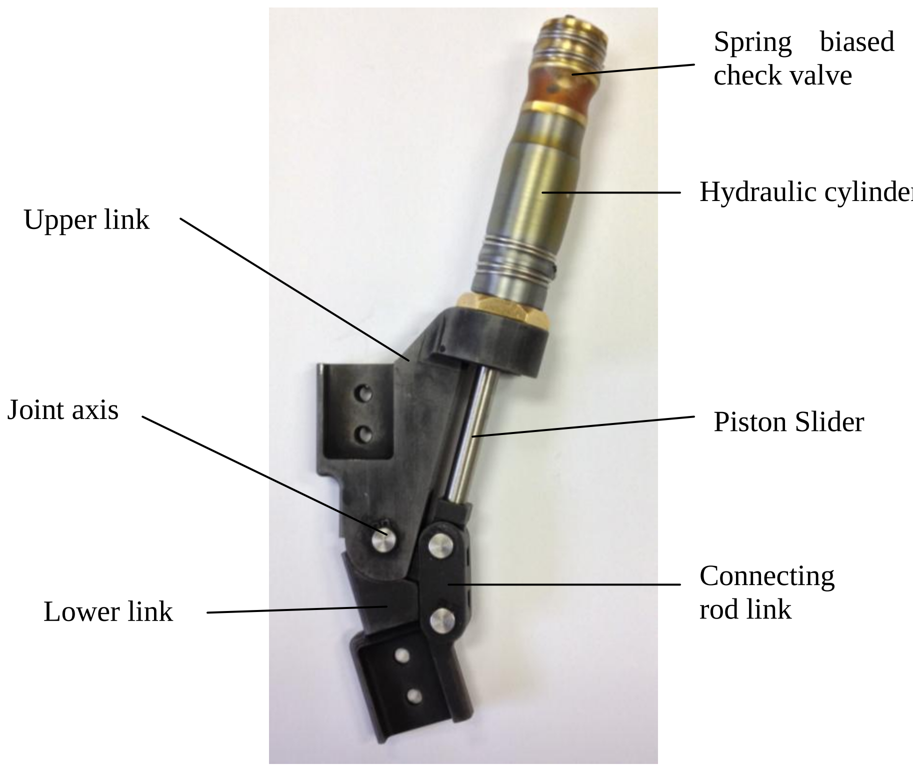


Figure 3.3: Current OWS joint.

The hydraulic cylinder was changed to the Vektek mini threaded 20-0105-07 (Appendix B), which has same stroke length but increased capacity (445 kg, 5000 psi maximum). Surgical tubing was used as the fluid reservoir and was placed around the outside of the cylinder.

### 3.3.2 Geometry

To determine orthotic joint forces, the positions, velocities and accelerations of the points A, B and C must be determined (Figure 3.4). Point A is selected as the origin of a joint-fixed coordinate system and an i-j coordinate system is fixed in the upper link (Figure 3.4). Equations 3.1 are used to determine the position, velocity, and acceleration of point C with respect to joint A in the i-j coordinate system, given by

$$\begin{aligned} \vec{R}_{C/A} &= \vec{R}_A + \vec{R}_{B/A} + \vec{R}_{C/\mathrm{B}} \\ \vec{v}_{C/A} &= \vec{v}_A + \vec{v}_{B/A} + \vec{v}_{C/\mathrm{B}} \\ \vec{a}_{C/A} &= \vec{a}_A + \vec{a}_{B/A} + \vec{a}_{C/B} \end{aligned} \tag{3.1}$$

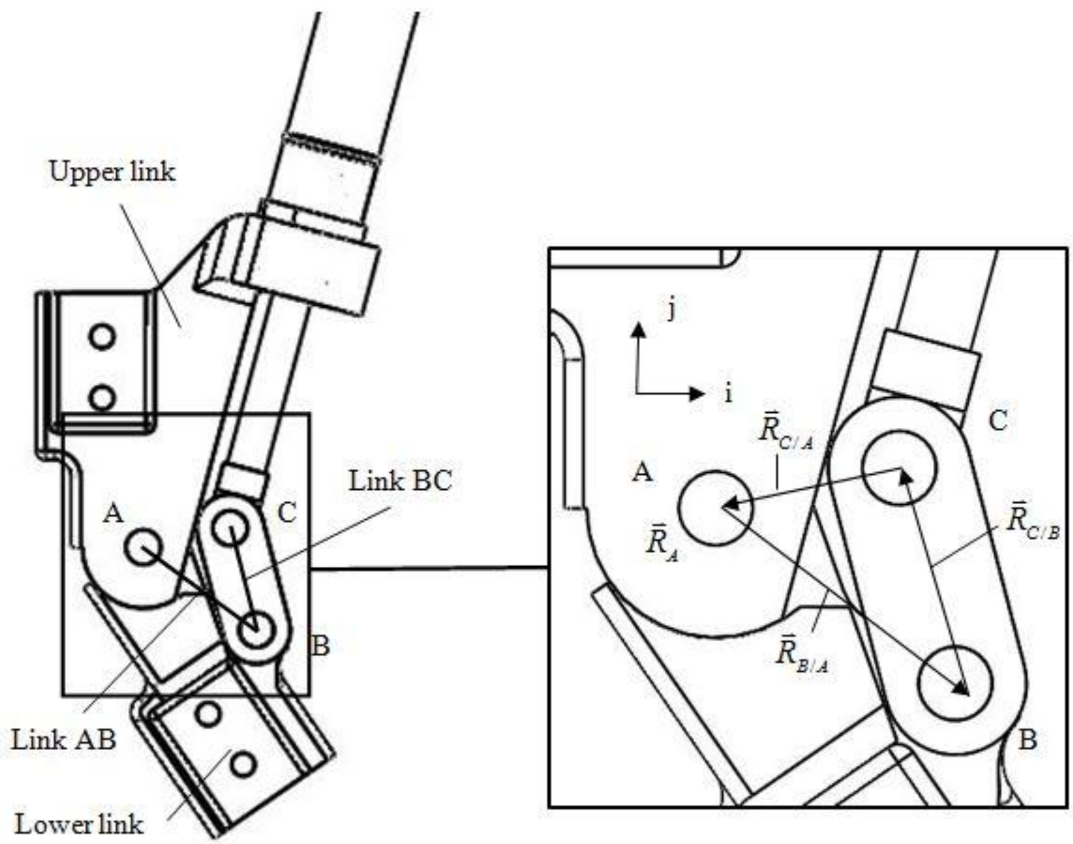


Figure 3.4: OWS joints A, B, C and links AB and BC. Vectors $\vec{R}_A$, $\vec{R}_{B/\mathrm{A}}$, $\vec{R}_{C/B}$, and $\vec{R}_{C/A}$.

The velocity ($\vec{v}$) and acceleration ($\vec{a}$) vector components are found by taking time derivatives of position ($\vec{R}$) and velocity vector components respectively:

$$\begin{aligned} \vec{v} &= \tfrac{d}{dt}\vec{R} \\ \vec{a} &= \tfrac{d}{dt}\vec{v} \end{aligned} \tag{3.2}$$

Points A and B are connected by a rigid link, therefore point B will move in a circular path about A. Equation 3.3 is the position of point B with respect to point A. $l_{AB}$ is the length of the link connecting points A and B (link AB), and $\theta$ is the knee joint's flexion angle (0˚ is an extended leg). $c_1$ is the angle $\vec{R}_{B/A}$ (link AB) makes with the horizontal of the i-j coordinate system when the knee is fully extended ($\theta$ = 0˚), and is equal to -70.73˚. Equations 3.4 and 3.5 are the velocity and acceleration of point B with respect to point A. $\dot{\theta}$ is the angular velocity $\ddot{\theta}$ is the angular acceleration of link AB.

$$\vec{R}_{\mathrm{B/A}} = \left(l_{ab}\cos(\theta+c_1)\right)\hat{i} + (l_{ab}\sin(\theta+c_1))\,j \tag{3.3}$$

$$\vec{v}_{B/A} = \tfrac{d}{dt}\vec{R}_{B/A} = \left(-l_{ab}\dot{\theta}\sin\left(\theta+c_1\right)\right)\hat{i} + \left(l_{ab}\dot{\theta}\cos\left(\theta+c_1\right)\right)j \tag{3.4}$$

$$\begin{aligned} \vec{a}_{B/A} = \tfrac{d}{dt}\vec{v}_{B/A} &= \left(-l_{ab}\ddot{\theta}\sin\left(\theta+c_1\right) - l_{ab}\dot{\theta}^2\cos\left(\theta+c_1\right)\right)\hat{i} \\ &\quad + \left(l_{ab}\ddot{\theta}\cos\left(\theta+c_1\right) - l_{ab}\dot{\theta}^2\sin\left(\theta+c_1\right)\right)j \end{aligned} \tag{3.5}$$

Equation 3.6 is the position of point C with respect to point B. $l_{BC}$ is the length of the link connecting points B and C (link BC), and φ is the angle $\vec{R}_{C/B}$ (link BC) makes with the horizontal in the i-j coordinate system. Point C can only translate along the hydraulic piston's line of action (15˚ from vertical). Equations 3.7 and 3.8 are the velocity and acceleration of point C with respect to point B. $\dot{\varphi}$ is the angular velocity and $\ddot{\varphi}$ is the angular acceleration of link BC.

$$\vec{R}_{\mathrm{C/B}} = \left(l_{bc}\cos\phi\right)\hat{i} + (l_{bc}\sin\phi)\,j \tag{3.6}$$

$$\vec{v}_{\mathrm{C/B}} = \tfrac{d}{dt}\vec{R}_{\mathrm{C/B}} = (-l_{bc}\dot{\phi}\sin\phi)\hat{i} + (l_{bc}\dot{\phi}\cos\phi)\,j \tag{3.7}$$

$$\vec{a}_{\mathrm{C/B}} = \tfrac{d}{dt}\vec{v}_{\mathrm{C/B}} = (-l_{bc}\ddot{\phi}\sin\phi - l_{bc}\dot{\phi}^2\cos\phi)\hat{i} + (l_{bc}\ddot{\phi}\cos\phi - l_{bc}\dot{\phi}^2\sin\phi)\,j \tag{3.8}$$

Equation 3.9 is the position of point C relative to point A. Equations 3.10 and 3.11 are the velocity and acceleration of point C relative to point A.

$$\vec{R}_{C/A} = \vec{R}_{C/B} + \vec{R}_{B/A}$$
$$= (l_{ab}\cos(\theta + c_1) + l_{bc}\cos\phi)\hat{i} + (l_{ab}\sin(\theta + c_1) + l_{bc}\sin\phi)\, j \tag{3.9}$$

$$\vec{v}_{C/A} = \left(-l_{ab}\dot{\theta}\sin(\theta + c_1) - l_{bc}\dot{\phi}\sin\phi\right)\hat{i} + \left(l_{ab}\dot{\theta}\cos(\theta + c_1) + l_{bc}\dot{\phi}\cos\phi\right) j \tag{3.10}$$

$$\bar{a}_{C/A} = \left(-l_{ab}\ddot{\theta}\sin(\theta + c_1) - l_{ab}\dot{\theta}^2\cos(\theta + c_1) - l_{bc}\ddot{\phi}\sin\phi - l_{bc}\dot{\phi}^2\cos\phi\right)\hat{i} +$$
$$\left(l_{ab}\ddot{\theta}\cos(\theta + c_1) - l_{ab}\dot{\theta}^2\sin(\theta + c_1) + l_{bc}\ddot{\phi}\cos\phi - l_{bc}\dot{\phi}^2\sin\phi\right) j \tag{3.11}$$

If the upper link, where the i-j coordinate system is fixed, is at an angle, $\alpha$ (angle of the thigh to vertical), the new coordinates of points B and C can be found in the i-j coordinate system (coordinate system fixed to the upper link), or converted to a coordinate system where j' (vertical) aligns with gravity (i'-j' coordinate system) (Figure 3.5). The coordinates of points B and C in the i'-j' (primed) coordinate system can be found via a rotation matrix (equation 3.12) [53]

$$\begin{bmatrix} i' \\ j' \end{bmatrix} = \begin{bmatrix} \cos\alpha & -\sin\alpha \\ \sin\alpha & \cos\alpha \end{bmatrix} \begin{bmatrix} \hat{i} \\ j \end{bmatrix} \tag{3.12}$$

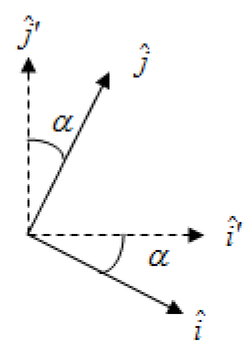


Figure 3.5: Diagram of i-j coordinate system rotated at an angle α to the vertical.

### 3.3.2.1 Velocity polygon

Determining the velocity and acceleration in the above analysis requires the angular velocity and acceleration of link BC ($\dot{\varphi}$ and $\ddot{\varphi}$) to be known. This is used to determine the linear velocity of point C for a given knee joint angular velocity ($\dot{\theta}$) [54]. Knee joint angular velocity is defined as the angular velocity of link AB. Figure 3.6 is a diagram of points A, B and C (identical to the previous analysis) and the position vector loop. Point D is a fixed point placed on the axis along which point C translates (dotted line), where point A would perpendicularly intersect this axis. Points A and D are fixed, and point B moves in a circle around point A. Equation 3.13 is the vector loop equation and equation 3.14 is the time derivative of the vector loop.

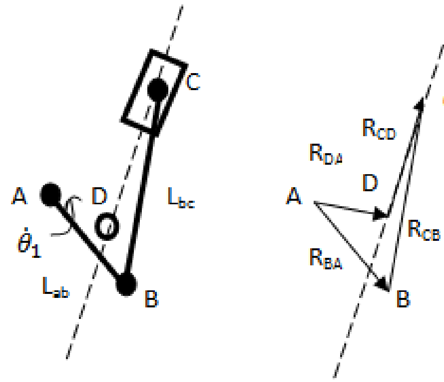


Figure 3.6: Position vector loop used for the velocity polygon analysis.

$$\vec{R}_{C/B} + \vec{R}_{B/A} = \vec{R}_{C/D} + \vec{R}_{D/A} \tag{3.13}$$

$$\vec{v}_{C/B} + \vec{v}_{B/A} = \vec{v}_{C/D} + \vec{v}_{D/A} \tag{3.14}$$

The position vector $\vec{R}_{D/A}$ is between two fixed points, therefore the velocity of point D with respect to point A ($\vec{v}_{D/A}$) is zero. The position vectors $\vec{R}_{B/A}$ and $\vec{R}_{C/B}$ represent rigid links (constant length), therefore $\vec{v}_{B/A}$ and $\vec{v}_{C/B}$ can only have tangential velocity components (the directions of $\vec{v}_{B/A}$ and $\vec{v}_{C/B}$ are perpendicular to the position vectors $\vec{R}_{B/A}$ and $\vec{R}_{C/B}$, respectively). Equation 3.15 is the equation for the velocity of joint B with respect to A (link AB). Equation 3.14 can then be simplified to equation 3.16, as shown in Figure 3.7.

$$v_{B/A} = \dot{\theta}_1 R_{B/A} \tag{3.15}$$

$$\vec{v}_{C/D} = \vec{v}_{B/A} + \vec{v}_{C/B} \tag{3.16}$$

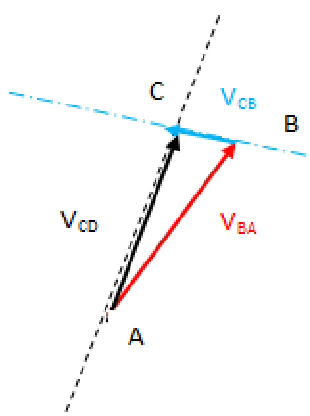


Figure 3.7: Velocity polygon to determine piston linear velocity for a given angular velocity.

The tangential velocity position and direction for link AB, velocity path for point C with respect to B (perpendicular to link BC), and $\vec{v}_{C/D}$ path are known. The orientation of link BC can be determined for any knee angle from the previous analysis. Geometry can then be used to solve for the magnitudes of vectors $\vec{v}_{C/D}$ and $\vec{v}_{C/B}$. Equation 3.17 is used to determine the velocity of link C with respect to B (angular velocity of link BC, $\dot{\varphi}$ ).

$$\dot{\varphi} = \frac{\left|\vec{v}_{C/B}\right|}{\left|\vec{R}_{C/B}\right|} \tag{3.17}$$

3.3.2.2 Acceleration polygon

The piston's linear acceleration (point C) can be determined for a known knee angular velocity and acceleration ($\dot{\theta}$, $\ddot{\theta}$) and link BC angular velocity ($\dot{\varphi}$) [54]. Equation 3.18 is the second time derivative of equation 3.13. Accelerations for both links can be divided into tangential and normal components (equation 3.19).

$$\vec{a}_{C/D} = \vec{a}_{B/A} + \vec{a}_{C/B} \tag{3.18}$$

$$\vec{a}_{C/D} = \vec{a}^{t}_{B/A} + \vec{a}^{n}_{B/A} + \vec{a}^{t}_{C/B} + \vec{a}^{n}_{C/B} \tag{3.19}$$

Equations (3.20) are for the normal acceleration components and equation 3.21 is the tangential acceleration component of link AB.

$$\begin{aligned} \vec{a}^{n}_{B/A} &= -\dot{\theta}^{2}\vec{R}_{B/A} \\ \vec{a}^{n}_{C/B} &= -\dot{\varphi}^{2}\vec{R}_{C/B} \end{aligned} \tag{3.20}$$

$$a^{t}_{B/A} = \ddot{\theta} R_{B/A} \tag{3.21}$$

The acceleration polygon's components are shown in Figure 3.8. Normal accelerations ( $\vec{a}^{n}_{B/A}$ and $\vec{a}^{n}_{C/B}$) are oriented along the link axes and tangential accelerations are perpendicular to the links. Figure 3.9 is the acceleration polygon used to determine the piston's linear acceleration (point C), as per equation 3.19. Knowing the A, B and C point positions, the acceleration polygon can be solved with trigonometry to determine the linear velocity of point C. Equation 3.22 calculates the angular acceleration of point C with respect to B (link BC).

$$\ddot{\varphi} = \frac{\left|\vec{a}_{C/B}\right|}{\left|\vec{R}_{C/B}\right|} \tag{3.22}$$

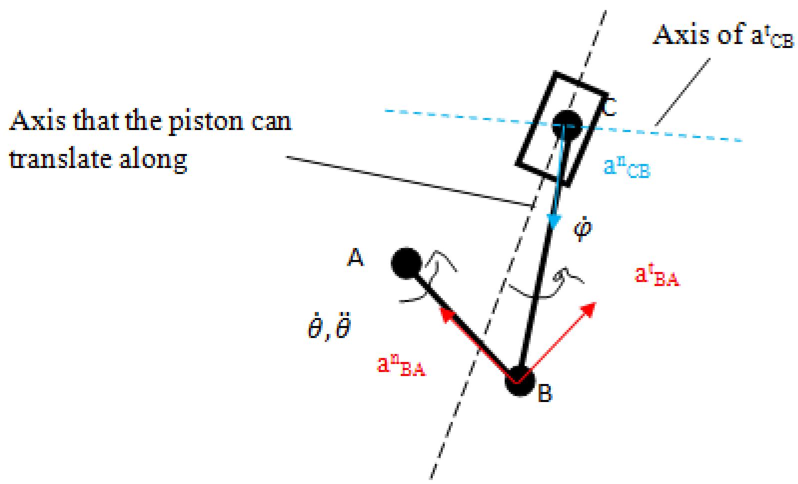


Figure 3.8: Acceleration polygon components.

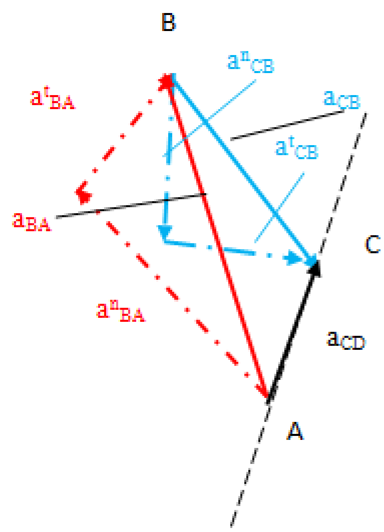


Figure 3.9: Acceleration polygon used to determine the linear acceleration of the piston for any given knee angular velocity and acceleration.

### 3.3.3 Force analysis

A quasi-static scenario was used for joint force analysis, with the variable resistance valve blocking fluid flow from the cylinder (i.e., this represents the largest possible forces because the cylinder has locked the joint from moving). The quasi-static analysis assumes that the effects of inertia of the links are ignored. The valve is in a closed position blocking fluid flow so the knee joint will remain motionless. This analysis determined forces on the joints and hydraulic cylinder. External flexion moments ($M_{Ext}$) were applied to the knee at angles ($\theta$) within the joint's ROM. Only knee flexion/extension was analyzed.

As shown in Figure 3.10, the moment $M_{Ext}$ is an external flexion moment acting at the knee via link AB. The knee joint angle ($\theta$) is 0° when fully extended. The link BC angle ($\varphi$) is determined from the previous analysis for a given knee angle.

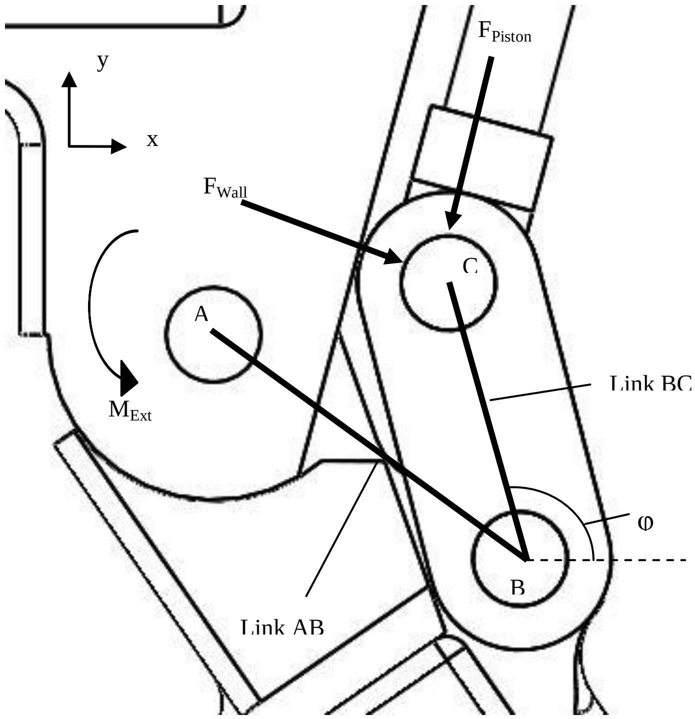


Figure 3.10: Joint force analysis diagram.

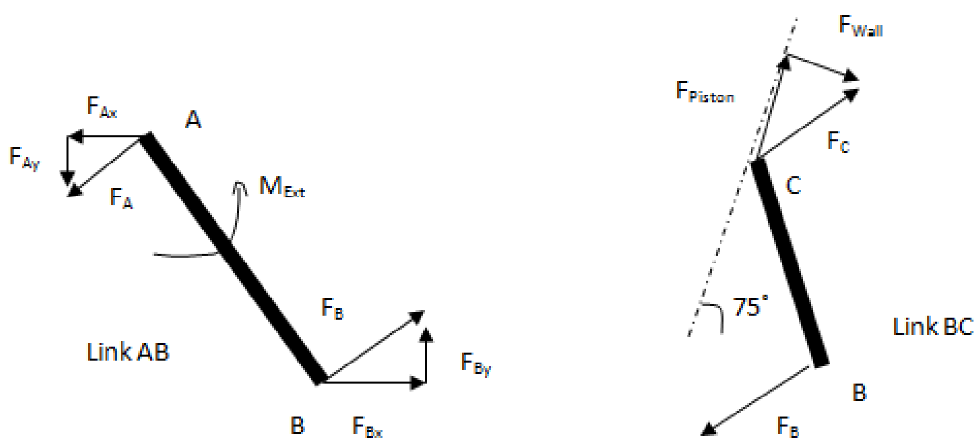


Figure 3.11: Free body diagrams of links AB and BC.

The links AB and BC can be separated into two free body diagrams (FBD), where each link is in equilibrium due to the quasi-static analysis (Figure 3.11). Equations 3.23 are the equilibrium force balances for link AB [55]. The internal forces at B ($F_B$) can be determined by solving these equations. The orientation and length of link AB are known ($l_{AB}$ = 25.4 mm).

$$
\begin{aligned}
\Sigma F_x &= 0 = F_{Ax} + F_{Bx} \\
\Sigma F_y &= 0 = F_{Ay} + F_{By} \\
\Sigma M_A &= 0 = M_{Ext} + l_{AB} F_B
\end{aligned}
\tag{3.23}
$$

$F_B$ is applied perpendicular to link AB (equation 3.24). $\theta$ is the knee angle. A 19.27˚ offset (angle from vertical of the link AB when the knee is fully extended, θ = 0) is added to the knee angle and 90˚ is added to the equation because $F_B$ is perpendicular to link AB.

$$\angle F_B = (\theta + 19.27^{\circ}) + 90^{\circ} \tag{3.24}$$

Since link BC is in equilibrium, the force at joint C ($F_C$) is equal and opposite to the force at joint B ($F_B$) (Figure 3.11). To determine the force that is transferred to the hydraulic cylinder ($F_{Piston}$) and the upper link ($F_{Wall}$), $F_C$ components need to be rotated +75˚ (equations 3.25).

$$
\begin{aligned}
F_{Piston} &= F_C \cos(75 - \angle F_B) \\
F_{Wall} &= F_C \sin(75 - \angle F_B)
\end{aligned}
\tag{3.25}
$$

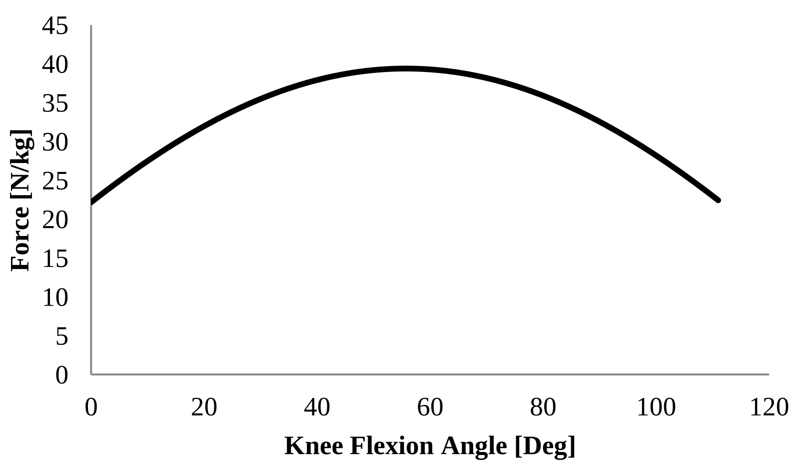


Figure 3.12: Normalized force on the hydraulic cylinder over the orthotic joint’s ROM.

Normalized piston forces due to normalized external knee flexion moments (Nm/kg) throughout the knee ROM (0-112˚) are shown in Figure 3.12. The highest piston force occurs at 56˚ knee flexion.

### 3.3.4 Component strengths

3.3.4.1 Hydraulic cylinder

The Vektek mini threaded 20-0105-07 hydraulic cylinder was used for the OWS design. This cylinder has a maximum operating pressure of 34.47 MPa (5000 psi), or a maximum force on the cylinder of 4.63 kN (980 lb) (Appendix B). The largest force on the piston occurs when the joint is locked at 56˚ (39.37 N/kg) (peak of graph in Figure 3.12); therefore, the maximum external knee moment for this cylinder is approximately 118 Nm. Maximum external knee moments during level ground walking are approximately 1.0 Nm/kg [14] and occur during the loading response and mid-stance sub phases. Since knee flexion during this portion of the gait cycle reaches approximately 25˚, the cylinder could resist an external knee moment of over 140 Nm. Therefore, the cylinder can withstand external knee moments during level ground walking for individuals that weigh up to 100 kg.

For stair descent, a large range of maximum external knee flexion moments have been reported in the literature (section 2.1.2). This maximum occurs during the single leg support. While larger cylinder loads are calculated with the static scenario, the valve will not be in a locked position during stair descent, thereby reducing the cylinder's load bearing requirements.

3.3.4.2 Pins

The joint pins must support large forces. For points A, B and C, the pin's diameter is 6.35 mm. From the analysis, the largest pin force would equal $F_B$. Equation 3.26 is the formula for shear stress, where $V$ is the internal resultant shear force, $A$ is the pin's cross sectional area, and $\tau$ is the shear stress. The joint is a double lap joint (two shear surfaces) therefore $V = F_B / 2$ . Equation 3.27 is the formula for allowable shear stress. F.S. is the factor of safety, $\tau_{Fail}$ is the failure shear stress, and $\tau_{Allow}$ is the allowable shear stress [55].

$$\tau = \frac{V}{A} \tag{3.26}$$

$$F.S. = \frac{\tau_{Fail}}{\tau_{Allow}} \tag{3.27}$$

To determine the pin's maximum shear force, these formulas can be combined to solve for $V \ \left(F_B / 2\right)$. The 4140 cold rolled steel used for the pins has an approximate $\tau_{Fail}$ of 249 MPa [56]. If a factor of safety of 2 is used, the allowable shear force on the joint would be 3.94 kN, or the largest allowable force on the joints would be 7.89 kN. Therefore, the joints should not fail during normal loading scenarios.

#### 3.3.4.3 Joint links

Analyses using SolidWorks (Dassault Systèmes, Waltham, MA) [57] simulation tools were performed on the upper link, lower link, and piston rod connection link to determine if there were any failure points in the design. A simulation example is shown in Figure 3.13. All links where machined with 4340 steel. Loads were applied to the components where large forces may occur. No material failures were predicted due to knee joint loading sagittal plane for individuals with a mass greater than 100 kg. The hydraulic cylinder would exceed its maximum operating pressure before material failure would occur in the links.

Large forces are only expected for flexion/extension because KAFO orientation during movement results in lower forces in the coronal (adduction/abduction) and transverse (internal rotation) planes. Simulated forces were applied to the joint links medial and lateral sides, where the uprights connect, to determine side loading effects on the joint. All the links were able to withstand forces up to 4000 N without material failure or significant deformation. The 4000 N force is much large than what would be expected from the side. The joint links should withstand perpendicular forces during walking and stair descent.

#### 3.3.4.4 Future joint modifications

To reduce the joint's weight, a hole was cut in the upper link model and SolidWorks simulations were performed to ensure the hole did not affect the upper link's strength (Figure 3.13). The same SolidWorks simulations were performed on the upper link with the hole as performed in section 3.3.4.3. The link was able to withstand forces up to 4000 N without material failure. The hole in the upper link reduced joint weight by 12.5 grams. The modified upper link technical drawing is found in Appendix A.

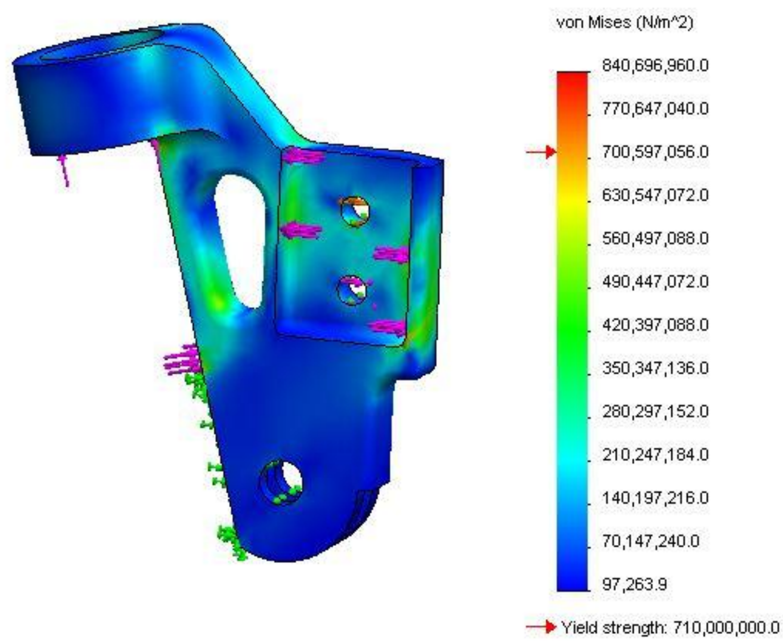


Figure 3.13: SolidWorks simulation of the upper link with the hole cut to reduce the weight.

## 3.4 Hydraulic circuit design

### 3.4.1 Criteria

The hydraulic circuit requires the following functions to meet the level, stairs, and sitting design criteria:

- A method for controlling knee joint flexion, with open (free flexion), closed (no flexion), and variable resistance (controlled flexion) settings to control fluid flow.
- A separate fluid path that bypasses the variable flow valve, allowing free knee extension.
- A fluid reservoir after the cylinder and variable flow valve. The reservoir must adapt to increasing fluid volume during joint flexion (compressed cylinder) and decreases during extension.
- Channels to fill the circuit with hydraulic fluid and remove air bubbles.

### 3.4.2 Circuit design

Figure 3.14 illustrates the hydraulic circuit's main components. During joint flexion, hydraulic fluid flows from the cylinder, through the variable flow valve, and into the reservoir. Fluid cannot flow from the cylinder, through the check valve, to the reservoir, so all fluid must pass through the variable flow valve. This valve controls fluid flow, and thus controls knee joint flexion. The check valve only allows fluid to move from the reservoir to the cylinder, bypassing the variable flow valve and allowing free knee extension even when the variable flow valve is closed. The reservoir must expand with the fluid's changing volume.

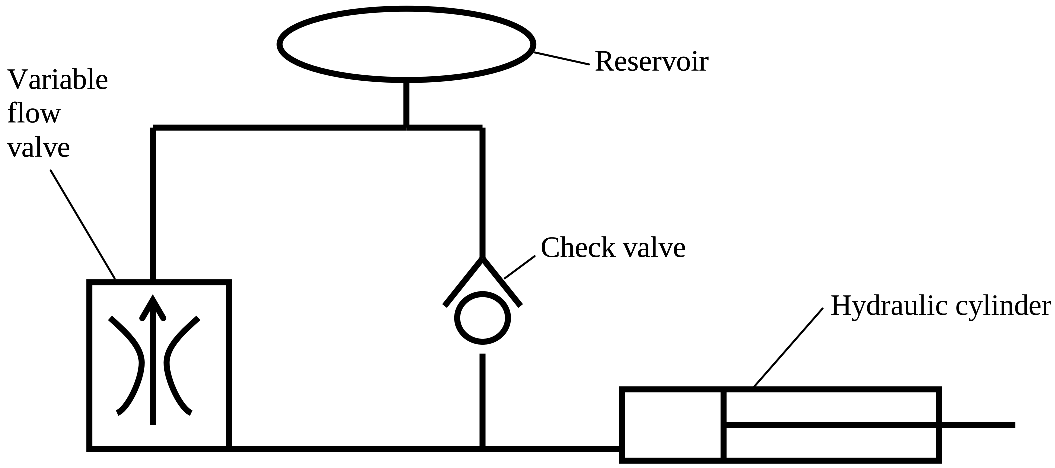


Figure 3.14: Hydraulic circuit diagram.

The circuit has high and low pressure sides. High pressures will occur between the cylinder and the check and variable resistance valves when a moment is applied to the joint and the variable resistance valve restricts or stops fluid flow. The circuit between the reservoir and the two valves will only experience slight back-pressure from the expandable reservoir.

### 3.4.3 Block design

The hydraulic circuit was designed with a high strength aluminum alloy L168 – 2014A block (50 mm x 40 mm x 17.5 mm). As shown in Figure 3.15 and Appendix A, a female tapped hole (M12x1.25) connects the cylinder with the block. A custom made male-male connection part threads between the cylinder and the block. The reservoir connection is a female tapped hole (M12x1.25). The check valve is positioned in an M8x1.0 female tapped hole. The check valve requires threading to position the valve seat, and is further explained in section 3.6. The ends of the fill points / plug channels are tapped (M5x0.8).

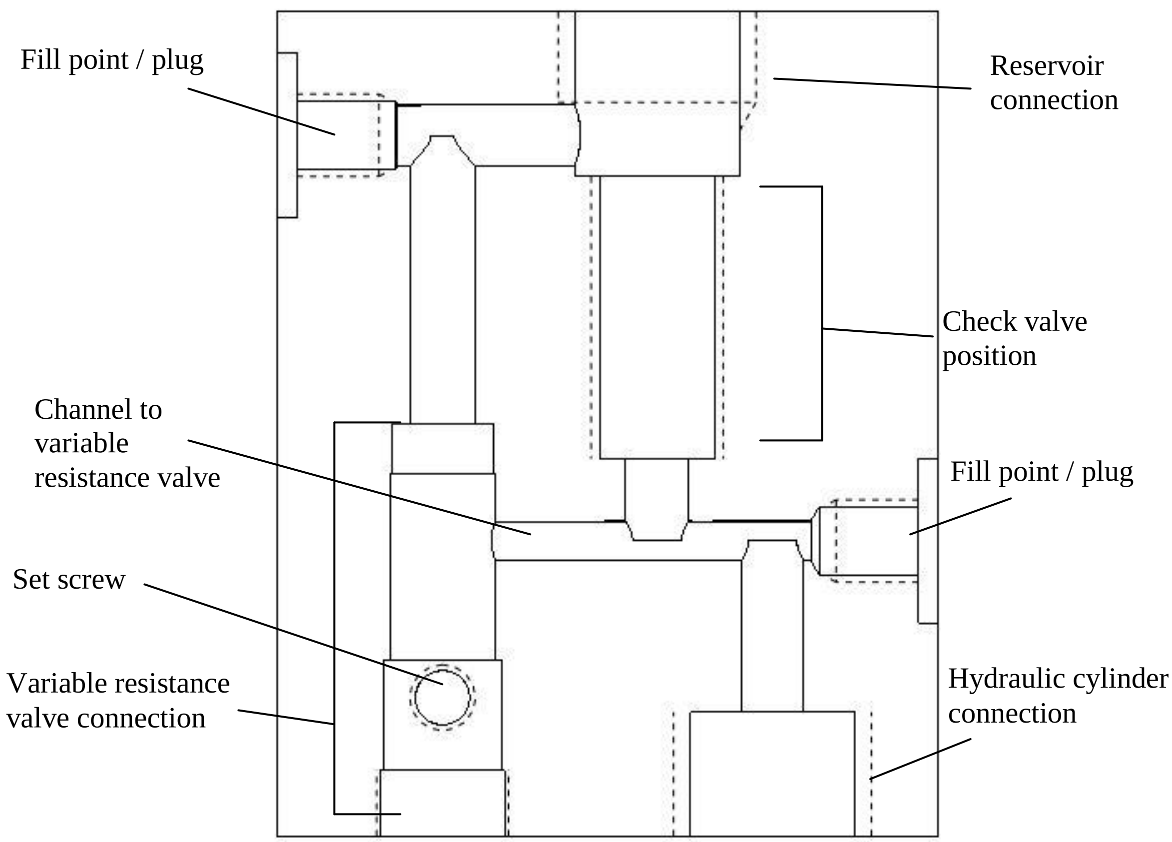


Figure 3.15: Hydraulic circuit block design.

The variable resistance valve connection channel requires precise machining for the valve to function correctly. The valve threads into the block through an M8x0.75 hole. A dog point set screw is required for valve positioning, and is a tapped M4x0.7 hole. The cut where the valve meets the channel leading to the valve requires very precise machining. This is where the variable resistance valve rotates and fluid passes through the valve, allowing the valve to rotate but preventing fluid from escaping between the valve and block. The variable resistance valve channel has a 2.4 mm diameter.

L168 – 2014A aluminum alloy was selected for the design to reduce weight. SolidWorks simulations were performed on the block to verify that this grade of aluminum would withstand the pressures associated with the design. Static simulations were performed where the holes on the high pressure side of the circuit were subjected to a maximum pressure of 34.47 MPa (5000 psi). No displacements were observed and the stresses due to the pressures did not surpass the aluminum yield strength.

## 3.5 Blatchford variable resistance valve

### 3.5.1 Original valve design

The variable resistance valve in this thesis was based on the variable flow hydraulic valve from Endolite's Elan prosthetic ankle (Figure 3.16). This valve provides variable resistances for the prosthetic ankle and is used successfully in practice. The valve uses hydraulic oil as the working fluid and is a compact design (10 mm diameter, 72 mm length) that could be integrated into the new orthotic knee design without having to greatly increase the joint's overall size envelope. The valve changes hydraulic flow via a motor assembly (DC motor, gear box, encoder) that turns the valve to expose different size holes to the input channel. Since these holes are sized for a prosthetic ankle, different hole sizes were needed for the knee orthosis application.

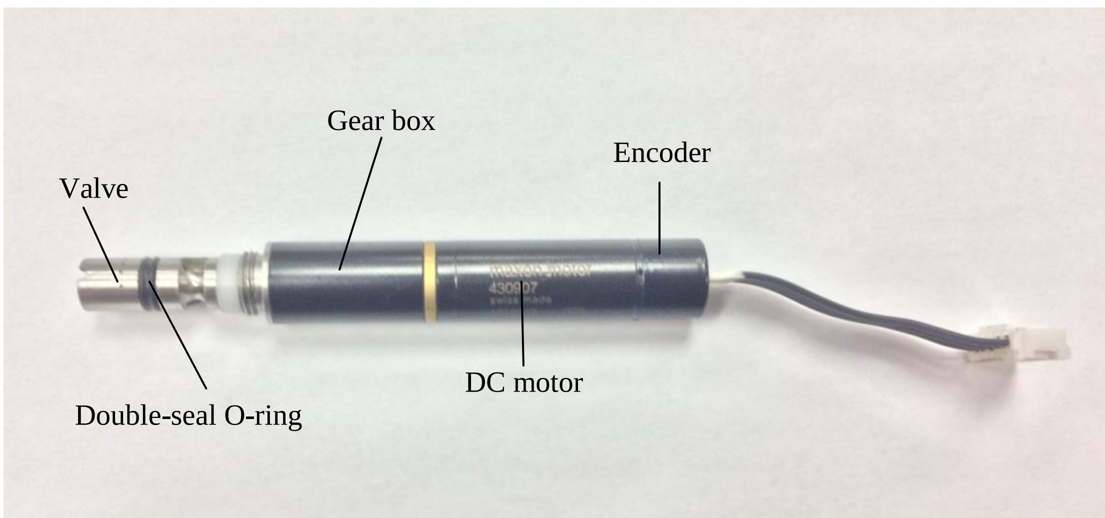


Figure 3.16: Blatchford's variable resistance valve.

Hydraulic oil flows from an input channel, through the holes on the valve's side, and exits through the valve's top (Figure 3.17). As the valve rotates axially, different holes are positioned in front of the channel to allow more or less fluid flow. A range slot is used to create a mechanical datum that is used by the control system to determine a consistent zero position for reliable rotation to valve hole positions.

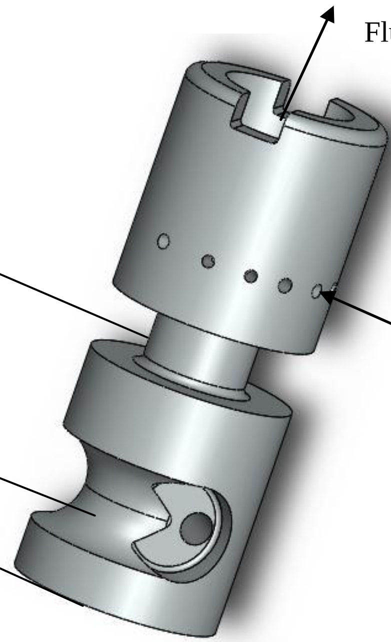


Figure 3.17: SolidWorks model of the valve portion of the variable resistance valve.

To use Blatchford's variable resistance valve with the orthotic knee joint, new hole sizes and patterns that matched the design criteria were determined. The motor assembly was also analyzed in relation to the orthotic knee joint requirements.

### 3.5.2 Hole pattern selection

An orthotic variable resistance valve requires closed and open settings for level ground walking: open to provide free knee flexion during swing and closed to stop knee flexion throughout stance. The joint also requires knee joint flexion resistance settings that allow users of different weights (50-100 kg) to safely descend stairs and sit. The goal was to not alter the valve's size, but only to change the hole pattern. This would result in cost savings, since the valve is currently in production, and reliability, since the valve design has already passed relevant mechanical and clinical tests.

Multiple methods were explored for determining the correct hole sizes. The volumetric flow rate equation (3.28) states that flow rate ($Q$) is equal to the flow's cross-sectional area ($A$) multiplied by the fluid's velocity ($v$).

$$Q_1 = A_1 v_1 = A_2 v_2 = Q_2 \tag{3.28}$$

Volumetric flow rate stays constant throughout a system. This equation does not account for losses due to sudden expansions and contractions or due to entrance and exit from a valve. Major and minor loss pipe system equations are not valid for this problem because these equations require fluid flow to be at a steady state and fully developed [58]. Since the piston's stroke is short and the piston will not move in constant motion, the flow will never be fully developed.

Piping system and volumetric flow rate equations were used to obtain an initial estimate of the hole sizes required for the hole pattern. However, it was determined that an experimental method was the best method of determining the required hole sizes. A physical experiment would account for losses due to changes in geometry of the channel that could not be calculated with the equations, and would also use the OWS joint to allow for a more realistic loading scenario.

3.5.2.1 Hole selection experiment

A physical experiment was designed to show the effects of fluid flowing from the hydraulic cylinder through different holes sizes, during a realistic loading scenario. This experiment accounted for major and minor losses due to the change in channel geometry (expansions, contractions and elbows in the channel from the hydraulic cylinder to the exit of the variable resistance valve hole), as well as friction in the cylinder and joint (there will be some friction from the OWS joint and the hydraulic cylinder that could not be accounted for in fluid equations). The experimental setup is shown in Figure 3.18.

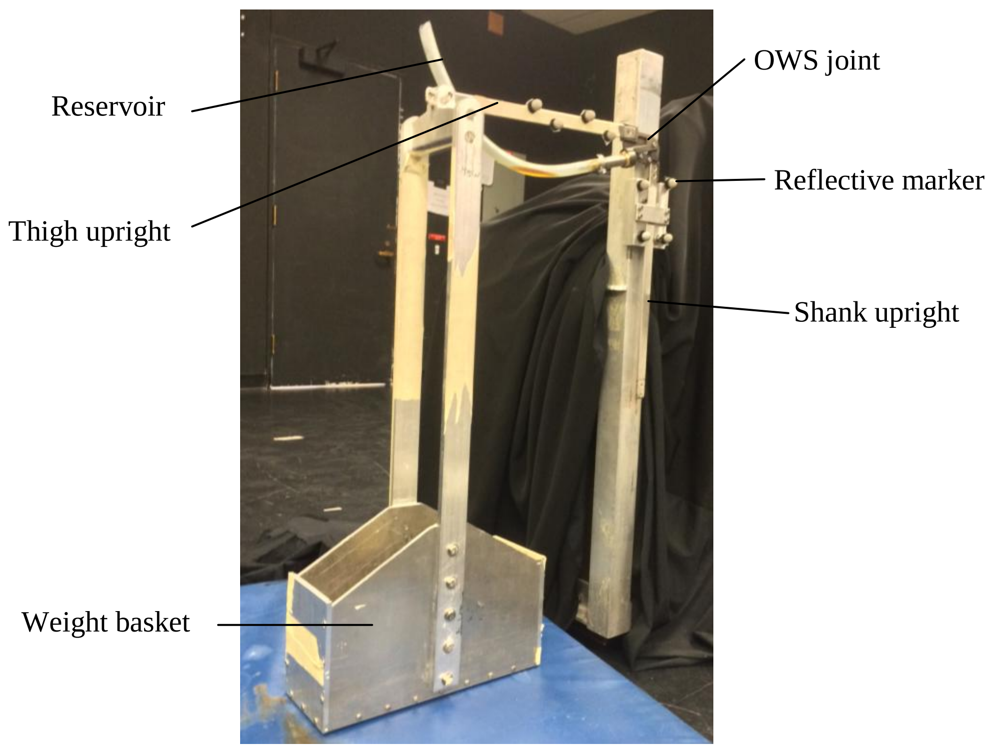


Figure 3.18: Testing setup for the hole selection experiment.

Standard orthotic steel uprights were attached to the OWS joint. The joint was held vertical by fixing the shank upright to a heavy bench. A weight basket was attached to the distal end of the thigh upright, 37.5 cm from the joint centre. Four different weights were used: 51 N, 111 N, 168 N, and 200 N. A custom-made orifice part was machined from brass and threaded onto the hydraulic cylinder (Figure 3.19). Hydraulic fluid was pushed out of the cylinder, through the orifice part, and into a reservoir. The orifice exit hole was re-drilled after each test to increase the diameter. Nine orifice sizes were tested between 0.25-2.00 mm in diameter (Table 3.3).

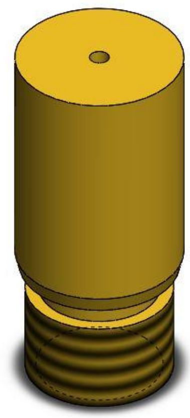

Figure 3.19: Custom made orifice part with 1.5 mm diameter exit hole.

The cylinder was filled with Turbospec 320 hydraulic oil (80 weight gear oil that was used in the OWS-Speed joint) and the piston was cycled multiple times until no air bubbles emerged from the exit orifice. Upright position was measured by an 8-camera motion capture system (Vicon Inc., Oxford, UK) in the TOHRC Rehabilitation Technology Lab (RTL). Eight reflective markers were adhered to the shank mounting arm and the thigh upright and marker movement was tracked at 100 Hz. The weight basket was filled with a known mass and dropped from a joint angle of approximately 30˚ to 95˚. For the nine orifice sizes, three drops per weight were collected (12 trials per orifice size).

Marker data were reconstructed and labelled using the Vicon Nexus (Vicon Inc., Oxford, UK) software and analyzed using Visual3D (C-Motion Inc., Rockville, MD). Marker data was filtered using a $4^{th}$ order low pass Butterworth filter with a cut-off frequency of 10 Hz. Joint angular position, velocity, and travel time were calculated. Figure 3.20 and Figure 3.21 show the time for the joint to flex 50˚ (40˚ - 90˚), for each hole size, at the four basket weights. Figure 3.20 shows the results for the smallest three hole sizes (0.25 mm, 0.37 mm, and 0.51 mm) and Figure 3.21 shows the results for larger six hole sizes (0.74 mm, 0.99 mm, 1.19 mm, 1.50 mm, 1.70 mm, and 2.00 mm). The times were averaged over the three trials at each weight.

Table 3.3: Orifice and drill bit sizes for the hole selection test.

| Hole | Drill Size | Decimal Equivalent (mm) |
|---|---|---|
| 1 | 0.25 mm | 0.25 |
| 2 | #79 | 0.37 |
| 3 | #76 | 0.51 |
| 4 | #69 | 0.74 |
| 5 | #61 | 0.99 |
| 6 | 3/64 in | 1.19 |
| 7 | 1.50 mm | 1.50 |
| 8 | #51 | 1.70 |
| 9 | 2.00 mm | 2.00 |

Hole sizes were determined based on angular position, flexion time, and moment applied to the joint by the weight basket. The joint's resistance settings were designed to support 50-100 kg individuals for 0.7 - 1.0 seconds during the stance phase of stair descent (approximately 65˚ of knee flexion) on the braced limb (Table 3.1). The time for the joint to flex 50˚ for each hole diameter tested was known (Figure 3.20 and Figure 3.21). With the known moment applied to the joint by the weight basket, the holes sizes were approximated that would support individuals during stair descents.

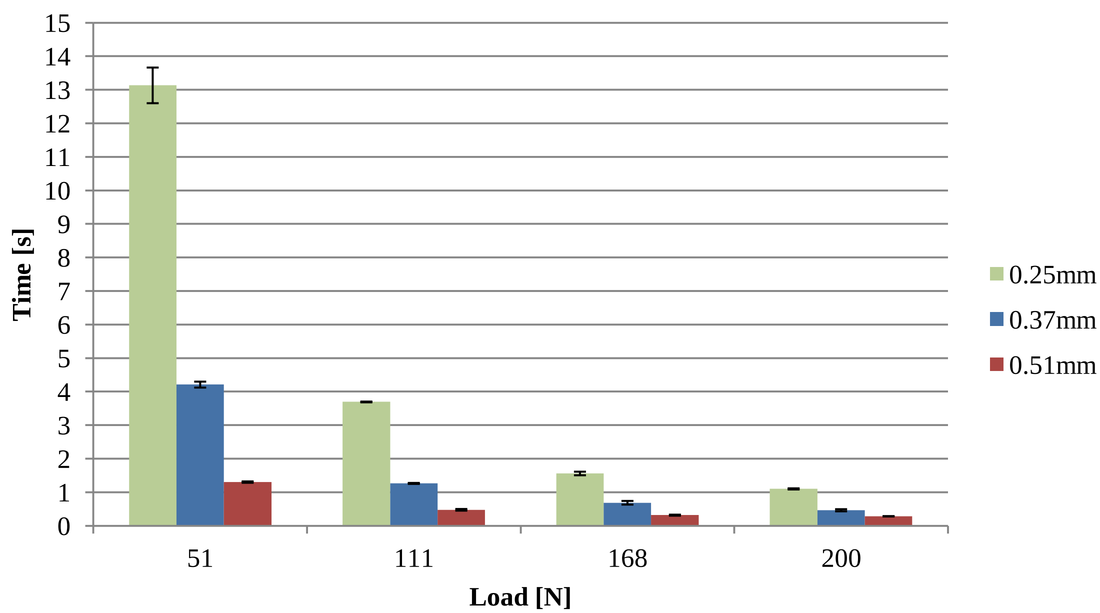


Figure 3.20: Time for the joint to flex 50˚ (40˚-90˚) for the 0.25 mm, 0.37 mm and 0.51 mm holes.

The 168 N and 200 N drop tests applied external moments to the orthotic joint that would be similar to the moments applied to a knee joint during stair descent. Hole diameters larger than 0.51 mm did not resist joint flexion that would support the user. Hole diameters of 0.25 mm, 0.37 mm, and 0.51 mm resisted joint flexion. For heavier individuals it would be beneficial to have a setting with a hole diameter smaller than 0.25 mm to further resist flexion. Hole sizes between 0.20 mm – 0.50 mm were selected for the resistance settings.

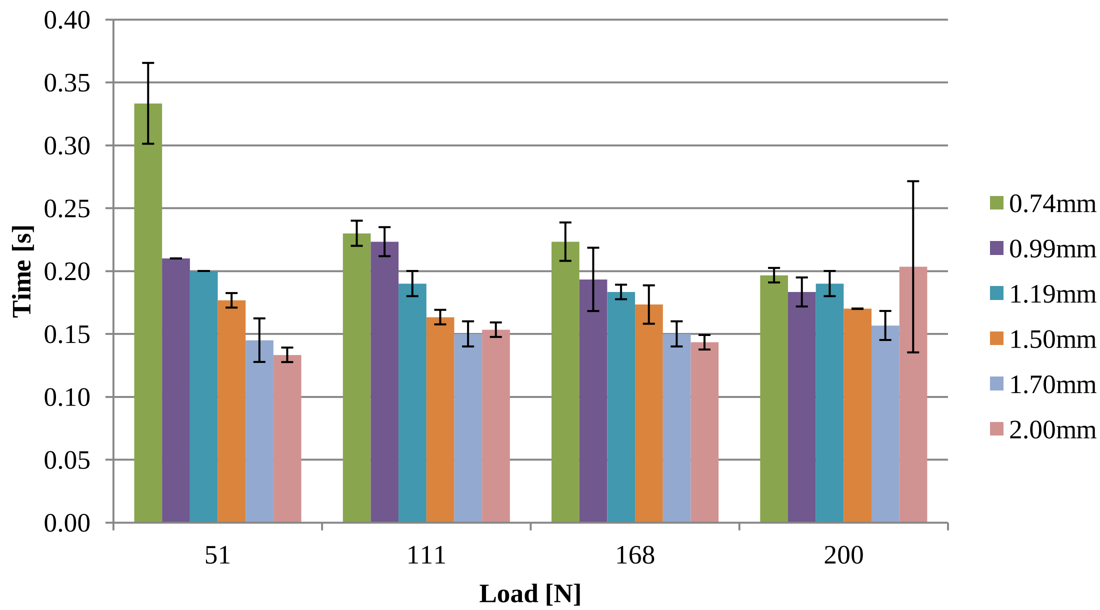


Figure 3.21: Time for the joint to flex 50˚ (40˚-90˚) for the 0.74 mm, 0.99 mm, 1.19 mm, 1.50 mm, 1.70 mm, and the 2.00 mm holes.

The value's open setting should allow the joint to flex freely with any input moment. Instantaneous angular velocities at joint angles 30˚, 45 ˚, 60 ˚, 75 ˚, and 90˚ were averaged and standard deviations were calculated for the 51 N drop test (Table 3.4). Standard deviations were higher than expected since the weight basket was dropped by hand, and therefore not dropped from exactly the same angle on every trial.

The joint's angular velocity increased with increased hole diameter. Hole sizes above 1.50 mm (holes 7-9) achieved angular velocities greater than 300˚/s with relatively low moments (51 N basket) applied to the joint. If the channel leading to the variable resistance valve has a diameter of 2.4 mm (the same diameter used in the Elan prosthetic ankle) joint flexion should not be restricted. The valve's open setting was selected have a diameter of 2.25 mm, which is a standard drill size slightly smaller than the channel leading to the valve.

Table 3.4: Instantaneous joint angular velocity averages and standard deviations at joint angles of 30˚, 45˚, 60˚, 75˚, and 90˚for the 51 N drop tests.

| **Hole (mm)** | **Angular Velocity at Specified Angle [˚/s]** | | | | |
|---|---|---|---|---|---|
| | **30˚** | **45˚** | **60˚** | **75˚** | **90˚** |
| 0.25 | 7.0 (1.4) | 5.8 (1.0) | 3.4 (1.2) | 5.0 (2.0) | 8.1 (1.4) |
| 0.37 | 18.6 (2.3) | 20.7 (1.5) | 16.9 (3.3) | 15.2 (1.1) | 20.5 (1.9) |
| 0.51 | 55.5 (12.4) | 47.3 (5.1) | 30.6 (1.7) | 46.0 (1.4) | 33.6 (6.3) |
| 0.74 | 109.2 (31.3) | 146.0 (33.3) | 152.4 (10.6) | 140.4 (8.0) | 142.6 (3.5) |
| 0.99 | 153.0 (8.9) | 220.6 (5.8) | 234.6 (8.1) | 243.6 (10.9) | 250.1 (2.7) |
| 1.19 | 93.2 (29.4) | 206.0 (6.2) | 247.4 (5.7) | 276.3 (1.3) | 298.8 (16.2) |
| 1.50 | 149.4 (22.2) | 240.1 (13.9) | 274.3 (11.6) | 307.3 (15.8) | 319.2 (11.6) |
| 1.70 | 241.1 (55.5) | 313.5 (42.3) | 331.0 (45.8) | 339.9 (29.9) | 335.9 (15.5) |
| 2.00 | 261.4 (16.2) | 320.2 (18.7) | 349.5 (16.9) | 376.8 (18.8) | 356.3 (16.3) |

3.5.2.2 Hole pattern

The range slot (Figure 3.17) was modified to allow 222˚ of valve rotation, to increase the number of settings. The hole pattern was designed to have the closed setting as the zero position, followed by the "open" setting, to minimize switching time. This design allowed for six holes, "open" and five "resistance" holes for controlled knee flexion (Table 3.5).

Table 3.5: Hole diameters for the variable resistance valve.

| **Hole Number** | **Hole Diameter (mm)** |
|---|---|
| 1 | 2.25 |
| 2 | 0.50 |
| 3 | 0.35 |
| 4 | 0.30 |
| 5 | 0.25 |
| 6 | 0.20 |

The "resistance" settings were designed so the valve could turn to expose a single hole or two holes to the channel leading to the variable resistance valve (2.4 mm in diameter). This provided 11 settings (closed, open, 9 varying resistance settings). Table 3.6 displays the setting number, holes used for the setting, total area of the holes for the setting, and the angular position displayed in degrees from the valve's zero position (mechanical stop).

Table 3.6: Hole pattern for variable resistance valve.

| Setting | Hole Number | Total Area ($mm^2$) | Angle from Zero Position (°) |
|---|---|---|---|
| 0 | No hole | 0.00 | 0.00 |
| 1 | 1 | 3.98 | 48.58 |
| 2 | 2 | 0.20 | 101.08 |
| 3 | 2,3 | 0.29 | 116.08 |
| 4 | 3 | 0.10 | 131.08 |
| 5 | 3,4 | 0.17 | 146.08 |
| 6 | 4 | 0.07 | 161.08 |
| 7 | 4,5 | 0.12 | 176.08 |
| 8 | 5 | 0.05 | 191.08 |
| 9 | 5,6 | 0.08 | 206.08 |
| 10 | 6 | 0.03 | 221.08 |

### 3.5.3 Motor/gearbox/encoder

The valve requires a motor, gearbox, and encoder to rotate accurately. These parts are manufactured by Maxon Motor (Maxon Motor AG, Sachseln, Switzerland) and are pre-assembled. The valve (manufactured by Endolite) is attached to the output shaft of the gear box, which is rotated by the motor, and the encoder converts the angular position of the motor shaft to a digital code. The Endolite Elan prosthetic ankle uses the following components:

- Motor: DC electric motor (Part #118397) 10 mm outer diameter, 1.5W, 6V, 9880rpm
- Gearbox: Planetary Gearhead (Part #218417) 10 mm out diameter, 0.01-0.15 Nm, 1:256 gear reduction
- Encoder: (Part #138061) 12 counts/turn, 2 channel, quadrature encoder

The design for the motor/gearbox/encoder of the OWVS should be similar to the design of the prosthetic ankle to reduce costs, since the motor combination is already in production for the ankle. The 1:256 gear reduction requires the motor to rotate 256 times for 1 output shaft rotation (equation 3.29). The relationship between input and output rotational speed, and gear reduction is given by

$$\omega_{Output} = \frac{\omega_{Input}}{GR} \tag{3.29}$$

where the $\omega$ terms are the rotational speeds (rpm) for the input (motor) and output (gearbox shaft) and $GR$ is the gear reduction (the motor's number of turns to turn the gearbox once). In an ideal situation, where the motor rotates at 9880 rpm (no load speed), the gear box output shaft rotates at 38.59 rpm or 0.64 rps.

The joint will primarily switch between settings 1 and 2 (Table 3.6), which are approximately 50˚ apart. Approximately 0.22 s would be required to rotate 50˚ (50/360 of a rotation). For level ground walking, the desired switching time between the open and closed setting was less than 0.10 seconds, so the current motor gear assembly was too slow. Therefore, a Maxon #218417 gearbox with a 1:64 gear reduction was used in the orthotic knee application. This gear box works with the same motor and encoder. With the DC motor rotating at 9880 rpm the gear box's output shaft would rotate at 154.38 rpm (2.57 rps). Approximately 0.05 seconds would be required for the valve to rotate 50˚. Even if the valve were rotating at 75% of it's no load speed, the time to rotate 50˚ would be 0.07 seconds, which is faster than the desired time of 0.10 seconds.

The trade-off from increasing valve rotational speed is a decreased ability to control valve position. The 12 counts per turn quadrature encoder combines two sensing channels to register movements four times smaller than the pattern printed on the code disk [59], so the encoder registers 48 counts per turn of the motor. If the 1:64 gearbox is used, the motor would turn 64 times to rotate the gearbox once, therefore the encoder would have a count of 3072 per rotation of the valve (equation 3.30). The valve rotates 0.12˚ (1/3072 rotations) for every count; therefore, the valve position error is 0.12˚ for every count.

$$Counts_{Output} = GR * Counts_{Input} \tag{3.30}$$

With a 1:64 gearbox instead of a 1:256 gearbox, the valve's rotation speed increases by a factor of 4, but valve accuracy will decrease by a factor of 4. The 1:64 gearbox is able to achieve the required switching times, so a motor/gearbox using this gear reduction was selected. The accuracy of the motor/gearbox should be sufficient for this design as each motor encoder position is equal to 0.12˚ of rotation. Tests were performed to verify the time to rotate between various valve settings (section 4.1).

## 3.6 Check valve

A check valve provided free knee extension by bypassing the variable resistance valve. A 5 mm diameter stainless steel ball, a metric compression spring ($k_{spring}$ = 0.33 lb/mm or 1.47 N/mm), and a custom made seat were used. The spring holds the ball against the seat so that the valve is closed during flexion. If a pressure greater than the spring force is applied opposite to the spring, the valve opens and allows fluid to pass from the reservoir to the cylinder (Figure 3.22).

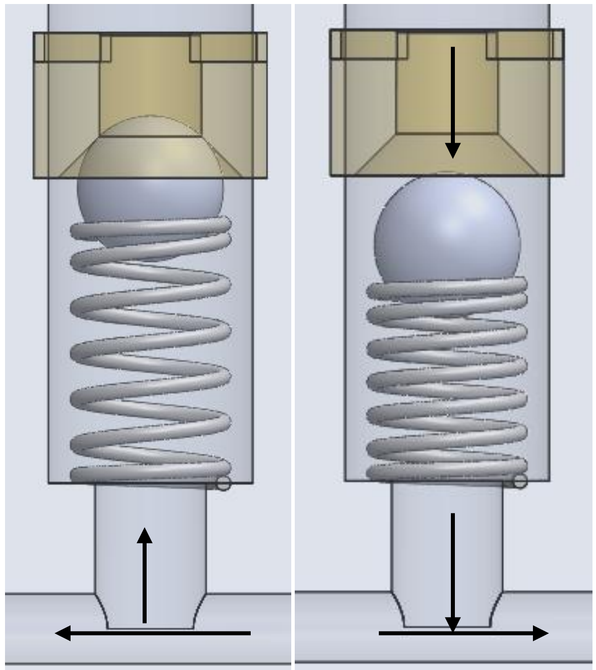

Figure 3.22: Check valve closed (left) and open (right). The valve is closed when the knee flexes and opens when the knee extends. Arrows indicate fluid flow direction.

Cracking pressure is the pressure required to open the check valve. A low cracking pressure is desirable so that the joint may quickly cycle between flexion and extension. The spring's purpose is to eliminate play in the valve, so when there is equal pressure on both sides the valve will default to flexion. The cracking pressure can be adjusted by threading the seat to change spring compression.

In a static situation where the valve is closed and fluid is not flowing, the force on the ball due to a difference in pressure must be greater than the spring's force to open the valve ($F_{Ball} > F_{Spring}$). The spring force is calculated using Hooke's Law ($F_{spring} = k_{spring} x$), where $k_{spring}$ is the spring's stiffness and $x$ is the distance the spring has been compressed.

The cracking pressure can then be calculated using equation 3.31,

$$P_{Cracking} > \frac{F_{Spring}}{A_{Ball}} \tag{3.31}$$

where $A_{Ball}$ is the sphere's cross sectional area used in the check valve. The cracking pressure is a linear function, depending on how far the seat has compressed the spring. If the spring is compressed by 2 mm, cracking pressure would be approximately 150 kPa. This low pressure should not interfere with check valve switching from flexion to extension.

The check valve has a conical seat, with an internal conical angle of 90˚ and with a 3.5 mm diameter through hole. The advantage of a conical design is that the ball self-centres when closing. The seat design with a 5 mm diameter ball implies that the seat contacts the ball at the cone's intersection and the through hole. This design yields a higher sealing force than having the ball contact tangent to the conical surface [60]. A steeper conical angle allows for easier alignment with the through hole, but more difficulty when releasing during reverse flow and reduced sealing quality. A 90˚ angle was selected, which commonly used in practice [60].

## 3.7 Additional components

This section discusses the additional components that were either manufactured or purchased to complete the OWVS.

### 3.7.1 Reservoir

The reservoir must be expandable, to collect fluid on the hydraulic circuit's low pressure side. The reservoir should not apply a large back pressure on the system that would cause the check valve to open. The reservoir's volume must be at least the hydraulic cylinders volume when fully expanded. The cylinder has a 2.41 $cm^3$ (0.147 cu. in) capacity.

A balloon style reservoir was selected for initial prototyping. A brass reservoir connection part was manufactured at the TOHRC machine shop and threaded into the hydraulic circuit block (M12x1.25). The connection part was designed with a lip at the reservoir end. Nozzle caps for caulking containers (Lee Valley Tools Ltd., Ottawa, Canada) [61]) were selected for the reservoir. These caps are made from thick natural latex, which should be appropriately durable for prototype testing, and the cap's volume was large enough when expanded. A more permanent reservoir will be designed after prototype testing is complete.

### 3.7.2 Case

The variable flow valve concentricity in the hydraulic circuit block is very important to the design so that the valve will rotate freely. A case was designed to protect the valve motor/gear assembly from accidental dislodgement (Appendix A). The case was designed to fit over the hydraulic circuit block and extend down to cover the variable resistance valve. The valve's control board can be mounted on the case. The case was made in ABS using the UP Plus 3D Printer (Tiertime Corp., NY, USA) [62].

### 3.7.3 Hardware

M5 machine screws, M5 pressure sealing washers (5000 psi), metric compression springs, and 5 mm diameter balls were ordered from McMaster-Carr (McMaster-Carr Supply Company, IL, USA) [63]. The parts can be seen in Figure 3.1, and technical drawings found in Appendix B.

## 3.8 Costs

The variable resistance prototype costs are shown in Table 3.7. The company or shop where each part was manufactured is also shown. Many of these costs would be decreased if the prototype were produced on a larger scale. The ordered parts (McMaster-Carr and Maxon Motors) would decrease in price with larger orders. Cost-effective methods of component manufacturing will be explored if the design proceeds to the manufacturing stage.

Table 3.7: Costs of Ottawalk-Variable Speed prototype. Table shows the part, cost and where the part was ordered or manufactured.

| Part | Source | Cost |
|---|---|---:|
| OWS Joint | TOHRC Machine Shop | $3375 CAD |
| Maxon Motor/Gearbox/Encoder | Maxon Motors | £150.00 GBP |
| Blatchford Valve | Blatchford Model Shop | £30.00 GBP |
| Hydraulic Circuit Block | Blatchford Model Shop | £60.00 GBP |
| Hydraulic Cylinder Adapter | TOHRC Machine Shop | $150.00 CAD |
| Reservoir Connection | TOHRC Machine Shop | $125.00 CAD |
| Check Valve Seat | TOHRC Machine Shop | $60.00 CAD |
| 5 mm Diameter Balls | McMaster-Carr | $7.89 (Pack of 100) USD |
| Metric Compression Spring | McMaster-Carr | $10.36 (Pack of 5) USD |
| M5 Machine Screws | McMaster-Carr | $6.88 (Pack of 50) USD |
| M5 Pressure Sealing Washers | McMaster-Carr | $15.50 (Pack of 10) USD |
| 3D Printed Case | Blatchford Model Shop | £0.50 GBP |

The total cost of the OWVS prototype was approximately $4200 CAD. The majority of the cost is for the manufacturing of the OWS joint at the TOHRC machine shop (Table 3.7). The new components added to the existing OWS joint cost approximately $810 CAD, which indicates that it is relatively inexpensive to convert existing OWS joints to the OWVS design. Other costs are associated with the valve control equipment. This includes a Bluetooth adapter, a printed circuit board, changer and interface cable. These components were used for testing the orthotic joint design (Chapter 4 and Chapter 5), and were supplied by Blatchford. The components cost approximately £100 GBP ($179 CAD), but were not designed specifically for the OWVS so were not included in the cost analysis.

# Chapter 4: Mechanical Testing

This chapter presents mechanical testing results from the variable resistance orthotic knee joint (OWVS). Three mechanical tests were performed on the joint to evaluate its performance.

Figure 4.1 is an image of the OWVS connected to the variable resistance valve control electronics. Blatchford provided the printed circuit board (PCB), batteries, Bluetooth adapter, and software to control the valve.

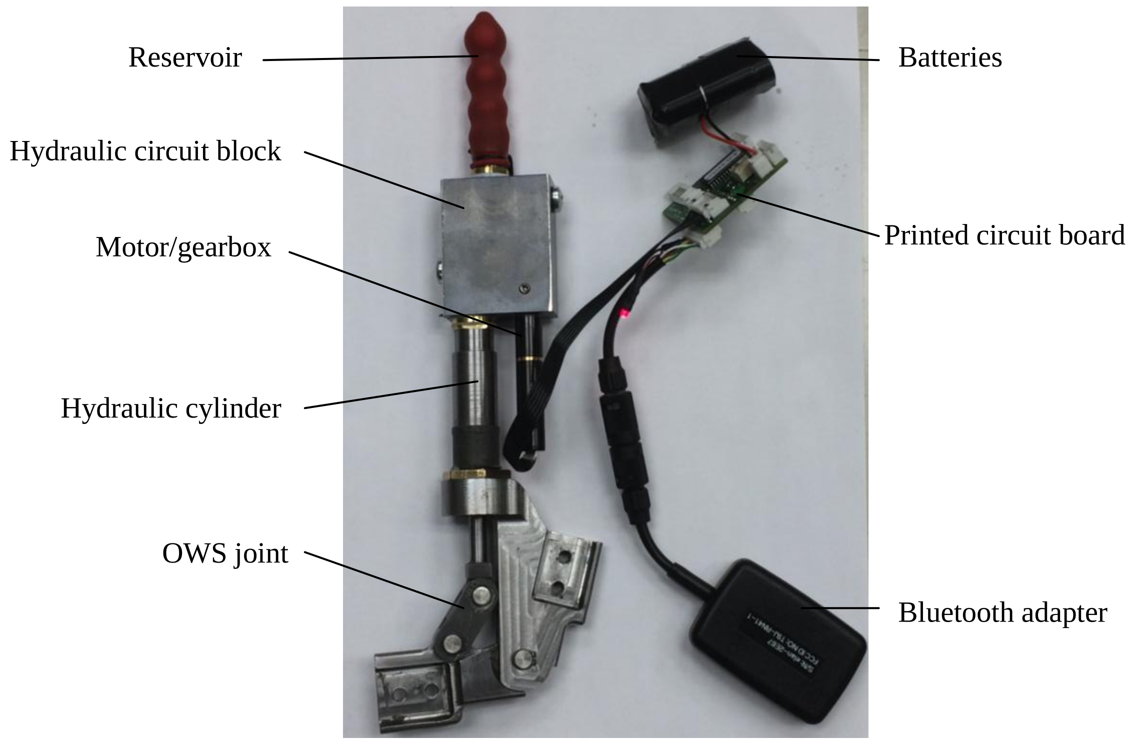


Figure 4.1: OWS joint, variable resistance valve, and control electronics.

The valve is controlled remotely with a computer via Bluetooth. As shown in Figure 4.2, the software contains buttons for the valve’s 11 settings. When a setting is selected, the valve rotates to the desired position. The software displays the current valve setting, time for the valve to rotate from the previous position to the current position (in milliseconds), motor encoder position demanded, and actual motor encoder position achieved.

The motor encoder counts 3072 positions per valve revolution, using the 1:64 gear reduction (section 3.5.3). Each count is equal to 0.12˚ of output shaft rotation. The software also graphically displays, in real time, the demanded motor encoder position and the actual motor encoder position (Figure 4.2). The yellow line on the graph is the reference line (the position demanded) and the green line is the actual valve position. The vertical line moves from the left to the right side of the screen, indicating the current valve position.

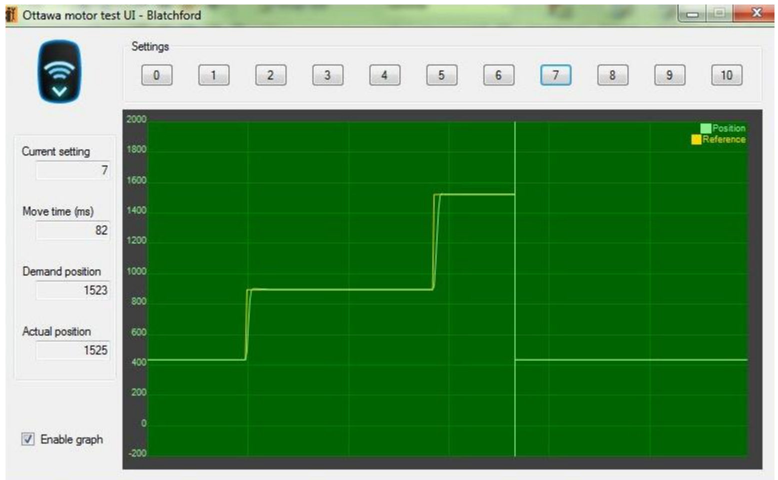


Figure 4.2: Software to control the variable resistance valve.

Table 4.1: Angle, encoder positions, and corrected encoder positions for the variable resistance valve.

| **Valve setting** | **Angle from zero position (˚)** | **Encoder position** | **Corrected encoder position** |
|---|---|---|---|
| 0 | 0.00 | 0 | 10 |
| 1 | 48.58 | 415 | 435 |
| 2 | 101.08 | 863 | 896 |
| 3 | 116.08 | 991 | 1013 |
| 4 | 131.08 | 1119 | 1139 |
| 5 | 146.08 | 1247 | 1267 |
| 6 | 161.08 | 1375 | 1400 |
| 7 | 176.08 | 1503 | 1523 |
| 8 | 191.08 | 1631 | 1651 |
| 9 | 206.08 | 1759 | 1779 |
| 10 | 221.08 | 1887 | 1910 |

The motor encoder positions for each valves setting are shown in Table 4.1. The table displays the valve setting, angle between the valve setting and the zero position, encoder position, and corrected encoder position. The corrected motor encoder positions were determined by an engineer at Blatchford. The positions were corrected slightly by visual inspection to better align the settings with the channel. The valve's closed position (setting 0) was changed from 0 to 10, so the valve wouldn't reach the extreme limit repeatedly.

## 4.1 Motor/gearbox test

The motor/gearbox test determined the time for the valve to switch between settings and was used to establish whether the 1:64 gearbox met the speed switching design criteria. As previously discussed, the joint should switch between settings 1 and 2 (closed and open settings) in less than 0.1 s.

### 4.1.1 Procedure

The hydraulic circuit was filled with hydraulic fluid (TurboSpec 320). The motor/valve was connected to the PCB, the PCB was connected to the power supply, and a Bluetooth connection was established between the computer and the control board. The valve was placed on its lateral side and all motor/gearbox tests were performed without a load to the hydraulic cylinder.

The valve was rotated between setting 0 and each of the other settings (1-10). For every rotation, the time to rotate and the position error were recorded (collected from the software). Ten trials were recorded for forward and backward movements, between position 0 and each of the possible settings (100 trials forward and 100 backward), and mean and standard deviation of the rotation time and position error were calculated.

### 4.1.2 Results and discussion

Figure 4.3 displays the average rotation time between setting 0 and settings 1-10.

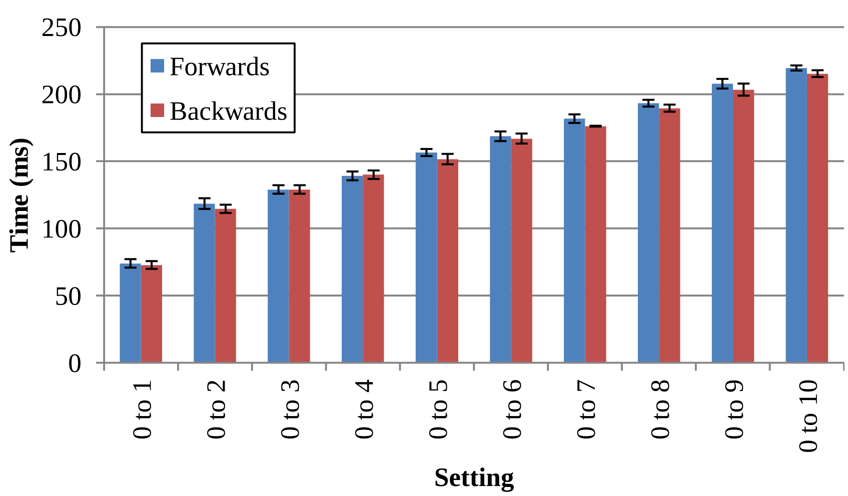


Figure 4.3: Average and standard deviations for valve rotation time between setting 0 and settings 1-10. The blue bars represent the valve turning in a ‘forward’ direction (from 0 to the desired position) and the red bars represent the valve turning ‘backward’ to setting 0.

Table 4.2: Average valve rotation time between setting 0 and settings 1-10 and average valve position error. Standard deviation is displayed in the brackets.

| Setting | Valve Rotation Time (ms) | Position Error (encoder count) |
|---|---|---|
| 0-1 | 73.4 (3.0) | 1.6 (0.5) |
| 0-2 | 116.6 (3.5) | 1.6 (0.8) |
| 0-3 | 129.0 (3.2) | 1.8 (0.4) |
| 0-4 | 139.6 (3.2) | 2.0 (0.0) |
| 0-5 | 154.1 (3.3) | 1.8 (0.5) |
| 0-6 | 167.8 (3.7) | 1.8 (0.6) |
| 0-7 | 178.9 (1.8) | 2.0 (0.2) |
| 0-8 | 191.4 (2.6) | 2.0 (0.0) |
| 0-9 | 205.5 (4.0) | 2.0 (0.0) |
| 0-10 | 217.3 (2.2) | 2.0 (0.2) |

The valve's average rotation time and average position error are displayed in Table 4.2. The rotation time between setting 0 (closed) and setting 1 (open) was 74.0 ± 3.2 ms rotating forward and 72.8 ± 2.9 ms backward. This met the design criteria time of 100 ms (0.1 s) to rotate between the open and closed settings.

The design goal was to switch between the closed and open setting (settings 0 and 1) in under 100 ms, but it is important to know and minimize the switching times to all the other settings (settings 2-10). The rotation time from setting 0 to setting 10 (largest rotation range of 221˚) was 219.4 ± 1.9 ms rotation forward and 215.2 ± 2.5 ms rotating backward, which are above 100 ms. Settings 2-10 are resistance settings designed to resist knee joint flexion during stair descents and stand-to-sit motions. These settings do not require the same rapid switching between settings, as they are intended to remain at the resistance setting throughout the entire motion being performed. Individuals with knee extensor weakness will likely approach and descend stairs carefully and slowly, so it is expected that the switching times to the resistance settings will be sufficient. For future designs of the variable resistance valve hole pattern, adding another closed setting at the opposite end valve (opposite end of the range slot where setting 10 is currently located) would be useful. This would provide another locked joint setting closer to the resistance settings, in the event the user were to stumble.

The largest valve position error was 2 motor encoder counts (0.24˚), which is sufficient for the OWVS design. Any rotational error under 1.0˚ (approximately 8 motor encoder counts) will not interfere with any of the hole settings. Hence, the 1:64 gearbox should be appropriate for the variable resistance valve.

## 4.2 Check valve test

The check valve test evaluated the check valve's functional performance. This valve was designed to allow the orthotic joint to extend freely, by allowing the hydraulic fluid travelling to the cylinder to bypass the variable resistance valve. Flow through the valve is blocked during knee flexion. A spring bias defaults the valve to the flexion setting (valve closed). This prevents fluid from flowing backwards through the check valve when there are equal pressures on both sides of the valve. A low cracking pressure is desired to provide low knee extension resistance.

### 4.2.1 Procedure

The check valve's seat was threaded into the hydraulic circuit block, to a depth that compressed the spring 2 mm. This distance was measured using a pin to determine the ball's depth from the hole's top. The variable resistance valve, reservoir, and hydraulic cylinder (without the joint) were assembled to the hydraulic circuit block and the circuit was filled with HydroSpec 320 oil. The block was clamped in horizontal position (Figure 4.4).

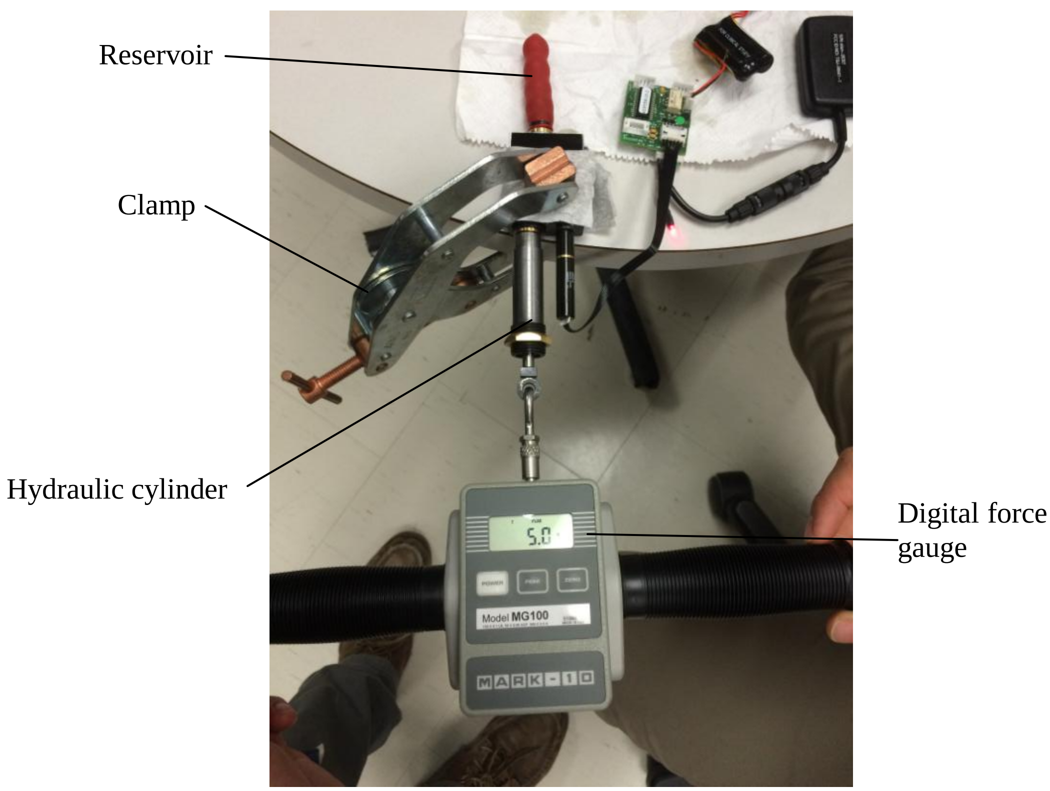

Figure 4.4: Check valve test setup.

The hydraulic cylinder was compressed by opening the variable resistance valve and allowing the reservoir to fill, simulating full knee flexion. The variable resistance valve was then closed (setting 0). The cylinder was extended by pulling on the piston shaft in the axial direction with an MG Series Digital Force Gauge (Mark-10 Corporation, NY, USA) that records peak tensile force (Figure 4.4). The maximum tensile force to extend the cylinder by a minimum of 2 mm was then recorded. Fifty trials were performed, extending the cylinder various lengths (between 2 mm and 19 mm of extension) and the peak tensile force was recorded in each case and then averaged. The forces were also converted to pressures in the hydraulic cylinder; however, this pressure was not the cracking pressure because it was not the pressure immediately after the check valve seat. The tensile force creates a pressure in the hydraulic cylinder that causes fluid to flow into the cylinder. The pressure should be similar to the 150 kPa calculated for the cracking pressure (section 3.6).

### 4.2.2 Results and discussion

The average tensile force required to extend the hydraulic cylinder was 18.42 ± 3.14 N, with a maximum force of 26 N and a minimum force of 13.5 N. The hydraulic cylinder pressure was calculated from the cylinder's inner diameter (12.7 mm) and equation $P = F/A$. The average pressure was 145.67 ± 24.81 kPa. This pressure is close to the desired cracking pressure and will not interfere with knee joint extension during locomotion. The joint should be able to move at an extension angular velocity of 350 °/s, which was verified in the biomechanical tests described in Chapter 5.

## 4.3 Resistance settings test

The resistance settings tests determined the flexion resistance of each valve setting. The prototype orthotic joint has nine resistance settings that were designed to allow users of different weights to descend stairs and perform stand-to-sit by safely lowering their centre of mass.

### 4.3.1 Procedure

4.3.1.1 Apparatus

The testing apparatus used in the hole-selection experiment (section 3.5.2.1) was modified for the resistance settings test (Figure 4.5). Similar to the hole-selection experiment, standard orthotic steel uprights were attached to the OWS joint. The joint was held vertically by fixing the shank upright to a heavy bench. A weight basket was attached to the distal end of the thigh upright (37.5 cm from the joint centre). The weight basket was lifted and a custom steel lever arm was used to hold the weight basket at a joint angle of 25˚. This lever arm released the weight basket at the same joint angle consistently, and allowed for an additional 10˚ of joint flexion compared to the hole-selection experiment.

Upright position was measured in the RTL with an 8-camera motion capture system (Vicon Inc., Oxford, UK). Eight reflective markers were adhered to the shank mounting arm and the thigh upright. Marker movement was tracked at 100 Hz.

4.3.1.2 Test procedure

The weight basket was filled with four different loads: 51 N, 111 N, 168 N, and 200 N. Using the custom lever arm, the weight basket was dropped from a 25˚ joint angle. Three trials per weight were collected for the eleven valve settings (12 trials per setting). Marker data were labelled and reconstructed using Vicon Nexus software and analyzed using Visual3D (C-Motion Inc., Rockville, MD). Marker data were filtered using a 4$^{th}$ order low pass Butterworth filter with a 10 Hz cut-off frequency. Joint angular position, velocity, and travel time were calculated.

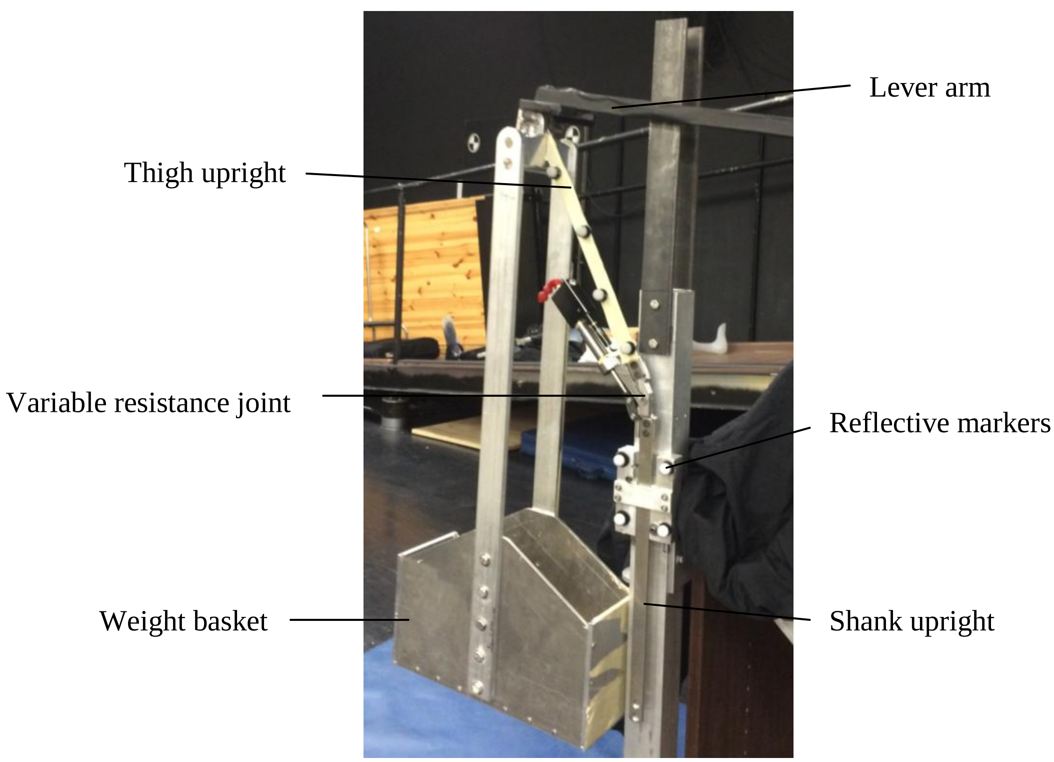


Figure 4.5: Testing apparatus for the resistance settings mechanical test. The weight basket was supported by the lever arm at a 25˚ joint angle.

### 4.3.2 Results and discussion

Table 4.3 shows the results for a 60˚ joint flexion range (30˚ to 90˚). An issue that was noticed during testing was that the hydraulic knee joint did not completely resist knee joint flexion at setting 0. This setting was designed to completely resist knee joint flexion, supporting the individual while the braced limb is in contact with the ground. Fluid was not leaking from the circuit (hydraulic cylinder, variable resistance valve hole, reservoir, fill points), so the fluid was likely bypassing either the variable resistance valve or the check valve and collecting in the reservoir. A mechanical test was performed to further investigate where the leak was occurring, why the leak occurred, and methods to correct it (section 4.4). Even though setting 0 did not completely resist knee flexion, flexion resistance was high. At a 200N load (40-75 Nm see Figure 4.6), the time to flex 60˚ was 18.83 ± 0.82 s (3.2 ˚/s). This resistance should provide safe knee flexion control during stance phase; however, small knee joint flexion during stance may adversely affect gait confidence for people with knee extension weakness. Biomechanical tests were performed in Chapter 5 to functionally evaluate the brace settings.

Table 4.3: Average and standard deviation (in brackets) for the time to flex 60˚ (30 ˚- 90˚), for all valve settings and four loads.

| Setting | Time for joint to flex 60˚ (30˚ - 90˚) [seconds] | | | |
|---|---|---|---|---|
| | **51 N** | **111 N** | **168 N** | **200 N** |
| 0 | 140.92 (20.75) | 54.21 (2.10) | 26.74 (2.61) | 18.83 (0.82) |
| 1 | 0.22 (0.00) | 0.22 (0.02) | 0.21 (0.01) | 0.20 (0.00) |
| 2 | 0.52 (0.04) | 0.29 (0.01) | 0.26 (0.01) | 0.24 (0.00) |
| 3 | 0.23 (0.02) | 0.24 (0.04) | 0.21 (0.02) | 0.20 (0.01) |
| 4 | 0.56 (0.01) | 0.31 (0.01) | 0.27 (0.01) | 0.25 (0.00) |
| 5 | 0.24 (0.03) | 0.21 (0.00) | 0.23 (0.06) | 0.21 (0.01) |
| 6 | 2.15 (0.14) | 0.73 (0.03) | 0.47 (0.01) | 0.40 (0.00) |
| 7 | 0.27 (0.01) | 0.22 (0.01) | 0.22 (0.02) | 0.21 (0.01) |
| 8 | 2.80 (0.01) | 0.77 (0.05) | 0.64 (0.14) | 0.59 (0.02) |
| 9 | 0.43 (0.04) | 0.29 (0.02) | 0.26 (0.04) | 0.20 (0.01) |
| 10 | 6.29 (0.06) | 1.51 (0.11) | 0.71 (0.03) | 0.53 (0.02) |

The moments applied to the joint during the drop tests increased as the joint flexion angle increased, due to the increasing moment arm length. For the four weights tested, the moments applied to the joint between 30˚ and 90˚ are shown in Figure 4.6. The 200 N weight basket applies the largest moments of 40 - 75 Nm. The 51 N weight basket only applies moments of 9.5 Nm – 19 Nm over this range.

Setting 1 is the valve's open setting. It is designed for free knee flexion, and has the largest hole diameter of all the settings (2.25 mm). Valve settings 2, 4, 6, 8, and 10 were designed to expose a single hole to the channel leading to the variable resistance valve (Table 3.6). The hole diameters are: 0.50 mm (setting 2), 0.35 mm (setting 4), 0.30 (setting 6), 0.25 mm (setting 8), and 0.20 mm (setting 10). Settings 3, 5, 7, and 9 expose two holes to the channel leading to the variable resistance valve, increasing flow though the valve and thereby decreasing the joint flexion resistance. The hole diameters are: 0.50 mm and 0.35 mm (settings 3), 0.35 mm and 0.30 mm (setting 5), 0.30 mm and 0.25 mm (setting 7), and 0.25 mm and 0.20 mm (setting 9) (Table 3.6). Figure 4.7 shows the joint flexion time results for the valve settings 1-10 over a 60˚ range (30˚ - 90˚), for the 168 N and 200 N drop tests.

As expected, the single hole settings (2, 4, 6, 8, and 10) provided more resistance to flexion than the double hole settings, particularly settings 6, 8 and 10 (Figure 4.7). For the 200 N drop test, 60˚ of joint flexion at settings 8 and 10 required 0.59 ± 0.02 s and 0.53 ± 0.02 s, respectively. Surprisingly, setting 10 provided less resistance than setting 8 for the 200 N drop test. Setting 10 provided the most resistance of all the settings for 51 N, 111 N and 168 N tests (Table 4.3). This inconsistency may be because the valve was not able to fully resist motion at the locked setting. At larger weights, more pressure is applied to the variable resistance valve. If a leak occurs at the variable resistance valve, setting 10 may be more susceptible to fluid escaping at higher pressures.

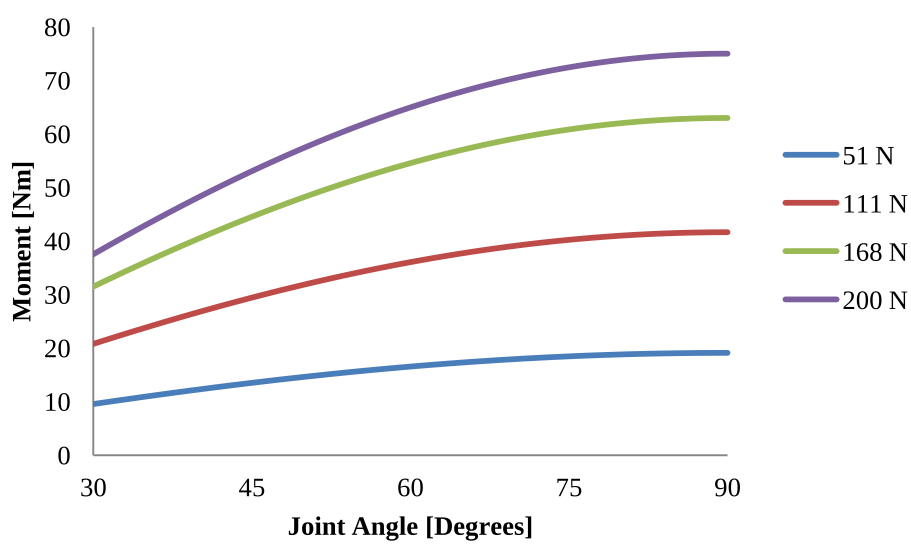


Figure 4.6: Moments applied to the joint between 30˚ and 90˚ for the four test weights.

Overall, the resistances were lower than predicted. From the hole selection experiment (section 3.5.2.1), a 0.25 mm hole (equivalent to setting 8) required 1.1 ± 0.02 s to flex the joint 50˚ (i.e., approximately twice as long as the time from the resistance setting test). The lower resistance results are likely due to hydraulic fluid leaking past the variable resistance and/or check valves and collecting in the reservoir.

The joint's resistance settings were designed to support individuals for 0.7 - 1.0 seconds during the stance phase of stair descent (approximately 65˚ of knee flexion) on the braced limb to safely lower the body's centre of mass to the next step. The settings provided less resistance than expected, but the drop test experiments do not replicate knee motion or loading during stair or stand-to-sit motions. Settings 6, 8 and 10 did resist joint flexion and should be tested functionally to determine performance (Chapter 5). These tests will provide a better understanding of whether the resistance settings are sufficient for users, even though resistance moments were lower than expected. From the results, settings 8 and 10 will likely be used as resistance settings for stair descent, and setting 6 may be appropriate for lighter individuals.

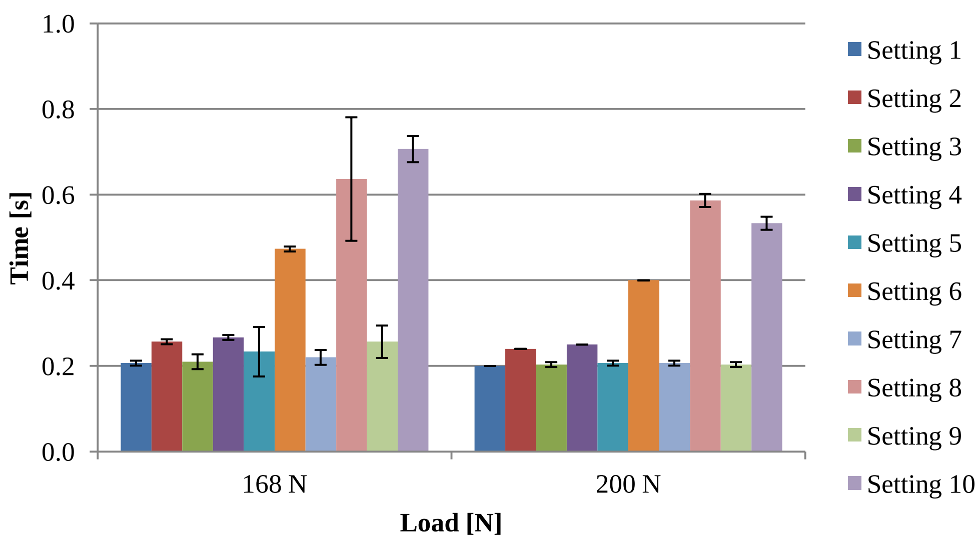


Figure 4.7: Time for the joint to flex 60˚ (30˚ - 90˚) for settings 1-10 at 168 N and 200 N loads.

The double hole settings (3, 5, 7, and 9) provided little flexion resistance. The 60˚ flexion times were similar to the open setting and did not provide enough flexion resistance for any of the target activities. This is not surprising since these settings use a combination of two holes. Having these settings allowed for a larger range of test results from different hole sizes but future OWVS designs may not need to include these double hole settings. Future hole pattern design should be modified to include a range of more appropriate resistance settings.

Instantaneous angular velocities at 45 ˚, 60 ˚, 75 ˚, and 90˚ joint angles were averaged and standard deviations were calculated for the 51 N drop test (Table 4.4). For the open setting, the joint should be able to move freely in flexion (> 325 ˚/s) with a relatively small knee moment.

As expected, the joint's angular velocity increased with increased hole diameter (Table 4.4). Setting 1 (open) achieved a flexion angular velocity of 348.6 ± 8.6 at 75˚, which met the design criteria. The 51 N drop test applied a low moment to the joint, and the joint was still able to move at velocities above the desired 325˚/s. The knee joint should permit free knee flexion at the valve's open setting.

Table 4.4: Instantaneous joint angular velocity averages and standard deviations at 45˚, 60˚, 75˚, and 90˚ joint angles for the 51 N drop tests for valve settings 1 – 10.

| **Setting** | **Instantaneous Angular Velocity at Specified Angle [˚/s]** | | | |
|---|---|---|---|---|
| | **45˚** | **60˚** | **75˚** | **90˚** |
| 1 | 207.7 (21.4) | 301.4 (4.6) | 348.6 (8.6) | 317.3 (9.7) |
| 2 | 143.8 (39.5) | 116.3 (9.5) | 100.5 (13.1) | 106.4 (3.9) |
| 3 | 211.3 (6.7) | 295.6 (31.5) | 344.9 (7.0) | 311.1 (3.9) |
| 4 | 147.5 (6.6) | 92.3 (16.2) | 69.1 (6.3) | 84.2 (3.3) |
| 5 | 185.1 (13.5) | 316.8 (12.4) | 324.1 (4.1) | 312.2 (8.8) |
| 6 | 45.0 (1.8) | 40.1 (4.7) | 19.1 (4.7) | 8.1 (7.3) |
| 7 | 204.9 (3.5) | 269.3 (7.3) | 224.7 (24.8) | 199.9 (4.0) |
| 8 | 27.9 (1.7) | 24.4 (3.3) | 13.6 (2.5) | 3.0 (0.9) |
| 9 | 180.3 (9.4) | 172.2 (6.1) | 81.8 (7.3) | 90.4 (18.4) |
| 10 | 2.1 (1.2) | 5.9 (3.0) | 5.0 (1.5) | 2.5 (3.6) |

## 4.4 Leak identification experiment

The OWVS was unable to completely resist flexion at setting 0 (locked setting). Setting 0 was designed to allow no fluid flow from the hydraulic cylinder to the reservoir. This experiment identified where the leak occurred and potential reasons for the leak.

During all joint testing, fluid did not leak from the circuit, including the hydraulic cylinder-block interface, variable resistance valve-block interface, external reservoir, or fill points. Therefore, the leak occurred internally, bypassing either the variable resistance valve or the check valve.

Visual inspection was performed by filling the high pressure side of the circuit (hydraulic cylinder) with oil and setting the valve to position 0 (closed). Steel uprights were attached to the joint and the shank upright was fixed to a heavy bench. The low pressure side of the reservoir was not filled with oil and the joint was flexed by applying a load. The oil appeared to be leaking from the variable resistance hole.

To prove that the fluid was bypassing the variable resistance valve, a plug needed to be made that blocked the variable resistance valve pathway. If the joint did not rotate when this pathway was plugged, the leak could be localized at the valve-pathway interface.

### 4.4.1 Plug design

Figure 4.8 show a SolidWorks model of the plug designed for the leak identification experiment. To avoid modifying the block, the plug was designed to thread into the block where the variable resistance valve is usually connected.

The plug was made from brass, and the main body had the same outer diameter as the variable resistance valve. An M8x0.75 thread allowed the plug to be inserted in the place of the variable resistance valve. A Teflon washer was placed on top of the plug and held in place by a socket head cap screw. When the plug was threaded into the block, the Teflon washer was compressed against the variable resistance valve's exit channel (leading to the reservoir), preventing any fluid escaping. The double-seal O-ring prevented fluid from leaking toward the threads. The slot at the bottom of the plug allowed for the plug to be tightened with a screw driver to ensure that the Teflon washer was compressed at the valve's exit channel.

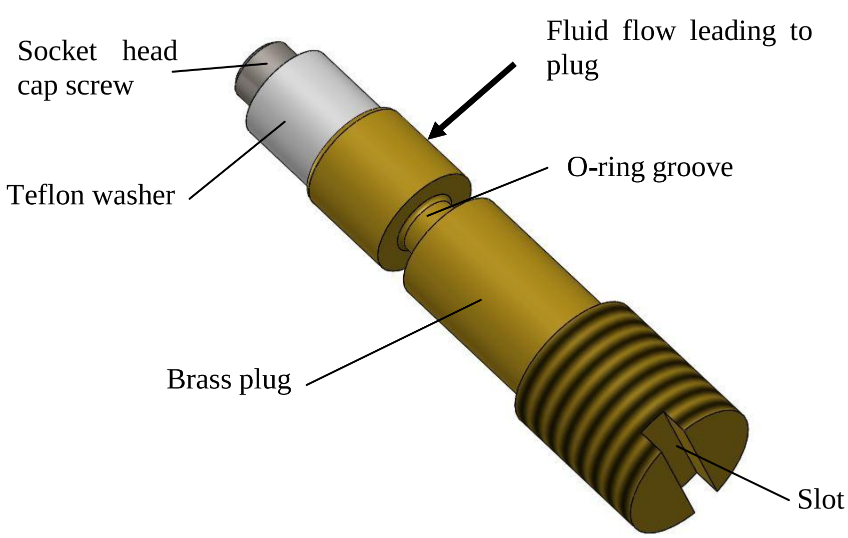


Figure 4.8: SolidWorks model of the plug designed for the leak identification experiment.

### 4.4.2 Procedure

The testing apparatus from the resistance settings test (section 4.3) was used for the leak identification experiment. Standard orthotic steel uprights were attached to the OWS joint. The joint was held vertically by fixing the shank upright to a heavy bench. A weight basket was attached to the distal end of the thigh upright (37.5 cm from the joint centre) (Figure 4.9).

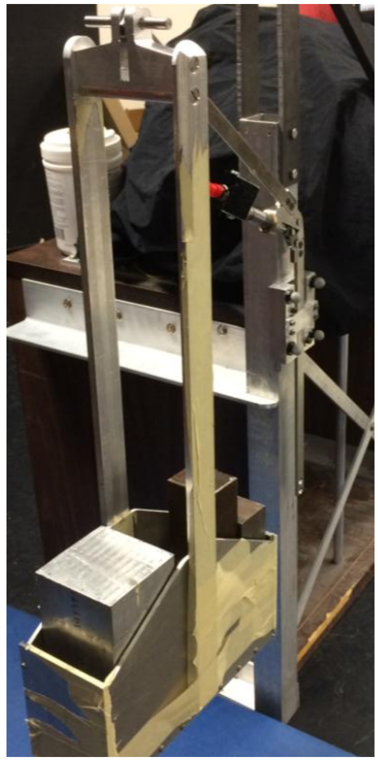

Figure 4.9: Testing apparatus for the leak identification experiment.

The custom plug was threaded into the variable resistance valve location and the hydraulic block and OWS were assembled normally. The hydraulic cylinder and high pressure side of the hydraulic block were filled with TurboSpec 320 hydraulic oil. The weight basket was filled with a 255 N load (55 N additional load from the maximum load in the resistance settings test) and the basket was suspended at 45˚, 60˚, and 90˚ joint angles. The basket was left for two minutes at each test angle, and the angle after two minutes was measured with a digital level.

### 4.4.3 Results and discussion

The moments applied to the joint from the 255 N weight basket were: 67.6 Nm at a 45˚ joint angle, 82.8 Nm at a 60˚ joint angle, and 95.6 Nm at a 90˚ joint angle. At each setting, no movement was observed during the two minute test period. The plugged joint completely resisted flexion, confirming that fluid was bypassing the variable resistance valve. No fluid bypassed the check valve or left the circuit.

The variable resistance valve was designed to the same specifications as Endolite's Elan prosthetic ankle. The optimum clearance between the valve and hydraulic circuit block, valve outer diameter (OD) and block housing inner diameter (ID), should be 2-5 μm, with a surface finish on both components of approximately 0.1 Ra (Ra is the arithmetic average of a set of surface peaks and valleys measured in μm [64], [65]). After speaking with an engineer from Blatchford, it was determined that the connector block bore, where the variable resistance valve rotates and fluid is exchanged, had to be opened slightly to allow for smooth rotation. The bore's ID was measured with a coordinate measuring machine (CMM), and the clearance between the valve OD and the block bore ID was 17-18 μm, after opening the hole. This is likely why the leak occurred at the variable resistance valve-bore interface. The fluid could then leak upwards to the exit channel of the variable resistance valve or around the side and into other valve hole.

Roundness and cylindricity are important factors to minimize friction between the valve and bore, which contributes to eliminating leaks between the components. Concentricity is also an important factor when the clearances between mating components are very small. Methods for improving the design for the next version are proposed in section 6.2. This section discusses the use of a coupling to improve the concentricity of the valve and bore, and different manufacturing methods to improve the clearances.

Even though a small leak was found, the joint still provided substantial joint flexion resistance at the closed setting (setting 0) and at the higher resistance settings (settings 6, 8 and 10) (Table 4.3). Functional evaluation of the OWVS was required for a better understanding of how the joint performed in realistic scenarios (Chapter 5).

# Chapter 5: Biomechanical Testing

Biomechanical testing was performed to evaluate the functionality of the variable resistance joint prototype (OWVS) when used in a SCKAFO during three common activities: level ground walking, stair descent, stand-to-sit transition. Biomechanical testing was used to determine if the joint supported the user throughout stance, allowed the knee to move freely during swing, and allowed the user to descend stairs and sit with a more natural technique than moving with a locked knee.

Kinematic (knee joint angle and angular velocity) and kinetic (knee joint moment) measures were compared to the able-bodied, SCKAFO, and TF amputee prosthetics literature. The device should function similar to an SCKAFO or TF microprocessor-controlled prosthetic knee for level ground walking and similar to a TF microprocessor controlled prosthetic knee for stair descent.

This pilot study of the OWVS was approved by the Ottawa Health Science Network Research Ethics Board (Appendix E) and the University of Ottawa Health Science and Science Research Ethics Board (Appendix F).

## 5.1 Methods

Three functional tests were performed: level ground walking, stair descent, and stand-to-sit. These tests were performed in the RTL using an 8-camera motion capture system (Vicon Inc., Oxford, UK) and two force platforms (AMTI, Watertown, MA; Bertec Corporation, Columbus, OH) embedded in the floor.

### 5.1.1 Participant

A single able-bodied participant volunteered to participate in the pilot test (male, 28 years, 179 cm, 80.74 kg). One participant was appropriate for the initial pilot test of the OWVS since the results would determine whether the joint design needs modification, and whether more testing should be carried out with other participants and population groups. The inclusion criterion was:

- No injuries or health issues affecting walking or stair ascent/descent
- Age between 18-60 years
- Mass between 50-100 kg

- Ability to perform multiple stair descents, walk continuously for 10 minutes, and sit to stand 5 times
- Ability to wear the test KAFO with minimal modifications.

The exclusion criterion was:

- Those who do not meet the inclusion criteria
- Individuals with injury, pain, loss of motion or dysfunction in lower extremities or trunk
- Individuals who have sustained a lower body injury in the past two years
- Individuals with balance problems or medication that affects balance

The recruitment notice and the consent form for the biomechanical testing can be found in Appendix G and Appendix I, respectively.

For safety reasons, only able-bodied participants were considered for biomechanical testing, since a manual control method was used for joint actuation. If the joint malfunctioned, able-bodied users would be able to catch themselves in a stumble scenario. For initial prototype testing, orthosis function can be tested with the participants relaxing and letting the joint support their weight. Future testing on individuals with knee extensor weakness should be performed once safe joint functionality has been confirmed.

An existing carbon-fibre KAFO was fitted to the participant by a certified orthotist from the Prosthetics and Orthotics Service at the TOHRC, to ensure a proper fit. The medial joint was a standard orthotic single axis knee joint and the lateral side was the OWVS. Once the individual was properly fitted for the KAFO, they were given time to become accustomed to the brace and try the different settings (approximately 10 minutes).

Figure 5.1 shows the participant wearing the carbon-fibre KAFO with the OWVS on the lateral side. The electronics of the OWVS (PCB, Bluetooth adapter, batteries) were placed in a plastic bag and taped to the front of the orthosis. This was done so that the electronics would not be placed on the side of the brace, where the motion capture markers were placed. By placing the electronics on the front of the orthosis, the markers would be more easily seen by the cameras.

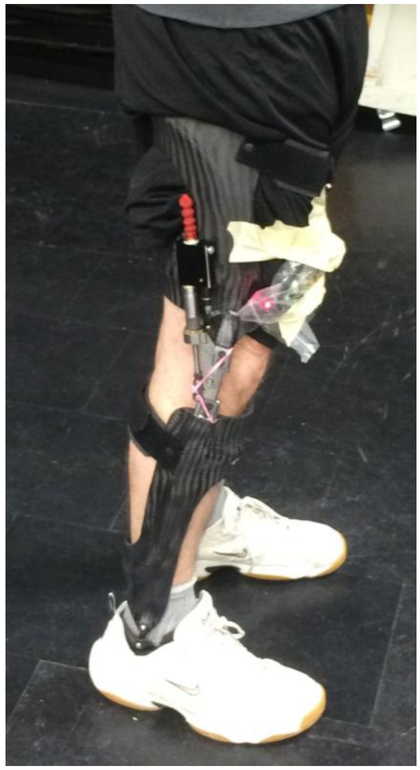

Figure 5.1: Participant wearing the carbon-fibre KAFO with the Ottawalk-Variable Speed orthotic joint on the lateral side and electronics taped to the front.

### 5.1.2 Walking tests

Three level ground walking tests were performed:

**Stance-control walking**: This test involved locking the knee joint during stance phase and unlocking the joint during swing. A manual switch was used to switch the valve between setting 1 (swing) and setting 0 (stance) states. Manual switching was done on a touch screen tablet that was connected to the valve by Bluetooth (i.e., operator selects open or closed valve position). The manual switching procedure is explained in section 5.1.6. The participant was asked to walk at a slow pace to allow for more accurate manual switching. Data was collected until five trails had been captured where the participant's foot on the braced limb fully contacted a force plate with proper manual switching (joint was locked at heel contact and unlocked at toe-off).

**Open (unlocked) joint test**: The variable resistance valve was set to setting 1 (open). The participant was asked to walk at a self-selected pace. Only trials where the foot of the braced limb fully contacted a force plate were collected. Five trials were collected.

**Locked joint test**: The variable resistance valve was set to setting 0 (closed). The participant was asked to walk at a self-selected pace. Only trials where the foot of the braced limb fully contacted a force plate were collected. Five trials were collected.

For all three tests, the participant walked along a level, 8m walkway in the RTL. Trials where the foot of the braced limb fully contacted a force plate were collected for the purpose of collecting kinetic data. Trials were constantly collected for the stance-control testing so that the effects of opening/closing the valve early/late could be observed.

### 5.1.3 Stair descent test

The participant descended a custom-made 4-step staircase in the RTL (Figure 5.2). Each step had a rise of 190.5 mm (7.5 in) and step depth of 247.7 mm (9.75 in).

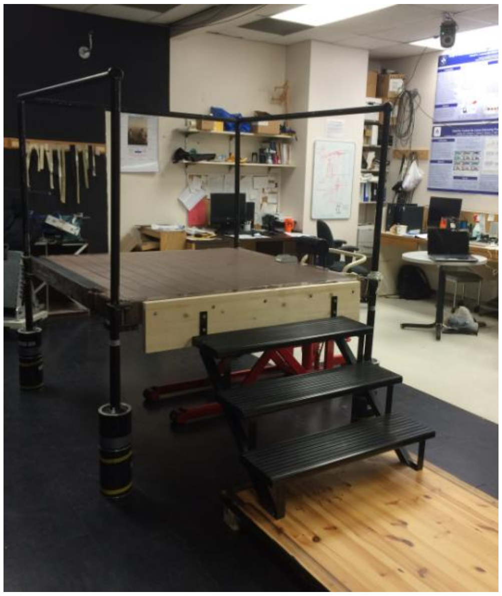

Figure 5.2: Custom made 4-step staircase in the RTL.

The participant performed stair descents using three different settings (setting 1, 8 and 10). Six stair descent trials were collected for each setting, three trials starting with the left foot stepping down first and three trials with the right foot first. This provided six kinematic stair descent cycles on the braced limb. Only kinematic data could be collected for the stair descent test because the stair set was not instrumented with force plates. A total of 18 stair descent trials were collected, six trials for each of the three settings.

### 5.1.4 Stand-to-sit test

For the stand-to-sit trials, the participant was instructed to begin in a standing position with each foot on a force plate (Figure 5.3). The participant was then instructed to sit on a bench placed behind him and, once sitting, the participant was asked to return to a standing position (without using his arms to assist). The participant performed 10 stand-to-sit-to-stand trials, at 1, 8, and 10 flexion resistance settings. 30 stand-to-sit motions were performed (10 stand-to-sits at each of the three settings). Kinematic and kinetic data were collected for the stand-to-sit tests.

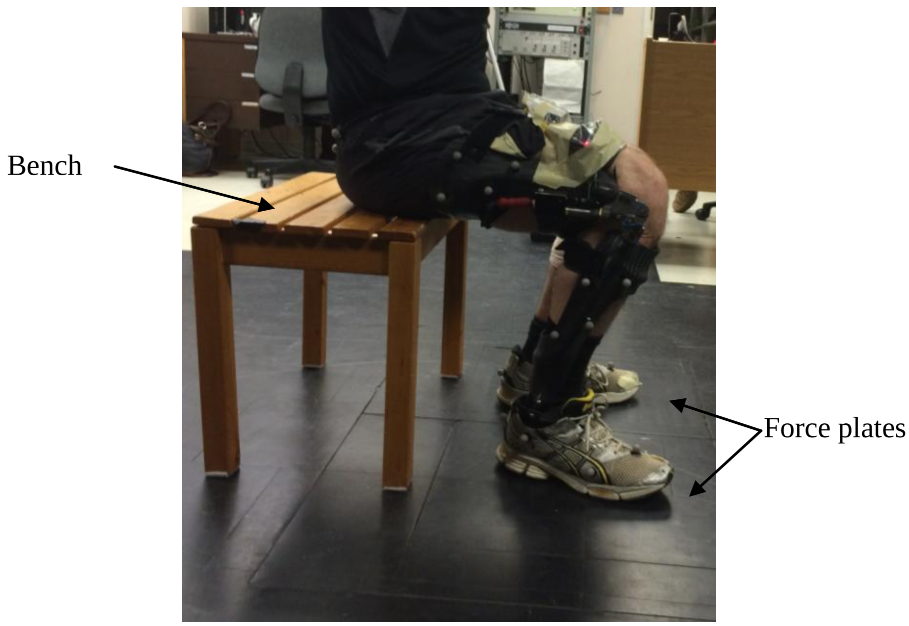

Figure 5.3: Testing configuration for stand-to-sit test.

### 5.1.5 Data collection

Three-dimensional marker data were collected at 100 Hz, using the 8-camera motion-capture system (Vicon Inc., Oxford, UK). A lower body 6 degree of freedom (DoF) marker set was used, adapted from Collins *et al.* [66] (Figure 5.4). Thirty reflective markers were placed on the subject's pelvis, thighs, shanks, and feet using two-sided tape. Thigh and shank plates (four marker clusters) were attached to the non-braced side, with the braced side's thigh and shank markers placed directly on the KAFO to tracking orthosis movement rather than movement of the limb within the orthosis.

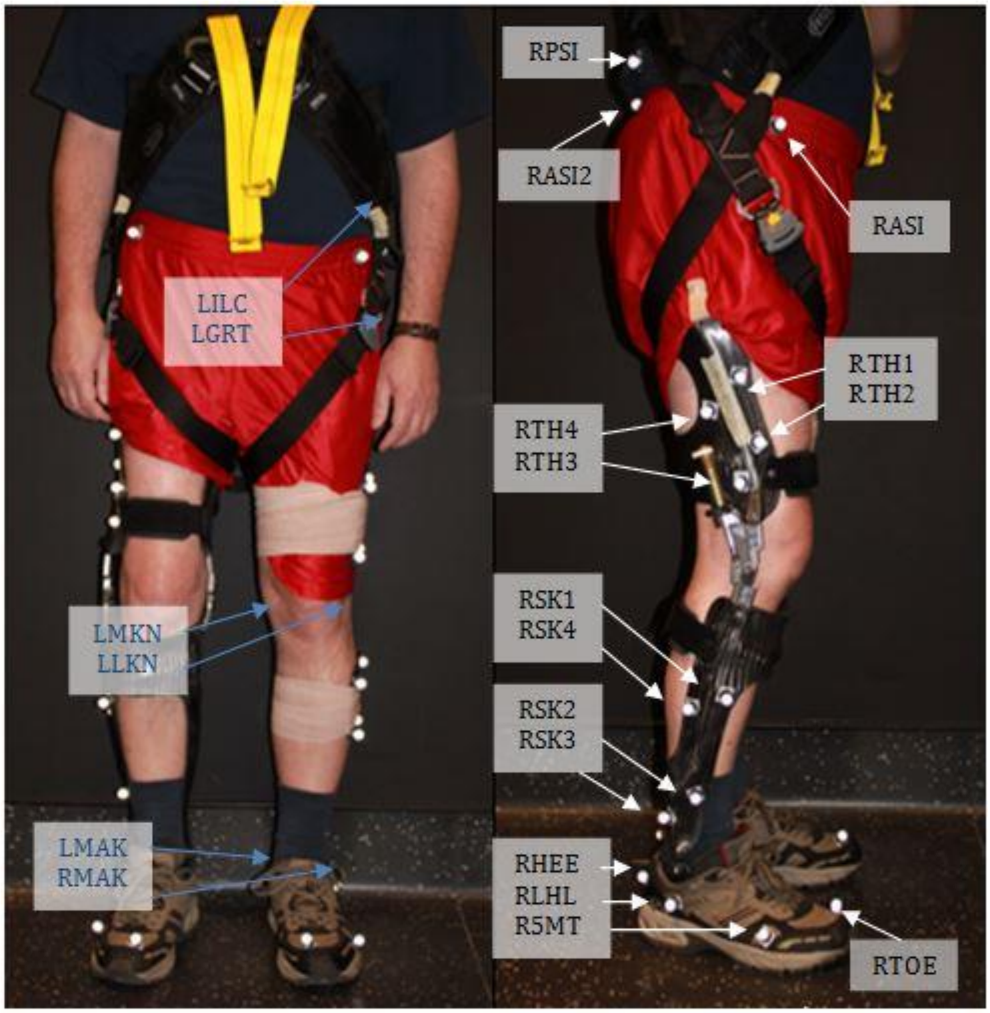


Figure 5.4: Lower body 6 degree of freedom marker set. The 6 anatomical locations are labeled on the left and 15 tracking markers are labeled on the right (adapted from [67]). Marker acronyms are explained in Table 5.1.

In addition to the tracking markers, 12 anatomical locations (6 per side) were digitized on the medial and lateral malleolus, medial and lateral knee joint centres, greater trochanter, and iliac crest using a digitizing wand (markers labeled in blue in Figure 5.4). Visual3D (C-Motion Inc., Rockville, MD) software was used to recognize the custom wand and place virtual markers at the specified locations [68]. All markers and segments are summarized in Table 5.1.

Table 5.1: Marker names and segments tracked (adapted from [67]).

| Segment | Tracking Markers (Left) | Tracking Markers (Right) |
|---|---|---|
| Anterior superior iliac spine | LASI | RASI |
| Posterior superior iliac spine | LPSI | RPSI |
| Hip Reference | LASI2 | RASI2 |
| Thigh | LTH1, LTH2, LTH3, LTH4 | RTH1, RTH2, RTH3, RTH4 |
| Shank | LSK1, LSK2, LSK3, LSK4 | RSK1, RSK2, RSK3, RSK4 |
| Toe | LTOE | RTOE |
| 5th metatarsal | L5MT | R5MT |
| Lateral heel | LLHL | RLHL |
| Heel | LHEE | RHEE |
| Greater trochanter (digitized) | LGTR | RGTR |
| Iliac crest (digitized) | LILC | RILC |
| Knee joint centre (digitized) | LMKN, LLKN | RMKN, RLKN |
| Ankle joint centre (digitized) | LMAK, LLAK | RMAK, RLAK |

Force plate data were collected at 1000 Hz for the walking and sitting tests. These force plates were connected to the Vicon system and controlled and synchronized with Vicon Nexus software.

### 5.1.6 Orthotic joint control

The OWVS was controlled manually for biomechanical testing. The control software connected to the valve using Bluetooth for remote control by computer or tablet (explained in Chapter 4). For the walk test, manual switching between setting 0 (closed) and setting 1 (open) was performed. The operator closely monitored the participant and selected setting 0 from braced limb foot contact to foot off. Just prior to foot off, at the beginning of pre-swing, setting 1 (open) was selected to allow free knee flexion.

The stair descent and sitting tests did not require setting switching. Prior to each stair descent or stand-to-sit sequence, the valve was set to the appropriate resistance setting.

### 5.1.7 Data analysis

Marker data were labelled and reconstructed using Vicon Nexus and analyzed using Visual3D. Marker and ground reaction force data were filtered with a $4^{th}$ order low-pass Butterworth filter at 10 Hz and 20 Hz cut-off frequencies, respectively. A seven segment lower body model (2 feet, 2 shanks, 2 thighs, pelvis) was created in Visual3D. Kinematic and kinetic data from the braced limb were normalized to 100% of the gait cycle (heel strike to heel strike of the braced limb) for the stair, walk, and stair descent tests. For the stand-to-sit tests, braced limb kinematic and kinetic data were normalized to 100% of the stand-to-sit cycle.

Kinematic and kinetic values were averaged over the trials for the participant. The following are the number of strides collected for each test:

- **Stance-control walking**: 20 kinematic strides with proper (on time) switching and 5 kinetic strides
- **Walking**: 5 kinematic and kinetic strides for open joint (setting 1) and locked joint (setting 0)
- **Stair descent**: 6 kinematic strides per setting (settings 1, 8 and 10)
- **Stand-to-sit** :10 kinematic and kinetic trials per setting (settings 1, 8 and 10)

Descriptive statistics were used to evaluate the data and verify device function. Knee angle and angular velocity for both walking and stair descent were compared to the able-bodied, SCKAFO, and transfemoral prosthetics literature. For the walking test, the knee should not flex throughout stance phase but flex appropriately during swing phase (i.e., joint locked during stance and open during swing). The motion should be similar to SCKAFO amputee gait. Peak values for knee angle and angular velocity were collected. For the walking trials, peak values for knee joint net moments and powers were also compared to SCKAFO and able-bodied literature

For the stair descent trials, peak knee angles, angular velocities, and stride parameters of the braced side were analyzed and compared to the able-bodied and transfemoral amputee literature. Stair descent should be similar to stair descent for transfemoral amputees. Stride and stance time for walking and stair descent were compared to literature. For the stand-to-sit trials, peak values for knee joint angle, angular velocity, external moment and power were compared to the able-bodied, SCKAFO and transfemoral amputee literature.

## 5.2 Results

Biomechanical test results are presented in this section. Graphs for all the kinematic and kinetic analyses can be found in Appendix C and Appendix D.

### 5.2.1 Walking test

5.2.1.1 Spatial-temporal stride parameters

Table 5.2 summarizes the average stride parameters for the three walking tests. The participant was instructed to walk at a comfortable slow pace for the stance-control test, to allow for more accurate switching of settings. The participant had a reduced stride velocity (38.3%

slower than walking with the joint open or locked), and a reduced stride length (15.0% shorter than walking with the joint open and 16.8% shorter than walking with a locked knee joint). The stride time increased (43.4% longer than walking with an open joint and 40.0% longer than walking with a locked knee joint). There was no difference in the change in stance (% of gait) between the stance-control mode and the open mode. When walking with a locked knee joint, the participant had a decreased stance/swing ratio (4% less stance than the stance-control and open modes).

Table 5.2: Average stride parameters for the braced limb during walking. Standard deviations are presented in brackets.

| Joint Setting | Stride time (s) | Stride Length (m) | Stride Velocity (m/s) | Stance (% of stride) |
|---|---|---|---|---|
| Stance-control | 1.75 (0.33) | 1.19 (0.11) | 0.71 (0.16) | 63 (2) |
| Open | 1.22 (0.04) | 1.40 (0.02) | 1.15 (0.04) | 63 (1) |
| Locked | 1.25 (0.02) | 1.43 (0.03) | 1.15 (0.04) | 59 (2) |

### 5.2.1.2 Kinematics

Figure 5.5 shows the average sagittal knee joint angle graphs for the three walking tests. Specific minimum and maximum sagittal knee joint angles were collected ($LA_1$, $LA_2$, $LA_3$, and $LA_4$), and the positions of these values are displayed in Figure 5.5a. $LA_1$ and $LA_2$ are the minimum and maximum sagittal knee angle during weight acceptance (0-15% of the gait cycle, includes the initial contact and loading response sub-phases), respectively. $LA_3$ is the minimum knee angle during terminal stance and pre-swing (30-60% of the gait cycle). $LA_4$ is the maximum knee angle during the gait cycle, occurring during swing phase. These average angles are displayed in Table 5.3.

During stance-control walking, the knee joint experiences a small angle increase during weight acceptance and then a constant knee joint angle until the valve is opened and knee flexion occurs. During open joint walking, knee flexion is greater than stance-control walking during weight acceptance, the knee extends during single leg support, and then flexes again in swing phase. In locked joint walking, the joint flexes during weight acceptance and during pre-swing, but the knee remains fairly extended throughout the cycle.

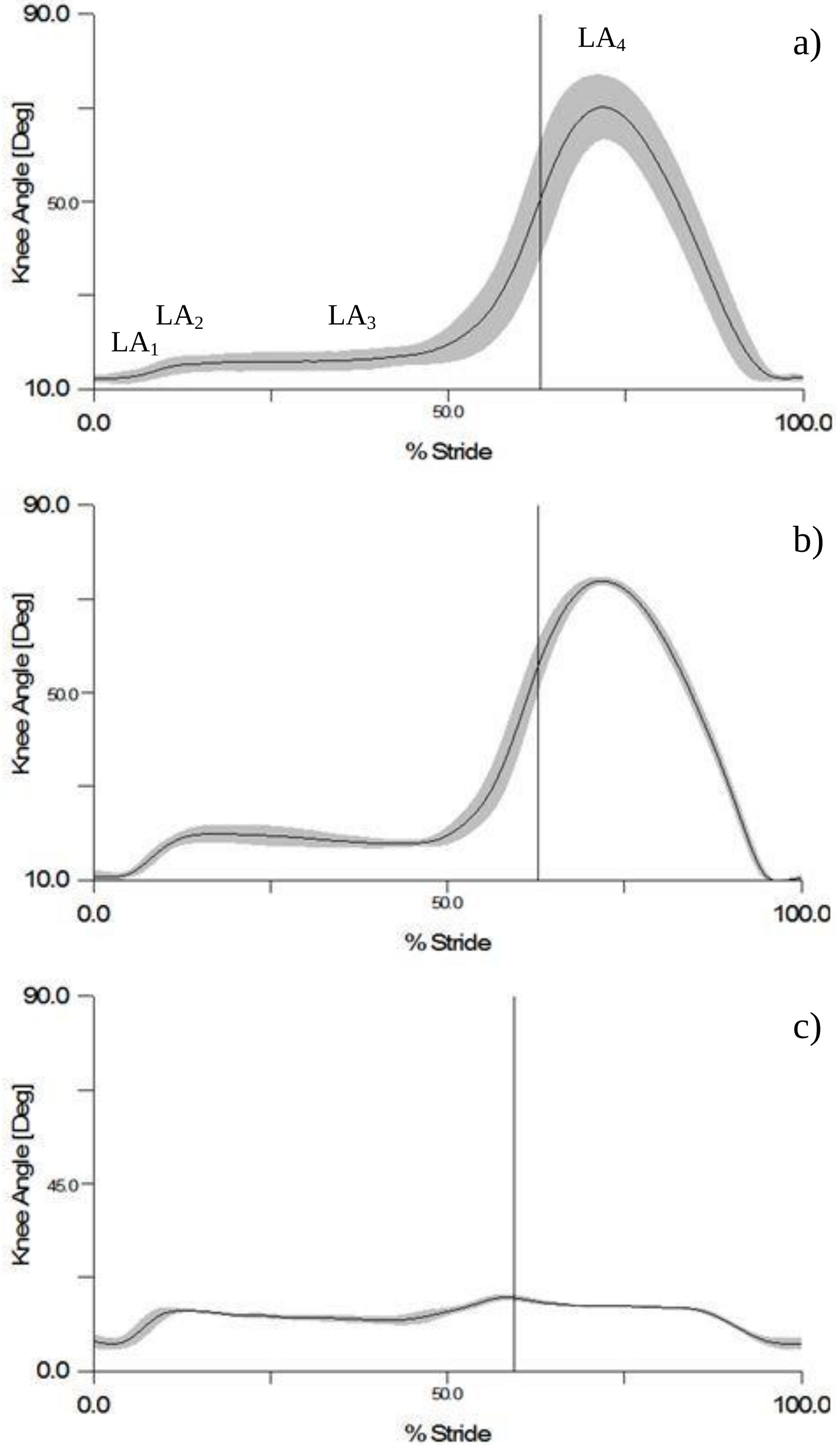


Figure 5.5: Average sagittal knee joint angles for a) stance-control walking, b) open joint walking (setting 1), c) locked joint walking (setting 0). The vertical line represents average toe-off. Left of the line is stance phase and right of the line is swing phase. Knee joint flexion is positive.

The orthosis had similar ranges of motion for stance-control and open settings walking, with approximately 5% greater range of motion (ROM) while walking with the joint open. The ROM for the locked joint test was 11.65 ± 1.36 ˚, with a large portion of the motion occurring during weight acceptance (8.33 ± 1.27 ˚). $LA_1$ (minimum angle during the weight acceptance task) were similar for stance-control and open tests, and had a more extended knee during the locked testing.

Figure 5.6 shows the average sagittal knee joint angular velocity graphs for the three walking tests. Specific minimum and maximum sagittal knee joint angular velocities were collected (Figure 5.6a). $LV_1$ is the maximum flexion angular velocity during weight acceptance (0-15% of the gait cycle), $LV_2$ is the maximum flexion angular velocity during swing limb advancement (50-100% of the gait cycle), and $LV_3$ is the minimum flexion angular velocity (maximum extension) during the gait cycle (Table 5.3).

Table 5.3: Average sagittal joint angles ($LA_1$, $LA_2$, $LA_3$, and $LA_4$) and angular velocities ($LV_1$, $LV_2$, and $LV_3$) collected from the walking test. The total ROM and the ROM during weight acceptance are also displayed. Standard deviations are displayed in brackets.

| | **Stance-control** | **Open** | **Locked** |
|---|---|---|---|
| **$LA_1$** [˚] | 12.0 (0.7) | 10.3 (1.2) | 6.3 (1.5) |
| **$LA_2$** [˚] | 15.6 (2.0) | 19.8 (1.8) | 14.6 (0.5) |
| **$LA_3$** [˚] | 15.5 (2.1) | 17.6 (0.9) | 12.0 (1.1) |
| **$LA_4$** [˚] | 71.9 (6.4) | 74.0 (1.0) | 18.0 (0.7) |
| **$LV_1$** [˚/s] | 45.3 (17.0) | 125.1 (31.2) | 133.3 (25.7) |
| **$LV_2$** [˚/s] | 289.9 (49.3) | 358.7 (9.9) | 55.5 (17.0) |
| **$LV_3$** [˚/s] | -216.4 (46.2) | -336.9 (19.8) | -73.2 (6.5) |
| **ROM Total** [˚] | 59.9 (6.6) | 63.7 (1.1) | 11.7 (1.4) |
| **ROM WA** [˚] | 3.7 (1.8) | 9.4 (1.5) | 8.3 (1.3) |

The angular velocity profile shapes were similar for the stance-control and open joint walking tests. The peak angular velocities were greater for the open joint settings (358.7 ± 9.9 ˚/s in flexion and 336.9 ± 19.8 ˚/s in extension), and much larger for the maximum angular velocity during weight acceptance ($LV_1$). Angular velocity for the locked joint tests experienced a peak during weight acceptance and remained low throughout the rest of the cycle.

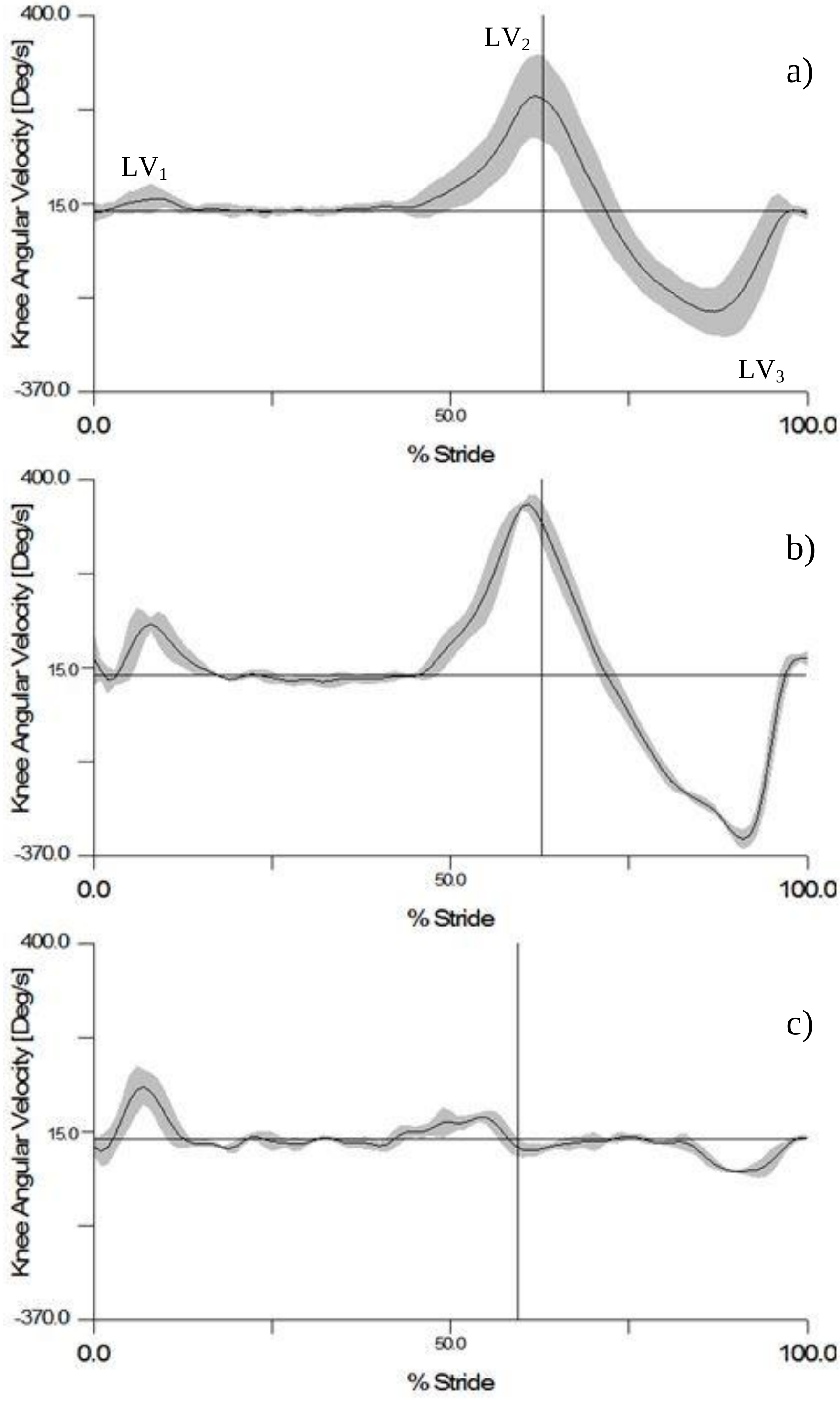


Figure 5.6: Average sagittal knee joint angular velocity for a) stance-control walking, b) open joint walking (setting 1), and c) locked-joint walking (setting 0). The vertical line represents average toe-off. Left of the line is stance phase and right of the line is swing phase. Knee flexion angular velocity is positive.

Figure 5.7 shows examples of individual stance-control walking trials where the valve was opened early (Figure 5.7a) and where the valve was opened late (Figure 5.7b). Premature knee flexion occurred when the valve opened early, prior to pre-swing. This caused the support limb to collapse and destabilized the participant, which also resulted in decreased knee ROM. When the valve opened late, knee flexion occurred after toe off. This resulted in decreased knee ROM and caused the participant to begin swing phase with an extended knee.

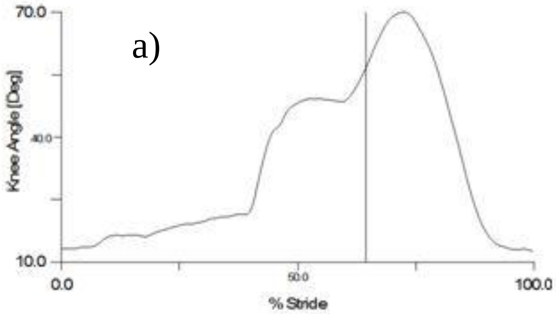


Figure 5.7: Average knee angle for stance-control walking where the valve was a) opened early and b) opened late. The vertical line represents average toe-off. Left of the line is stance phase and right of the line is swing phase. Knee flexion is positive.

5.2.1.3 Kinetics

Figure 5.8 and Table 5.4 show the average sagittal knee joint moment for the stance-control and open joint walking trials. $LM_1$ is the maximum knee flexion moment during weight acceptance (0-15% of gait cycle). $LM_2$ is the maximum knee extension moment during mid-stance (15-35% of gait cycle), and $LM_3$ and $LM_4$ are the minimum and maximum knee extension moments during pre-swing, respectively (50-65% of gait cycle).

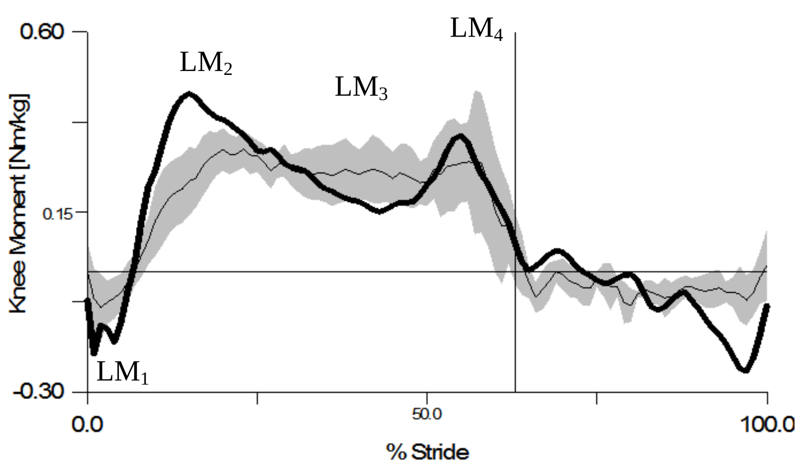


Figure 5.8: Average sagittal knee moment for stance-control walking (thin line with standard deviation) and open joint walking (bold line). Vertical line represents average toe-off. Left of the line is stance phase and right of the line is swing phase. Extension moment is positive.

The moment profiles were similar for stance-control and open joint walking. Open joint walking had larger and more distinct maximum and minimum moments. $LM_1$ (moment during weight acceptance) was the only flexion moment during stance.

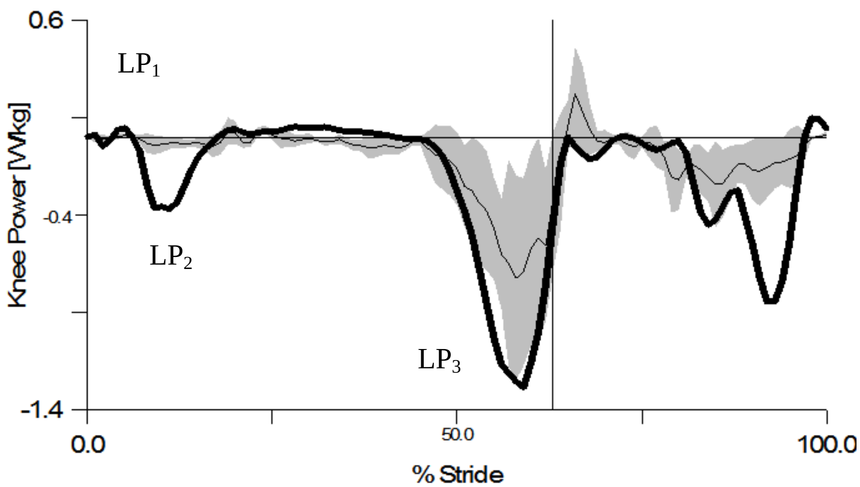


Figure 5.9: Average sagittal knee joint power for stance-control walking (thin line with standard deviation) and open joint walking (bold line). Vertical line represents average toe-off. Left of the line is stance phase and right of the line is swing phase. Positive powers indicate concentric contractions and negative powers indicate eccentric contractions.

Figure 5.9 and Table 5.4 show the average sagittal knee moments for stance-control and open joint walking trials. $LP_1$ and $LP_2$ are the maximum and minimum joint powers during early stance (0-25% of the gait cycle), respectively. $LP_3$ is the minimum joint power during the pre-swing (50-65% of the gait cycle).

The maximum powers experienced when walking were eccentric contractions occurring at $LP_2$ and $LP_3$. Open joint walking trials experienced the largest peak powers (Table 5.4).

Table 5.4: Average sagittal knee joint moments ($M_1$ - $M_4$) and powers ($P_1$ - $P_3$) for level walking (standard deviations in brackets). Extension moments and concentric contractions are positive.

| | **Stance-control** | **Open** | **Locked** |
|---|---|---|---|
| $\mathbf{LM_1}$ [Nm/kg] | -0.12 (0.07) | -0.23 (0.05) | -0.30 (0.09) |
| $\mathbf{LM_2}$ [Nm/kg] | 0.33 (0.05) | 0.46 (0.07) | 0.50 (0.16) |
| $\mathbf{LM_3}$ [Nm/kg] | 0.17 (0.04) | 0.12 (0.03) | 0.10 (0.07) |
| $\mathbf{LM_4}$ [Nm/kg] | 0.37 (0.08) | 0.37 (0.02) | 0.49 (0.03) |
| $\mathbf{LP_1}$ [W/kg] | 0.07 (0.04) | 0.10 (0.05) | 0.22 (0.06) |
| $\mathbf{LP_2}$ [W/kg] | -0.09 (0.03) | -0.48 (0.10) | -0.46 (0.26) |
| $\mathbf{LP_3}$ [W/kg] | -0.96 (0.34) | -1.43 (0.10) | -0.38 (0.09) |

## 5.2.2 Stair descent test

### 5.2.2.1 Temporal stride parameters

Table 5.5 is a summary of the braced limb average stride parameters for stair descent (joint settings 1 (open), 8, 10). The participant walked at a similar pace for all stair descent trials. Different settings had similar swing/stance ratios.

Table 5.5: Stride parameters for the braced limb during stair descent tests. Standard deviations are displayed in brackets.

| Setting | Stride Time (s) | Stance Time (s) | Swing Time (s) | Stance (% of stride) |
|---|---|---|---|---|
| 1 | 1.18 (0.09) | 0.74 (0.06) | 0.45 (0.04) | 62 (2) |
| 8 | 1.26 (0.12) | 0.77 (0.08) | 0.49 (0.06) | 61 (3) |
| 10 | 1.22 (0.06) | 0.77 (0.07) | 0.45 (0.03) | 63 (3) |

### 5.2.2.2 Kinematics

Figure 5.10 and Table 5.6 show average sagittal knee angles for stair descent tests using setting 10 and setting 1 (open). $SA_1$ and $SA_2$ are the minimum and maximum knee joint angles during weight acceptance (0-15% of the gait cycle), respectively. $SA_3$ is the maximum knee joint angle during the stride cycle.

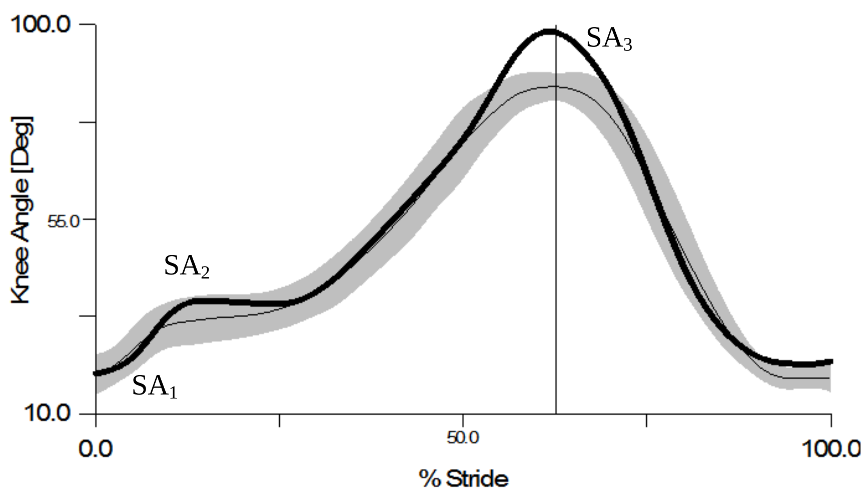


Figure 5.10: Average sagittal knee angle for stair descent using setting 10 (thin line with standard deviation) and setting 1 (bold line). The vertical line represents average toe-off. Left of the line is stance phase and right of the line is swing phase. Knee joint flexion is positive.

During stair descent, setting 1 (open) had a larger maximum knee flexion angle during weight acceptance compared to the other resistance settings. The knee also remained at the constant angle prior to lower the body's centre of mass during single leg support at setting 1, while the angle constantly increased for the resistance settings.

Figure 5.11 and Table 5.6 show average sagittal knee angular velocities for stair descent using setting 10 and setting 1 (open). $SV_1$ is maximum flexion angular velocity during weight acceptance (0-15% of the gait cycle), $SV_2$ is the maximum flexion angular velocity during terminal stance and pre-swing (30-65% of the gait cycle). $SV_3$ is the minimum flexion angular velocity (maximum extension) during the swing phase (60-100% of the gait cycle).

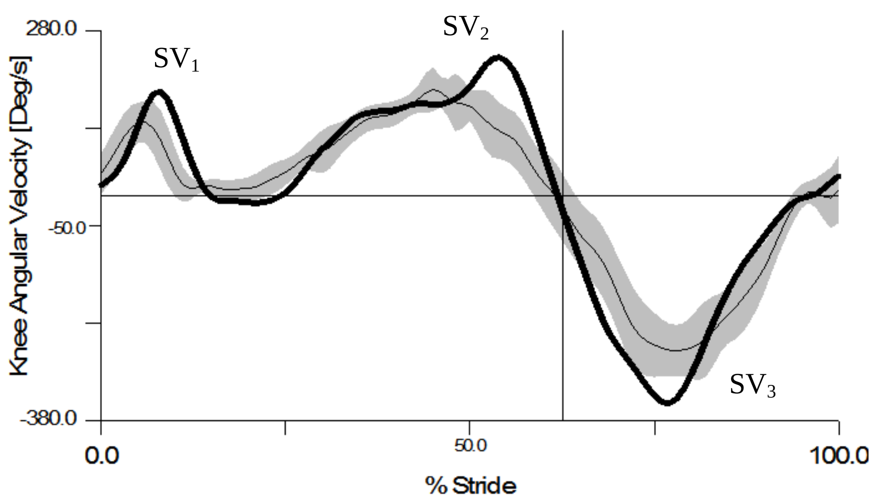


Figure 5.11: Average sagittal knee angular velocity for stair descent using setting 10 (thin line with standard deviation) and setting 1 (bold line). The vertical line represents average toe-off. Left of the line is stance phase and right of the line is swing phase. Flexion angular velocity is positive.

Table 5.6: Average sagittal joint angles ($SA_1$ - $SA_3$), angular velocities ($SV_1$ - $SV_3$), total ROM, and ROM during weight acceptance for stair descent (settings 1, 8, 10). Knee flexion and flexion angular velocities are positive. Standard deviations are displayed in brackets.

| | **Setting 1** | **Setting 8** | **Setting 10** |
|---|---|---|---|
| **$SA_1$** [˚] | 19.3 (4.1) | 16.5 (1.7) | 19.1 (4.7) |
| **$SA_2$** [˚] | 36.4 (3.6) | 29.4 (3.1) | 31.9 (5.5) |
| **$SA_3$** [˚] | 99.1 (1.2) | 91.7 (3.0) | 86.9 (3.5) |
| **$SV_1$** [˚/s] | 188.1 (25.7) | 144.2 (27.8) | 153.7 (32.4) |
| **$SV_2$** [˚/s] | 250.9 (20.1) | 190.3 (27.5) | 199.6 (24.1) |
| **$SV_3$** [˚/s] | -368.0 (25.1) | -299.7 (43.2) | -292.6 (29.0) |
| **ROM Total** [˚] | 79.8 (3.8) | 75.2 (4.0) | 67.7 (3.6) |
| **ROM WA** [˚] | 17.1 (2.8) | 12.9 (3.1) | 12.8 (3.3) |

ROM was largest for setting 1 (open) during stair descent. The ROM was 5.7% smaller while descending the stairs using setting 8, and was reduced by 15.1% while using setting 10. The ROM during the weight acceptance was also greatest using setting 1, and setting 8 and 10 had similar ranges of motion. Peak angular velocities were greatest for setting 1 (Figure 5.11). $SV_1$ for setting 1 was 23.3% greater than setting 8, and 18.3% greater than setting 10. $SV_2$ for setting 1 was 24.1% greater than setting 8, and 20.4 % greater than setting 10.

### 5.2.3 Stand-to-sit test

Figure 5.12 shows the average sagittal knee angle and angular velocity during the stand-to-sits tests using setting 10 and setting 1 (open) of the OWVS. The average sagittal knee angle and angular velocity profiles were similar when using the open and resistance settings.

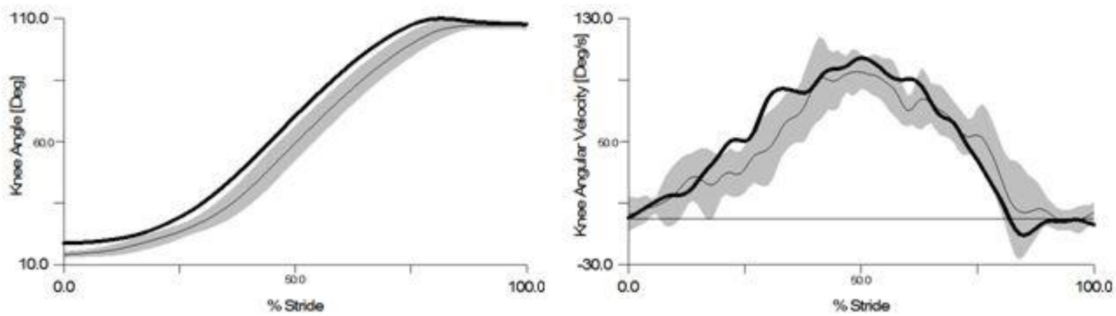


Figure 5.12: Graph of a) average sagittal knee angle and b) average sagittal knee angular velocity during stand-to-sit, using setting 10 (thin line with standard deviation) and setting 1 (bold line). Flexion is positive.

Figure 5.13 shows the average sagittal knee moment and power during the stand-to-sit tests using settings 10 and 1 (open).

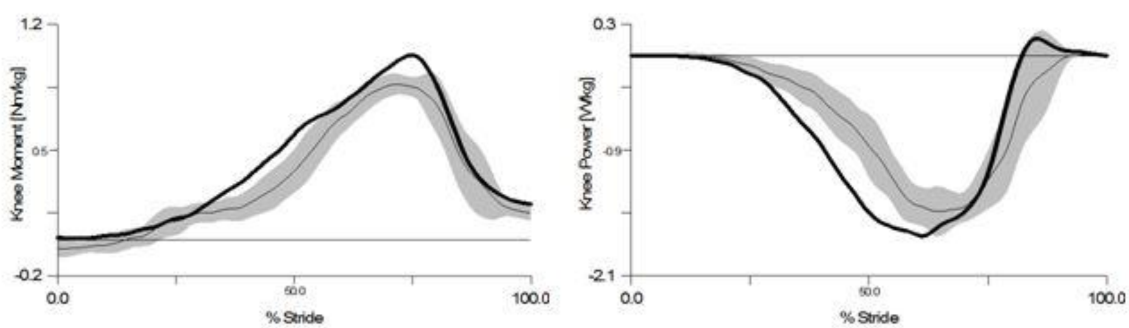


Figure 5.13: Graph of a) average sagittal knee moment and b) average sagittal knee power during stand-to-sits using setting 10 (thin line with standard deviation) and setting 1 (bold line). Extension moments and concentric contractions are positive.

Table 5.7 displays average maximum and minimum values for the stand-to-sit tests, using settings 1, 8, and 10 of the OWVS. The table displays the maximum and minimum sagittal knee joint angles, the maximum sagittal knee joint angular velocity, sagittal ROM of the knee joint, the maximum sagittal knee joint moment, and the minimum sagittal knee joint power.

Table 5.7: Average maximum and minimum sagittal knee angles (flexion is positive), maximum sagittal flexion knee angular velocity, sagittal knee ROM, maximum sagittal knee extension moment, and minimum sagittal knee power (negative powers indicate eccentric contractions).

| | **Setting 1** | **Setting 8** | **Setting 10** |
|---|---|---|---|
| **Sit time** [s] | 1.30 (0.12) | 1.40 (0.14) | 1.47 (0.11) |
| **Min. Angle** [˚] | 18.7 (1.6) | 16.1 (2.3) | 14.1 (1.3) |
| **Max. Angle** [˚] | 110.6 (0.9) | 107.6 (0.5) | 107.8 (1.4) |
| **ROM** [˚] | 91.9 (1.4) | 91.5 (2.1) | 93.8 (2.1) |
| **Max. Velocity** [˚/s] | 116.9 (8.8) | 121.0 (14.6) | 114.6 (10.5) |
| **Max. Moment** [Nm/kg] | 1.06 (0.07) | 0.89 (0.07) | 0.88 (0.05) |
| **Min. Power** [W/kg] | -1.81 (0.23) | -1.77 (0.25) | -1.59 (0.15) |

The time to perform a stand-to-sit motion was the longest while using setting 10, and fastest while using the open setting (setting 1). The ranges of motion were similar for the stand-to-sit trials at all joint settings tested. The maximum knee moments were similar for all settings, and only slightly larger for setting 1 (1.06 ± 0.07 Nm/kg).

## 5.3 Discussion

Overall, the biomechanical testing demonstrated that the OWVS design is promising. The joint resisted knee motion during stance phase and released the knee joint without restricting the knee's ROM. The joint provided flexion resistance during stair descent. Some testing limitations and issues with the joint design were also determined. This section discusses the results in more detail.

### 5.3.1 Walking test

The participant's stride length decreased during stance-control walking. The participant was asked to walk at a slow pace to help the operator manually switch the value setting at the correct time. Decreased stride length is a result of decreased walking velocity [69], so it was expected that the participant's stride lengths would be shorter than walking at a natural pace with the joint at the open setting.

The orthosis did not limit maximum knee joint flexion since the peak knee flexion angle ($LA_4$) for stance-control and open joint walking were comparable to able-bodied walking (i.e., approximately 70˚ of flexion [1], [2], [14]). The participant's knee extension was slightly limited. The minimum knee flexion angle (maximum knee extension) during weight acceptance ($LA_1$) for stance-control walking was slightly larger than able-bodied walking (approximately 0-5˚ of flexion [1], [14]). The limited knee joint extension during the weight acceptance task is probably due to the way the brace fit the participant. The KAFO used for testing was a pre-existing device that was made for a prior patient; the fit was appropriate for initial pilot testing but the knee centre of rotation did not perfectly match the mechanical joint centre of rotation. This likely limited the participant's knee extension during late swing (prior to foot contact). The maximum extension angle during the weight acceptance task ($LA_1$) for locked joint walking did extend more, proving that the ROM of the orthosis was not limited. Thus, the fit of the orthosis on the participant is likely the reason for the reduced knee joint extension. A custom fit orthosis would be a solution to this problem.

During stance-control walking, the orthosis locked knee flexion during single leg support (i.e., minimal change between angles $LA_2$ and $LA_3$). This is similar to the results reported by Irby *et al.* for individuals walking the Dynamic Knee Brace System (developed into the Otto Bock Sensor Walk) [70]. The Dynamic Knee Brace System used foot switches to lock the knee during stance and allowed free knee motion during swing. Differences in angle profiles between the Dynamic Knee Brace System and the OWVS occurred during weight acceptance and when the knee was released for knee joint flexion. The Dynamic Knee Brace System joint angle during the weight acceptance task remained constant, while the OWVS joint angle increased slightly. This indicates that the brace was not completely resisting joint flexion during weight acceptance. The OWVS also released the knee joint for flexion earlier (to prepare for swing) than the Dynamic Knee Brace System did. This difference was due to the different methods used to control the joints. The Dynamic Knee Brace System uses a footswitch to release the knee after toe off [70], while the OWVS was manually controlled, and the knee was released just prior to toe off.

The walking tests indicated an issue with ROM during weight acceptance. The joint was designed to completely resist joint flexion through the entire stance phase. The locked joint walking tests had a knee ROM of 8.3 ± 1.3˚ during weight acceptance. The joint should have been completely locked throughout the gait cycle during this test (i.e., little or no ROM). After inspecting the joint, some mechanical 'play' was found between 0-15˚ of flexion, allowing the joint to move freely between these angles. The movement was due to the connecting link rod not being held against the upper link of the joint (see section 6.2 for more detail and methods for correcting this problem).

The OWVS was manually switched between locked and open settings, locking before braced limb heel contact and opening just prior to toe off (for the stance-control walking tests). This allowed the participant to walk comfortably, but standard deviations were larger during the swing phase for the stance-control trials compared to the open joint walking trials. This could be because the manually switched valve did not open at the same point on every trial. For future testing, a control system should be implemented to provide consistent switching.

The peak flexion angular velocities for flexion and extension during the open joint tests were similar to able-bodied peak knee angular velocities [1], [14]. This indicates that the joint achieved free motion at the open setting. For stance-control walking, the joint resisted the peak knee flexion moments during mid-stance and remained at a constant angle when moments were applied to the joint.

### 5.3.2 Stair descent test

The participant descended the stairs at similar rates for all settings tested (1, 8, 10). All stance times met the design criteria of being able to remain in stance phase for 0.7 – 1.0 s. Although the participant attempted to relax his quadriceps and let the joint support body weight, it was difficult to determine if the able-bodied participant was still using knee extensor muscles to help resist joint motion. This is one of the limitations of testing with an able-bodied participant instead of an orthosis user with knee extensor weakness.

The joint's ROM decreased with increasing resistance settings. Knee ROM during stair descent is approximately 78 – 90˚ for able-bodied individuals [19]–[21]. The resistance settings ROM were lower than this range (75.2 ± 4.0˚ for setting 8, and 67.7 ± 3.6˚ for setting 10). This suggests that the orthotic joint was resisting knee joint flexion, but it is impossible to eliminate the possibility that the participant was not letting the joint lower their centre of mass completely to the following step. Peak flexion angular velocities also decreased for the resistance settings, compared to the open joint, indicating that the joint resisted flexion.

### 5.3.3 Stand-to-sit test

The participant was able to move comfortably from a standing to seated position at settings 1, 8, and 10. The ROM was similar for all settings, with maximum knee angles of approximately 110˚, meeting the design criteria that the joint should have a ROM of 0-110˚ to allow for the individual to sit comfortably.

As expected, stand-to-sit descent times were greatest for setting 10 and shortest for setting 1 (open). The resistance settings resisted joint flexion, lowering the body's centre of mass smoothly to the seat. The angle profiles were similar between the open and resistance settings, implying that the joint's flexion resistance did not change the participant's stand-to-sit movement pattern, but merely lengthened the time required to descend.

# Chapter 6: Conclusions and Future Work

## 6.1 Conclusions

In this thesis, the mechanical and hydraulic systems of a novel orthotic knee joint were designed and evaluated to address current SCKAFO device limitations. A variable resistance orthotic knee joint, the Ottawalk-Variable Speed (OWVS), was designed to allow individuals with knee extensor weakness to walk on level ground with a more natural gait pattern, descend stairs smoothly, and sit in a controlled manner. This design is low profile, so the orthosis will fit beneath normal clothing. The OWVS was based on the Ottawalk-Speed, developed at the Ottawa Hospital Rehabilitation Centre, and a variable flow hydraulic valve adapted from a commercial prosthetic ankle designed by Endolite Prosthetics and Orthotics Products (Chas A. Blatchford & Son Limited, Basingstoke, UK).

Table 6.1 displays the target testable design criteria for the OVWS, determined in section 3.1, and the criteria achieved during testing.

The OWVS structural design met all requirements. The design was lightweight and compact, which would allow the user to wear the orthosis beneath standard fitting clothing. The OWVS was also designed to be used with standard orthotic components, and can be swapped with many existing KAFO and SCKAFO joints. Functionally, the joint was able to switch to the locked setting at any joint angle, and disengage from the locked setting at any angle without requiring a knee extension moment.

Mechanical testing revealed that the design always allowed free knee joint extension, allowed uninhibited knee flexion at the open setting, and that the variable resistance valve's motor/gearbox was sufficient for the design. Unfortunately, the OWVS did not completely resist joint flexion, at the locked setting during, mechanical testing since fluid leaked from the around the variable resistance valve's top. This leak allowed for joint flexion at the locked setting, and likely reduced flexion resistance at settings 2-10. Even though the OWVS provided substantial joint flexion resistance at the closed setting (setting 0) and at the higher resistance settings (settings 6, 8 and 10), the fluid leak problem should be addressed in future designs since the joint should be able to completely resist joint flexion.

Table 6.1: The Ottawalk-Variable Speed design criteria goals and the criteria achieved.

| Function | Design Criteria | OWVS Test Results | Summary |
|---|---|---|---|
| Total joint weight | <560 g | 418 g (without electronics), 526 g (with electronics) | Fully met |
| Connection to orthosis | Modular design that can be used with standard orthotic components | Criteria met, joint can be used with standard orthotic components, and swapped with certain orthotic joints | Fully met |
| Maximum medial-lateral profile | 30 mm | 23.7 mm | Fully met |
| Range of motion | 0 - 110˚ (fully extend limb and sit comfortably) | Full range of motion is 0-112˚ | Fully met |
| Function during stance | Lock and prevent knee joint flexion at any angle, allow knee joint extension | Joint can be switched to lock mode at any joint angle and always allows for knee joint extension (check valve design). Joint was unable to completely resist knee flexion at locked setting | Partially met. Joint partially resisted knee flexion at locked setting |
| Function during swing | Free motion (uninhibited knee flexion and extension) | Free motion was achieved. Joint had full ROM during the swing phase | Fully met |
| Function during stair walking | Resist knee flexion to lower body centre of mass smoothly (support user for 0.7 - 1.0 seconds during the stance phase of stair descent) | Stance phase for stair descents using settings 8 and 10 were within the target range (0.74 s open joint, 0.77 s setting 8 and 10) | Fully met, more testing required for better understanding of resistance settings |
| Function during stand-to-sit | Resist knee flexion to lower body centre of mass smoothly | Resistance settings 8 and 10 slowed participant's descent times (1.30 s open joint, 1.40 s setting 8, and 1.47s setting 10) | Fully met |
| Freely permit maximum flexion angular velocity | > 325˚/s | 358.7 ± 9.9 ˚/s (open joint walking) | Fully met |
| Freely permit maximum extension angular velocity | > 350˚/s | 368.0 ± 25.1 ˚/s (open joint stair descent) | Fully met |
| Valve reaction time | <100 ms (0.1 s) switching between the open and locked settings | 73.4 ± 3.0 ms between the open and locked setting (setting 0 and 1) | Fully met |

Biomechanical testing demonstrated that, overall, the OWVS design is promising, supporting an 80.74 kg participant. The joint resisted knee motion during stance and released the knee joint without restricting knee ROM. The OWVS provided flexion resistance during stair descent and stand-to-sit motions. A concern noticed during the walking tests was that the joint allowed for some knee flexion during weight acceptance. Some mechanical 'play' was found between 0-15˚ of flexion, allowing the joint to move freely between these angles. A solution to solve the mechanical 'play' for future designs is explained in section 6.2.2.

While the OWVS met the design requirement for stair descent (i.e., support the user for 0.7-1.0 s during stance phase of stair descent), it was difficult to determine if the participant was allowing the orthosis to completely lower their centre of mass or if the participant was aiding the orthosis with their knee extensor muscles. A future testing protocol with individuals with knee extensor weakness is required to confirm joint function on stair descent. During stand-to-sit, the orthosis resisted knee motion, increasing the user's descend time, but did not restrict knee ROM.

Overall, the OWVS is a promising design for a microprocessor controlled SCKAFO. The low profile will allow users to wear the orthosis beneath their clothing and the variable resistance design allows users to negotiate different terrain types, unlike most SCKAFOs that are designed for level ground walking. The cost of producing the prototype OWVS was approximately $4200 CAD, of which the majority of the cost was related to machining the OWS components ($3375 CAD). Compared to microprocessor controlled SCKAFOs, this is relatively inexpensive, especially considering that the per unit machining cost would decrease significantly if the joint were put into production.

## 6.2 Future work

While the OWVS design was promising, some improvements can be made in future designs and additional tests that should be performed prior to using the orthosis on the target population. This section outlines the design changes that should be made in future designs to improve OWVS function and new testing procedures for the prototypes.

### 6.2.1 Variable resistance valve leak

The primary concern during testing was that the orthosis was unable to completely resist knee flexion at the locked setting. The tests in section 4.4 determined that the variable resistance valve was allowing hydraulic oil to pass around the valve when in the locked setting and collect in the reservoir. This likely reduced the valve's flexion resistance at the other resistance settings.

The leak occurred because the bore where the valve rotates had to be opened slightly to allow for smooth valve rotation. The clearance between the bore's inner diameter and valve's outer diameter should ideally be 2-3μm, but was 18 μm after opening the hole. This is likely why the leak occurred at the variable resistance valve-bore interface.

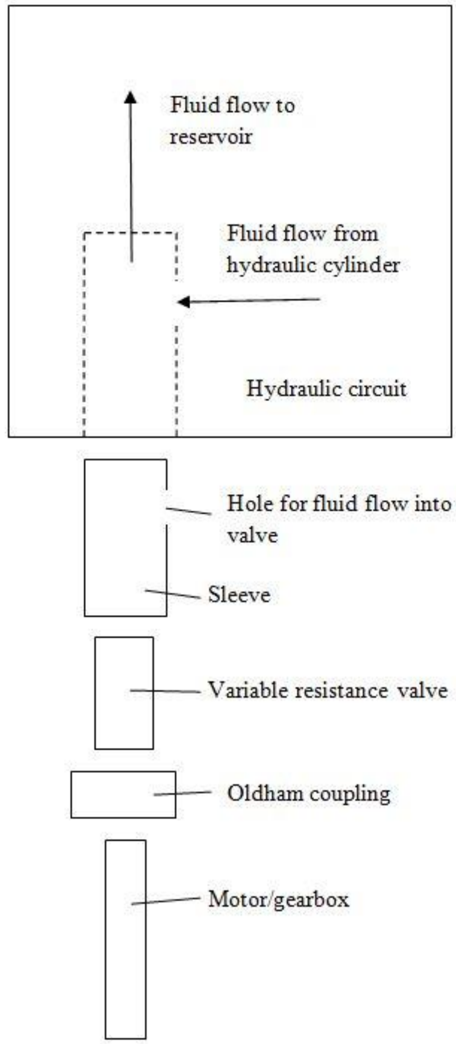


Figure 6.1: Block diagram of the variable resistance valve assembly concept for the future design of the Ottawalk-Variable Speed.

A possible solution for this problem would be to create a 'sleeve' in which the valve and motor/gearbox are assembled. This sleeve would be a cylinder machined to a very high tolerance, with an inner diameter allowing for the 2-3 μm clearance between the valve and the hole. A hole in the side of the sleeve would be cut to match the diameter of the channel leading to the variable resistance valve. The valve would rotate in this sleeve, but with the ideal clearance no fluid would escape. The sleeve would be inserted into the hydraulic circuit and aligned with the bore.

Concentricity of the valve and motor is also very important to allow the valve to rotate without rubbing against the wall and creating friction. An Oldham coupling could be positioned between the gearbox output shaft and the valve. Oldham couplings are designed to transmit torque from an input to an output shaft with axial misalignment [71]. The Oldham coupling can be purchased ([71], [72]) and applied to the design.

A simple block diagram of the sleeve concept is shown in Figure 6.1. The final design would consist of the motor/gearbox coupled to the valve with an Oldham coupling, which would be assembled in the sleeve. This assembly would allow for the valve to rotate within the sleeve, even with some axial misalignment between the gearbox output shaft and the valve. This assembly would then be bonded to the hydraulic circuit with the hydraulic cylinder, reservoir, and check valve (similar to the current design).

Roundness and cylindricity are important factors to minimize friction between the valve and bore, which in turn helps eliminate leaking between components. If the valve was made in a production environment, cylindrical grinding could be performed on the mating faces of the valve and bore where the valve sits in order to further reduce friction.

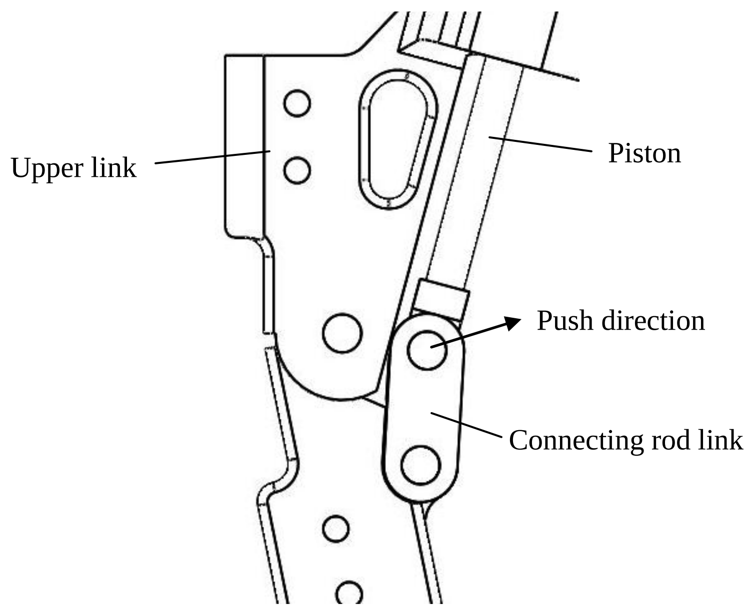


Figure 6.2: Mechanical play in the OWS joint. When the joint is fully extended and a flexion motion is applied, the connecting rod link is briefly pushed away from upper link.

### 6.2.2 Mechanical play in joint

Some mechanical ‘play’ was found between 0-15˚ of flexion, allowing the joint to move freely between these angles. This was noticed during the walking tests, where the joint was flexing during the weight acceptance task. When a flexion motion was applied to the joint from a fully extended position, the connecting rod link briefly pushed outwards, away from the upper link of the OWS joint (Figure 6.2). When the link was pushed outwards, the motion was not resisted, allowing for a small amount of joint flexion, and also applying a shear force to the piston of the hydraulic cylinder. The joint was designed so that the connecting link rod would remain in contact with the upper link constantly, guiding the motion of link.

A solution for this problem would be to add a spring or elastic band to the design to keep the connecting rod link in contact with the upper link of the joint. This design would guide the direction of the connecting rod link and allow for only axial force to be transmitted to the piston.

### 6.2.3 Electronics casing

A design to attach the electronics to the brace needs to be determined. The electronics include the PCB, Bluetooth adapter, and batteries. For testing, these devices were placed in a bag and taped to the orthosis. A more permanent and aesthetically pleasing design needs to be developed for a final product. Ideally, the design would safely secure the electronics to the lateral side of the orthosis, have minimal dimension, and allow the device to be worn beneath standard fitting clothing.

### 6.2.4 Testing

Once a new OWVS prototype that addresses the issues mentioned above has been manufactured, the joint will require further mechanical and biomechanical testing. The resistance setting test (section 4.3) should be performed again to verify that the joint completely resists flexion at the locked setting and whether the resistance settings have changed with the new design.

The biomechanical test procedure should remain similar. For the stance-control walking tests, the control system should be able to accurately switch between the appropriate settings during gait. This is needed to ensure that the joint is locked and unlocked consistently during biomechanical testing.

Hand railings should be added to the stair case for future testing. These railings would help the participant feel more confident about placing their entire weight on the orthosis and letting their leg muscles relax. This test would better determine how the resistance settings work for stair descent. During the stair descent test reported above, it was unclear whether the participant was aiding the OWVS to resist knee flexion.

### 6.2.5 Control system

When the OWVS mechanical and hydraulic systems are finalized, an embedded method for automatically controlling the variable resistance valve will be required. The control system should use wearable sensors to determine the individual's limb movements, categorize these moments, and switch the valve accordingly.

# References

[1] J. Perry and J. M. Burnfield, *Gait analysis : normal and pathological function*, 2nd ed.. Thorofare, NJ: SLACK, 2010.

[2] P. Bowker, D. N. Condie, D. L. Bader, and D. J. Pratt, *Biomechanical basis of orthotic management*. Oxford England; Boston: Butterworth-Heinemann, 1993.

[3] A. Cullell, J. C. Moreno, E. Rocon, A. Forner-Cordero, and J. L. Pons, "Biologically based design of an actuator system for a knee–ankle–foot orthosis," *Mech. Mach. Theory*, vol. 44, no. 4, pp. 860–872, Apr. 2009.

[4] M. K. Taylor, "Use of KAFOs for Patients with Cerebral Vascular Accident, Traumatic Brain Injury, Spinal Cord Injury," *J. Prosthet. Orthot.*, vol. 18, no. 7, pp. 202–203, 2006.

[5] C. Slemenda, K. D. Brandt, D. K. Heilman, S. Mazzuca, E. M. Braunstein, B. P. Katz, and F. D. Wolinsky, "Quadriceps Weakness and Osteoarthritis of the Knee," *Ann. Intern. Med.*, vol. 127, no. 2, pp. 97–104, Jul. 1997.

[6] K. Shamaei, P. C. Napolitano, and A. Dollar, "Design and Functional Evaluation of a Quasi-Passive Compliant Stance Control Knee-Ankle-Foot Orthosis," *IEEE Trans. Neural Syst. Rehabil. Eng.*, vol. 22, no. 2, pp. 258–268, Mar. 2014.

[7] T. Yakimovich, E. D. Lemaire, and J. Kofman, "Engineering design review of stance-control knee-ankle-foot orthoses," *J. Rehabil. Res. Dev.*, vol. 46, no. 2, pp. 257–267, 2009.

[8] A. G. McMillan, K. Kendrick, J. W. Michael, J. Aronson, and G. W. Horton, "Preliminary Evidence for Effectiveness of a Stance Control Orthosis," *J. Prosthet. Orthot.*, vol. 16, no. 1, pp. 6–13, Jan. 2004.

[9] E. D. Lemaire, R. Samadi, L. Goudreau, and J. Kofman, "Mechanical and biomechanical analysis of a linear piston design for angular-velocity-based orthotic control," *J. Rehabil. Res. Dev.*, vol. 50, no. 1, pp. 43–52, 2013.

[10] B. Zacharias and A. Kannenberg, "Clinical Benefits of Stance Control Orthosis Systems: An Analysis of the Scientific Literature," *J. Prosthet. Orthot.*, vol. 24, no. 1, pp. 2–7, Jan. 2012.

[11] C. W. Martin and D. Edeer, "E-MAG Active, a newer Stance Control Knee Ankle Foot Orthosis (SCKAFO) in the context of workers' compensation," WorkSafeBC Evidence-Based Practice Group, Dec. 2010.

[12] M. Whittle, *Gait analysis an introduction*, 4th ed.. Edinburgh ; New York: Butterworth-Heinemann, 2007.

[13] StudyBlue Inc., “Gait & Movement Analysis,” *StudyBlue*, 2013. [Online]. Available: http://www.studyblue.com/notes/note/n/gait--movement-analysis/deck/8375260. [Accessed: 01-Oct-2014].

[14] D. A. Winter, *The biomechanics and motor control of human gait : normal, elderly and pathological.*, 2nd ed.. Waterloo, Ont: University of Waterloo Press, 1991.

[15] D. A. Winter, *Biomechanics and Motor Control of Human Movement*, Fourth Edition. John Wiley & Sons, Inc, 2009.

[16] D. A. Winter and D. G. E. Robertson, “Joit torque and energy patterns in normal gait,” *Biol. Cybern.*, vol. 29, no. 3, pp. 137–142, Sep. 1978.

[17] R. Riener, M. Rabuffetti, and C. Frigo, “Stair ascent and descent at different inclinations,” *Gait Posture*, vol. 15, no. 1, pp. 32–44, Feb. 2002.

[18] B. J. McFadyen and D. A. Winter, “An integrated biomechanical analysis of normal stair ascent and descent,” *J. Biomech.*, vol. 21, no. 9, pp. 733–744, 1988.

[19] O. S. Mian, J. M. Thom, M. V. Narici, and V. Baltzopoulos, “Kinematics of stair descent in young and older adults and the impact of exercise training,” *Gait Posture*, vol. 25, no. 1, pp. 9–17, Jan. 2007.

[20] N. D. Reeves, M. Spanjaard, A. A. Mohagheghi, V. Baltzopoulos, and C. N. Maganaris, “The demands of stair descent relative to maximum capacities in elderly and young adults,” *J. Electromyogr. Kinesiol.*, vol. 18, no. 2, pp. 218–227, Apr. 2008.

[21] A. Protopapadaki, W. I. Drechsler, M. C. Cramp, F. J. Coutts, and O. M. Scott, “Hip, knee, ankle kinematics and kinetics during stair ascent and descent in healthy young individuals,” *Clin. Biomech.*, vol. 22, no. 2, pp. 203–210, Feb. 2007.

[22] A. C. Novak and B. Brouwer, “Sagittal and frontal lower limb joint moments during stair ascent and descent in young and older adults,” *Gait Posture*, vol. 33, no. 1, pp. 54–60, Jan. 2011.

[23] “One Degree of Separation,” *Christopher & Dana Reeve Foundation*, 2009. [Online]. Available:http://www.christopherreeve.org/site/c.ddJFKRNoFiG/b.5091685/k.58BD/One_Degree_of_Separation.htm. [Accessed: 03-Sep-2014].

[24] S. C. Government of Canada, “Statistics Canada: Canada’s national statistical agency,” 2014. [Online]. Available: http://www.statcan.gc.ca/start-debut-eng.html. [Accessed: 03-Sep-2014].

[25] J. N. Russell, G. E. Hendershot, F. LeClere, L. J. Howie, and M. Adler, *Trends and differential use of assistive technology devices: United States, 1994.* 1997.

[26] “Foot Drop and Stroke.” [Online]. Available: http://www.stroke-rehab.com/foot-drop.html. [Accessed: 08-Aug-2014].

[27] Custon Orthotic Design Group Ltd., “CODG - Knee Ankle Foot Orthoses (KAFO).” [Online]. Available: http://www.customorthotic.ca/. [Accessed: 29-Sep-2014].

[28] Capstone Orthopedic, “KAFOs - Knee ankle foot orthoses,” *Capstone Orthopedic*. [Online]. Available: http://www.capstoneorthopedic.com. [Accessed: 31-Oct-2013].

[29] K. R. Kaufman, S. E. Irby, J. W. Mathewson, R. W. Wirta, and D. H. Sutherland, “Energy-Efficient Knee-Ankle-Foot Orthosis: A Case Study.,” *J. Prosthet. Orthot.*, vol. 8, no. 3, pp. 79–85, 1996.

[30] S. Hwang, S. Kang, K. Cho, and Y. Kim, “Biomechanical effect of electromechanical knee–ankle–foot-orthosis on knee joint control in patients with poliomyelitis,” *Med. Biol. Eng. Comput.*, vol. 46, no. 6, pp. 541–549, Jun. 2008.

[31] B. Phillips, “Predictors of Assistive Technology Abandonment,” vol. 5, no. 1, pp. 36–45, Jun. 1993.

[32] Ottobock, “Ottobock Advanced Orthotics.” Apr-2013.

[33] “Becker Orthopedic.” [Online]. Available: http://www.beckerortho.com/index.htm. [Accessed: 18-Aug-2014].

[34] “Fillauer Orthotics Line.” [Online]. Available: http://fillauer.com/Orthotics/. [Accessed: 04-Nov-2013].

[35] E. D. Lemaire, L. Goudreau, T. Yakimovich, and J. Kofman, “Angular-Velocity Control Approach for Stance-Control Orthoses,” *IEEE Trans. Neural Syst. Rehabil. Eng.*, vol. 17, no. 5, pp. 497–503, 2009.

[36] “Horton’s Stance Control.” [Online]. Available: http://www.stancecontrol.com/. [Accessed: 04-Nov-2013].

[37] T. Yakimovich, J. Kofman, and E. D. Lemaire, “Design and Evaluation of a Stance-Control Knee-Ankle-Foot Orthosis Knee Joint,” *IEEE Trans. Neural Syst. Rehabil. Eng.*, vol. 14, no. 3, pp. 361–369, 2006.

[38] Otto Bock Health Care, “Ottobock Advanced Orthotics: Stance Control KAFOs and Unilateral Joints.” 2013.

[39] “Ottobock,” *ottobock.*, 2014. [Online]. Available: http://professionals.ottobockus.com/cps/rde/xchg/ob_us_en/hs.xsl/index.html. [Accessed: 18-Aug-2014].

[40] T. Shlomovitz and R. Shelly, “Knee-ankle-foot orthotic device,” US7462159 B1, 09-Dec-2008.

[41] Kiser's Orthotics Prosthetics Services Inc., "Orthotics Prosthetics NE (New England)," *Orthotics Prosthetics NE (New England)*. [Online]. Available: http://www.orthoticsprostheticsne.com/home/. [Accessed: 24-Sep-2014].

[42] T. Yakimovich, E. D. Lemaire, and J. Kofman, "Preliminary kinematic evaluation of a new stance-control knee–ankle–foot orthosis," *Clin. Biomech.*, vol. 21, no. 10, pp. 1081–1089, Dec. 2006.

[43] J. M. Naft and W. S. Newman, "Orthosis knee joint," US6770045 B2, 03-Aug-2004.

[44] S. E. Irby, K. R. Kaufman, J. W. Mathewson, and D. H. Sutherland, "Automatic control design for a dynamic knee-brace system," *IEEE Trans. Rehabil. Eng.*, vol. 7, no. 2, pp. 135–139, Jun. 1999.

[45] J. C. Moreno, F. Brunetti, E. Rocon, and J. L. Pons, "Immediate effects of a controllable knee ankle foot orthosis for functional compensation of gait in patients with proximal leg weakness," *Med. Biol. Eng. Comput.*, vol. 46, no. 1, pp. 43–53, Jan. 2008.

[46] R. Auberger, "Knee orthosis, and method for controlling a knee orthosis," US20110071452 A1, 24-Mar-2011.

[47] A. D. Segal, M. S. Orendurff, G. K. Klute, M. L. McDowell, J. A. Pecoraro, J. Shofer, and J. M. Czerniecki, "Kinematic and kinetic comparisons of transfemoral amputee gait using C-Leg and Mauch SNS prosthetic knees," *J. Rehabil. Res. Dev.*, vol. 43, no. 7, pp. 857–870, Dec. 2006.

[48] A. C. Novak and B. Brouwer, "Kinematic and kinetic evaluation of the stance phase of stair ambulation in persons with stroke and healthy adults: a pilot study," *J. Appl. Biomech.*, vol. 29, no. 4, pp. 443–452, Aug. 2013.

[49] T. Schmalz, S. Blumentritt, and B. Marx, "Biomechanical analysis of stair ambulation in lower limb amputees," *Gait Posture*, vol. 25, no. 2, pp. 267–278, Feb. 2007.

[50] K. A. Bernhardt and K. R. Kaufman, "Loads on the uprights of a knee-ankle-foot orthosis," *Prosthet. Orthot. Int.*, vol. 35, no. 1, pp. 106–112, Mar. 2011.

[51] K. A. Bernhardt, S. E. Irby, and K. R. Kaufman, "Consumer opinions of a stance control knee orthosis," *Prosthet. Orthot. Int.*, vol. 30, no. 3, pp. 246–256, Dec. 2006.

[52] A. I. Batavia and G. S. Hammer, "Towrd the development of consumer-based criteria for the evaluation of assistive devices," *J. Rehabil. Res. Dev.*, vol. 27, no. 4, pp. 425–436, 1990.

[53] E. W. Weisstein, "Rotation Matrix," *MathWorld - A Wolfram Web Resource*. [Online]. Available: http://mathworld.wolfram.com/RotationMatrix.html. [Accessed: 24-Oct-2014].

[54] C. E. Wilson, *Kinematics and dynamics of machinery*, 3rd ed.. Upper Saddle River, NJ: Prentice Hall, Pearson Education, 2003.

[55] R. C. Hibbeler, *Mechanics of materials*, 8th ed.. Boston: Pearson Prentice Hall, 2011.

[56] AZO Materials, "AISI 4140 Alloy Steel (UNS G41400)," *AZO Network*. [Online]. Available: http://www.azom.com/article.aspx?ArticleID=6769. [Accessed: 03-Nov-2014].

[57] Dassault Systèmes, "SolidWorks." [Online]. Available: http://www.solidworks.com/. [Accessed: 03-Nov-2014].

[58] F. M. White, *Fluid Mechanics Sixth Edition*. McGraw-Hill Higher Education, 2008.

[59] E. Eitel, "Basics of rotary encoders: Overview and new technologies," *Machine Design*, 07-May-2014. [Online]. Available: http://machinedesign.com/sensors/basics-rotary-encoders-overview-and-new-technologies-0. [Accessed: 27-Jan-2015].

[60] Bal-tec Inc., "Ball Check Valves,Ball Poppet Valves, Ball and Seat Valves, Ball Valves, Diamond Impregnated Lapping Ball, Diamond Impregnated Lapping Ball on a Stem," *Bal-tec*, 10-Sep-2014. [Online]. Available: https://www.precisionballs.com/ball_valve.php. [Accessed: 10-Sep-2014].

[61] Lee Valley Tools Ltd., "Lee Valley Tools - Woodworking Tools, Gardening Tools, Hardware," *Lee Valley & veritas*. [Online]. Available: http://www.leevalley.com/en/home.aspx. [Accessed: 18-Nov-2014].

[62] Tiertime Corporation, "tiertimecorporation," *tiertimecorporation*. [Online]. Available: http://www.tiertimecorp.com/. [Accessed: 18-Nov-2014].

[63] McMaster-Carr Supply Company, "McMaster-Carr." [Online]. Available: http://www.mcmaster.com/. [Accessed: 18-Nov-2014].

[64] Harrison Electropolishing L.P., "Ra & RMS Surface Roughness Calculation - Surface Finish Formulas," *Harrison Electropolishing L.P.* [Online]. Available: http://www.harrisonep.com/electropolishing-ra.html. [Accessed: 09-Feb-2015].

[65] S. Kalpakjian, *Manufacturing engineering and technology*, 5th ed.. Harlow: Prentice Hall, 2006.

[66] T. D. Collins, S. N. Ghoussayni, D. J. Ewins, and J. A. Kent, "A six degrees-of-freedom marker set for gait analysis: Repeatability and comparison with a modified Helen Hayes set," *Gait Posture*, vol. 30, no. 2, pp. 173–180, Aug. 2009.

[67] W. S. Montgomery, "Development and Application of a Virtual Reality Stumble Method to Test an Angular Velocity Control Orthosis," 2013.

[68] "C-Motion | Digitizing Pointer." [Online]. Available: http://www.c-motion.com/products/digitizing-pointer/. [Accessed: 25-Nov-2014].

[69] J. P. Holden, "Changes in knee joint function over a wide range of walking speeds," *Clin. Biomech.*, vol. 12, no. 6, pp. 375–382.

[70] S. E. Irby, “Gait of stance control orthosis users: The Dynamic Knee Brace System,” *Prosthet. Orthot. Int.*, vol. 29, no. 3, pp. 269–282, Dec. 2005.

[71] Ruland, “Oldham Coupling: Shaft Couplings for Servo Applications,” *Ruland*. [Online]. Available: http://www.ruland.com/ps_couplings_oldham.asp. [Accessed: 15-Feb-2015].

[72] Huco Engineering Industries Ltd, “Huco: World Leaders in Small Precision Couplings,” *Huco Dynatork*. [Online]. Available: http://www.huco.com/. [Accessed: 13-Feb-2015].

[73] Vektek Inc., “Vektek: Products: Hydraulic: Cylinders: Threaded Mini.” [Online]. Available: http://vektek.com/Product.aspx?CategoryUid=65. [Accessed: 15-Dec-2014].

# Appendix A: Technical Drawings

Component drawings are included in this section. Dimensions are not included at the request of the industrial partner.

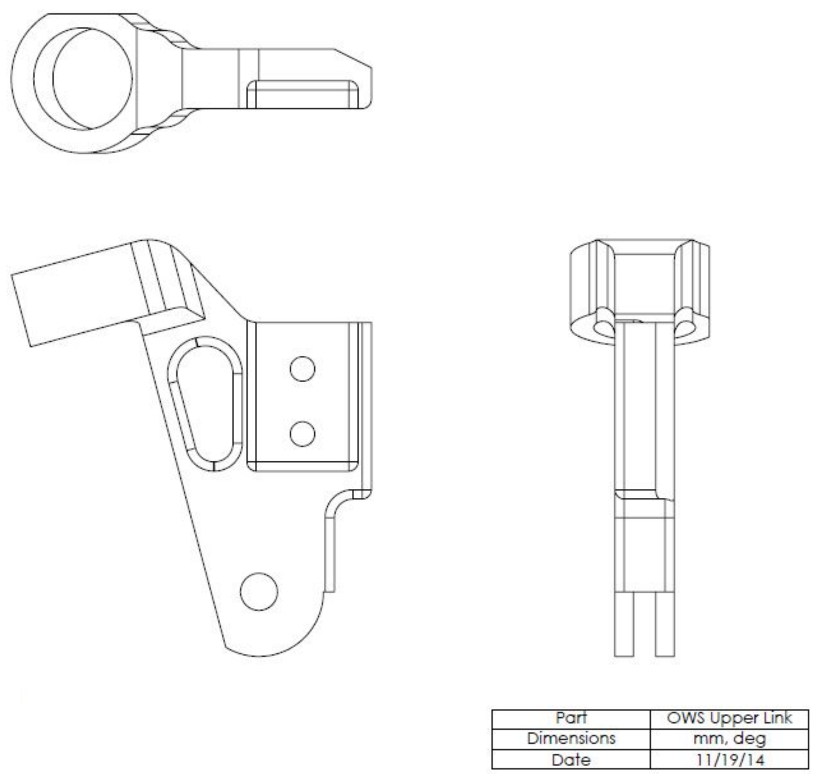


Figure A.1: OWS upper link.

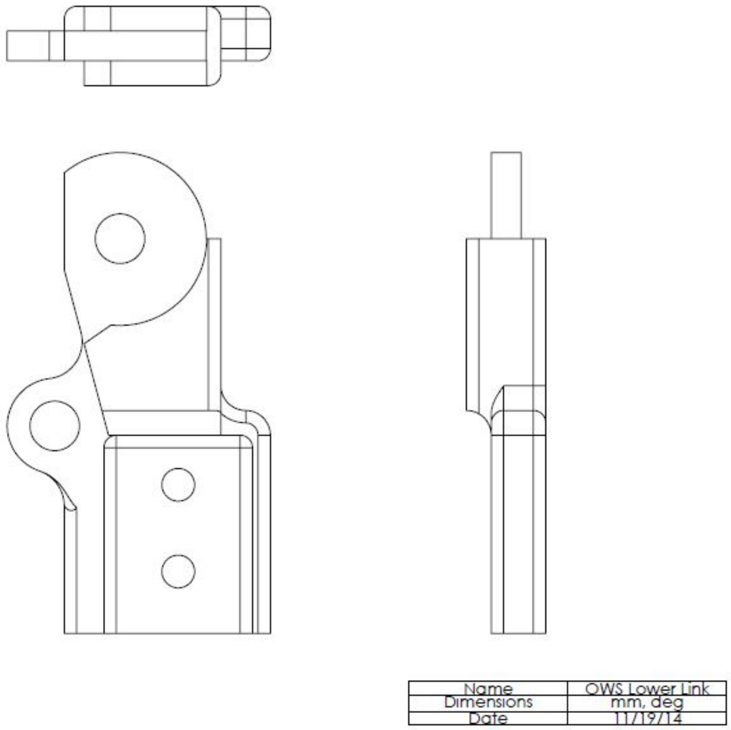


Figure A.2: OWS lower link.

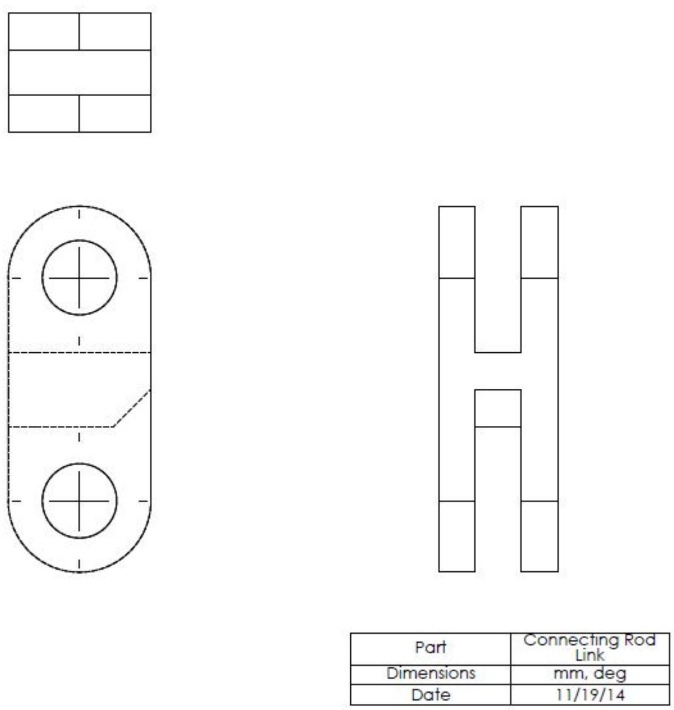


Figure A.3: OWS connecting rod link.

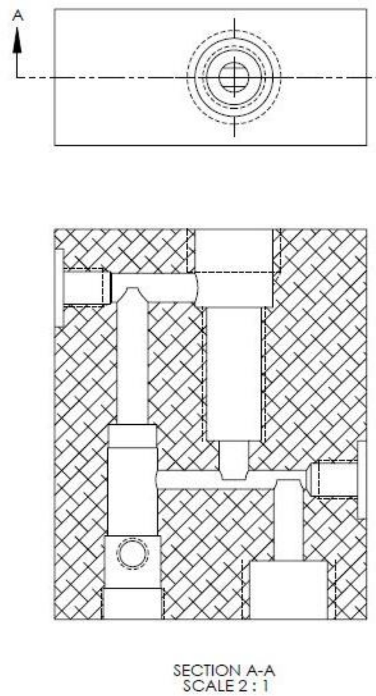


| Part | Hydraulic Block |
|---|---|
| Dimensions | mm |
| Date | 11/19/14 |

Figure A.4: Hydraulic circuit block.

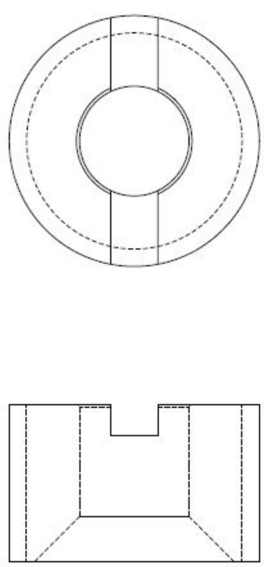

| Name | Check Valve Seat |
|---|---|
| Dimensions | mm |
| Date | 11/19/14 |

Figure A.5: Check valve seat.

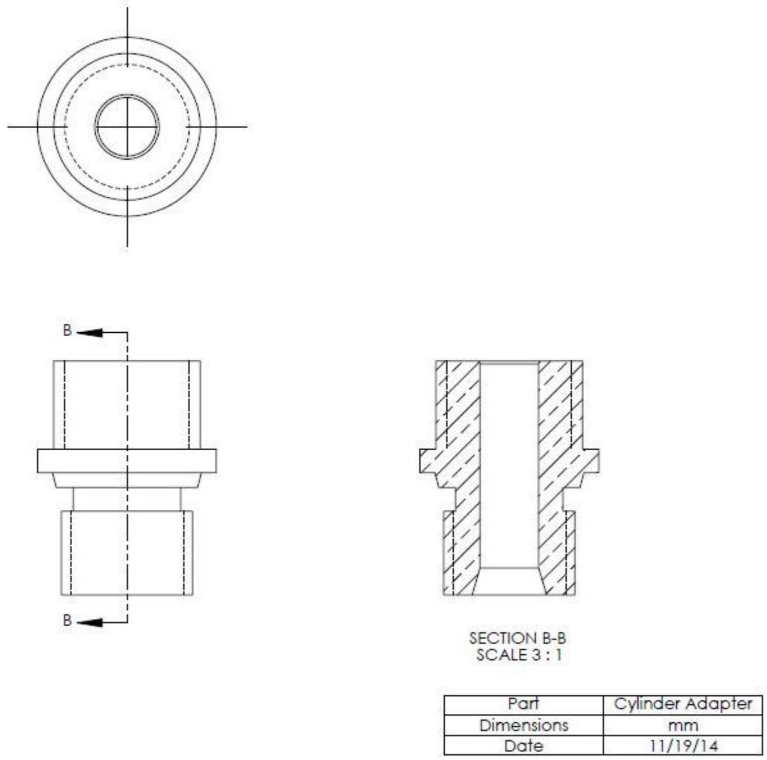


Figure A.6: Cylinder adapter.

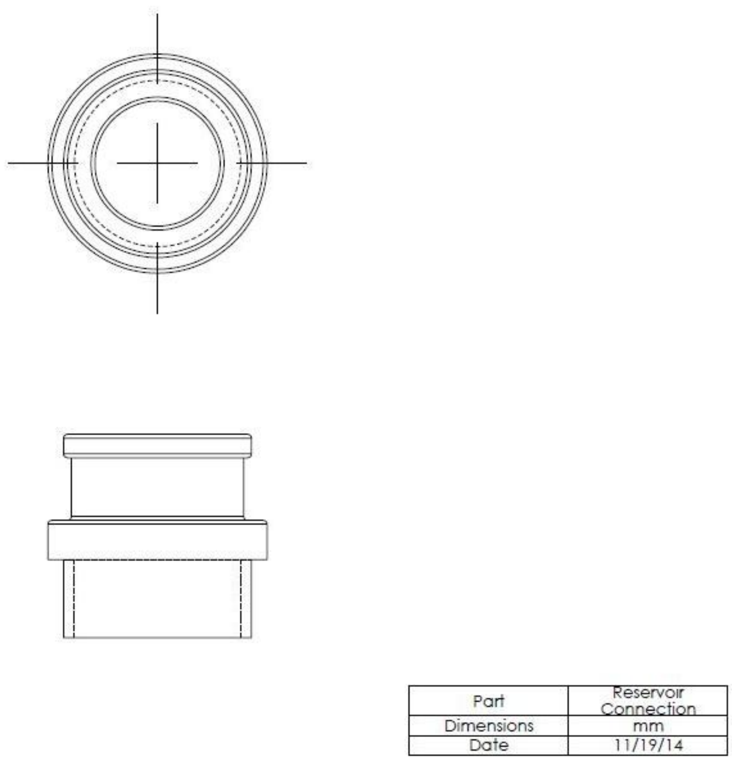


Figure A.7: Reservoir connection.

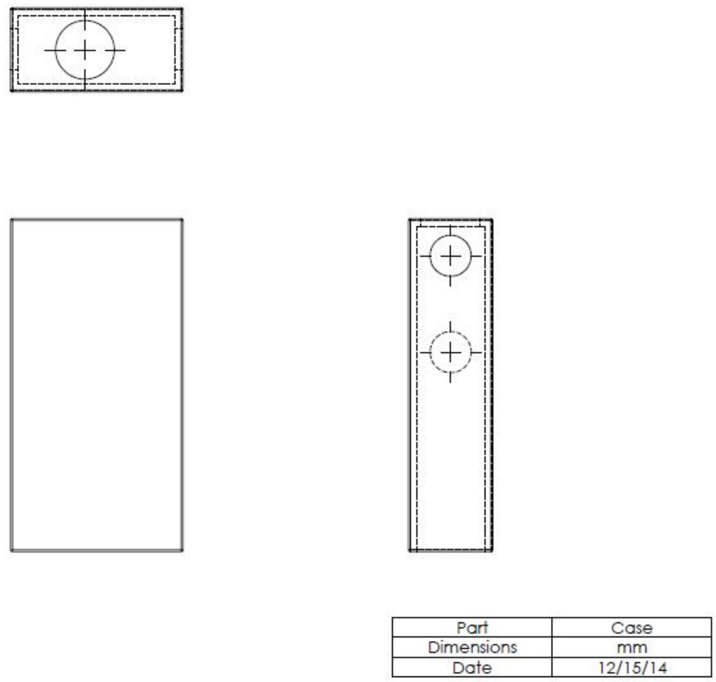


Figure A.8: 3D printed case.

# Appendix B: Purchased Components Specifications

Table B.1 displays the specification of the Vekek mini threaded hydraulic cylinder used in the variable resistance orthotic knee joint design. The model of the cylinder is 20-0105-07. The cylinder was modified at the TOHRC machine shop to remove some of the body thread and remove the spring on inside of the cylinder. Table B.2 displays the specification of the parts ordered form McMaster-Carr used in orthotic knee joint design.

Table B.1: Vektek mini threaded hydraulic cylinder specifications (model 20-0105-07). Cylinder capacity is at 5000 psi maximum operating pressure (table adapted from [73]).

| | |
|---|---|
| Cylinder Capacity (lb) | 980 |
| Stroke (in.) | 0.75 |
| Body Thread | ¾-16 |
| Minimum Length (in.) | 2.63 |
| Effective Piston Area (sq. in.) | 0.196 |
| Oil Capacity (cu. in.) | 0.147 |

Table B.2: Specifications of parts ordered from McMaster-Carr [63].

| Part | Part Number | Specifications |
|---|---|---|
| 5 mm Diameter Balls | 292K39 | • Bearing-quality E52100 alloy steel<br>• Hardened ball<br>• 5 mm diameter |
| Metric Compression Spring | 94125K422 | • Metric compressing spring (0.33 lb/mm)<br>• Music wire,<br>• 9.4 mm overall length<br>• 5.50 mm OD<br>• 0.5 mm wire |
| M5 Machine Screws | 92005A315 | • Metric pan head Phillips machine screw<br>• Zinc-plated steel<br>• M5 size<br>• 5 mm length<br>• 0.8 mm pitch |
| M5 Pressure Sealing Washers | 93786A100 | • Pressure-sealing washer<br>• Zinc-plated steel<br>• M5 screw size<br>• 4.8 mm ID<br>• 9.8 mm OD |

# Appendix C: Biomechanical Testing Kinematic Data

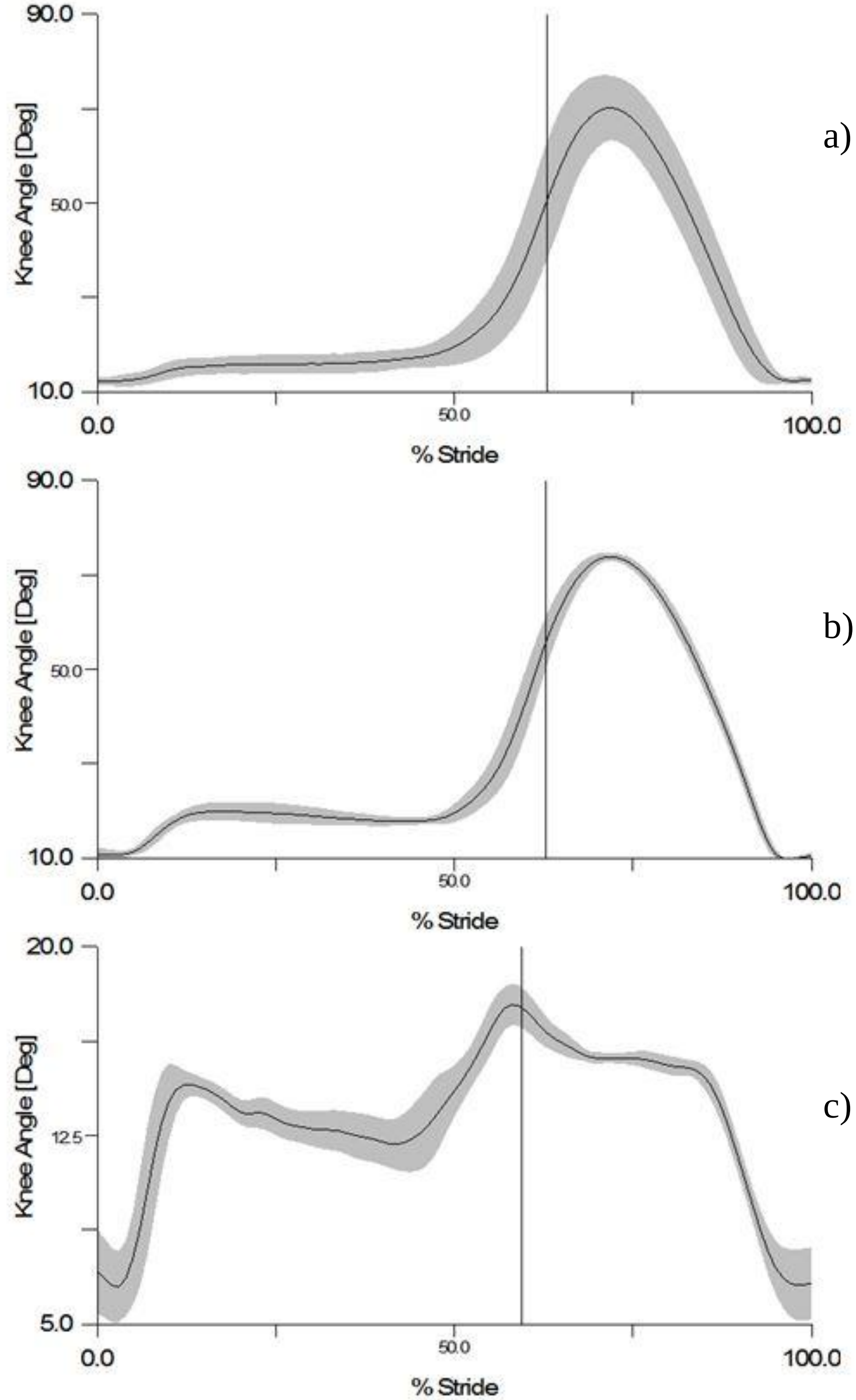


Figure C.1: Average sagittal knee angles for a) stance-control walking, b) open joint walking (setting 1), c) locked joint walking (setting 0). The vertical line represents average toe-off. Left of the line is stance phase and right of the line is swing phase. Knee flexion is positive.

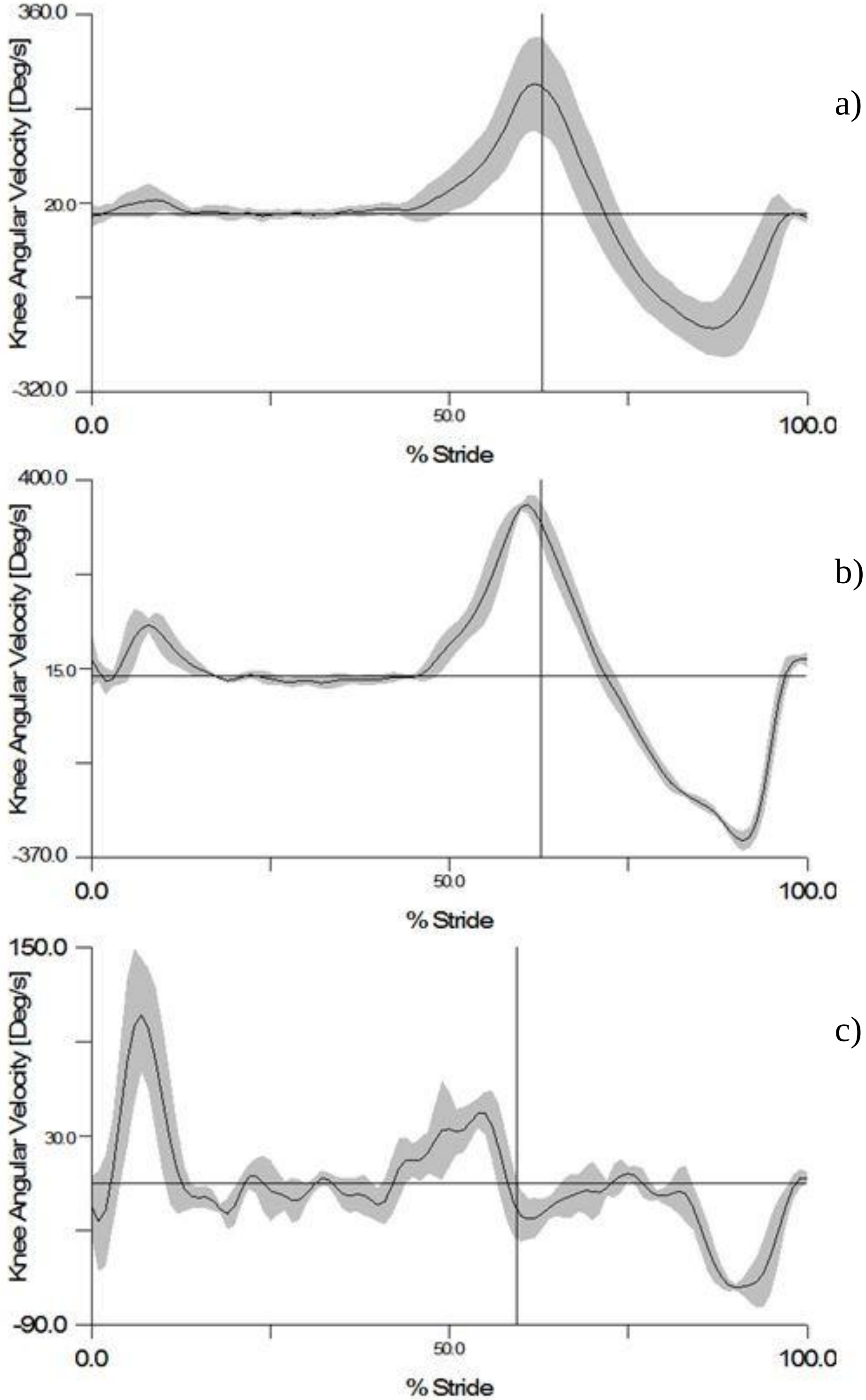


Figure C.2: Average sagittal knee angular velocity for a) stance-control walking, b) open joint walking (setting 1), and c) locked-joint walking (setting 0). The vertical line represents average toe-off. Left of the line is stance phase and right of the line is swing phase. Knee flexion angular velocity is positive.

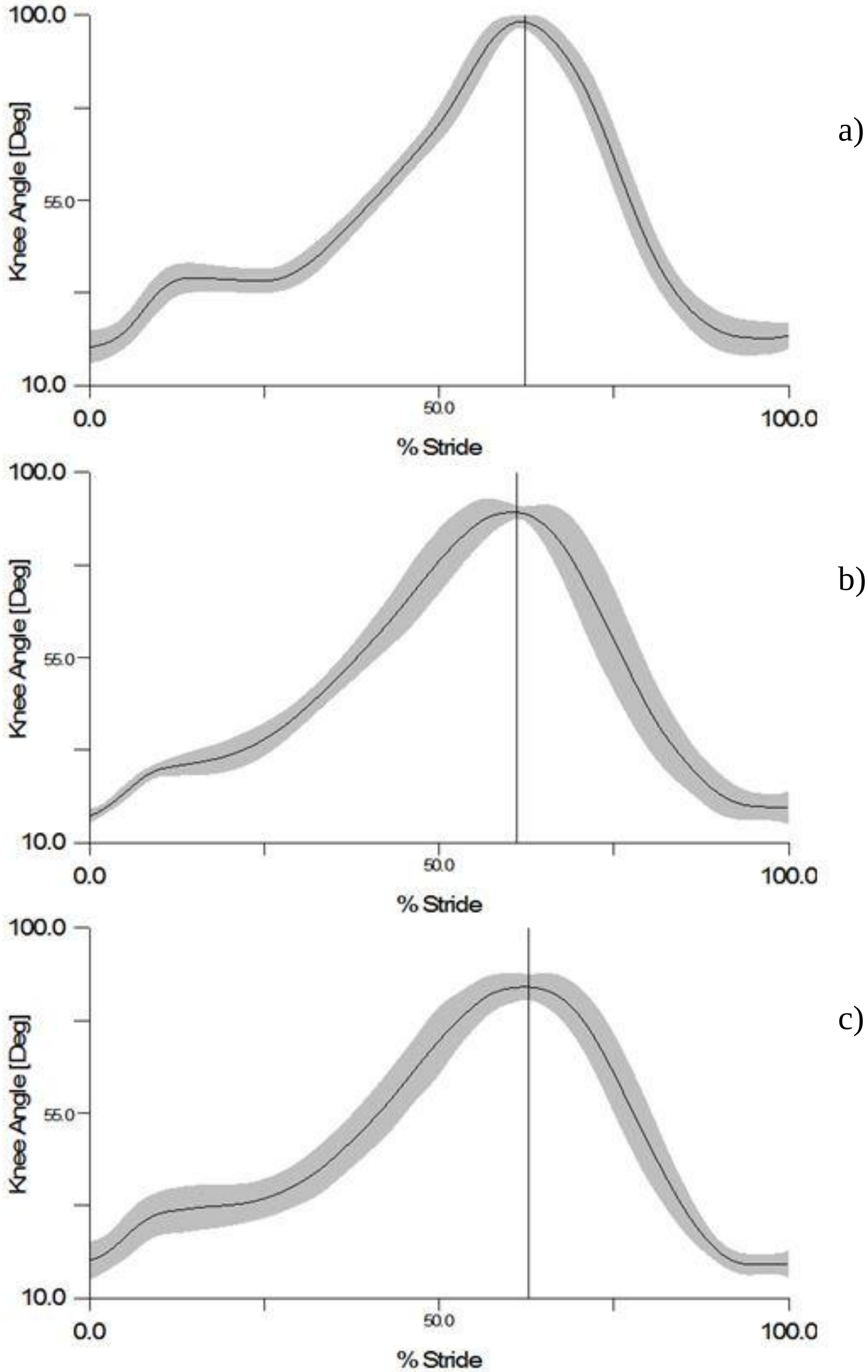


Figure C.3: Average sagittal knee angles for stair descent using a) setting 1 (open), b) setting 8, c) setting 10. The vertical line represents average toe-off. Left of the line is stance phase and right of the line is swing phase. Knee flexion is positive.

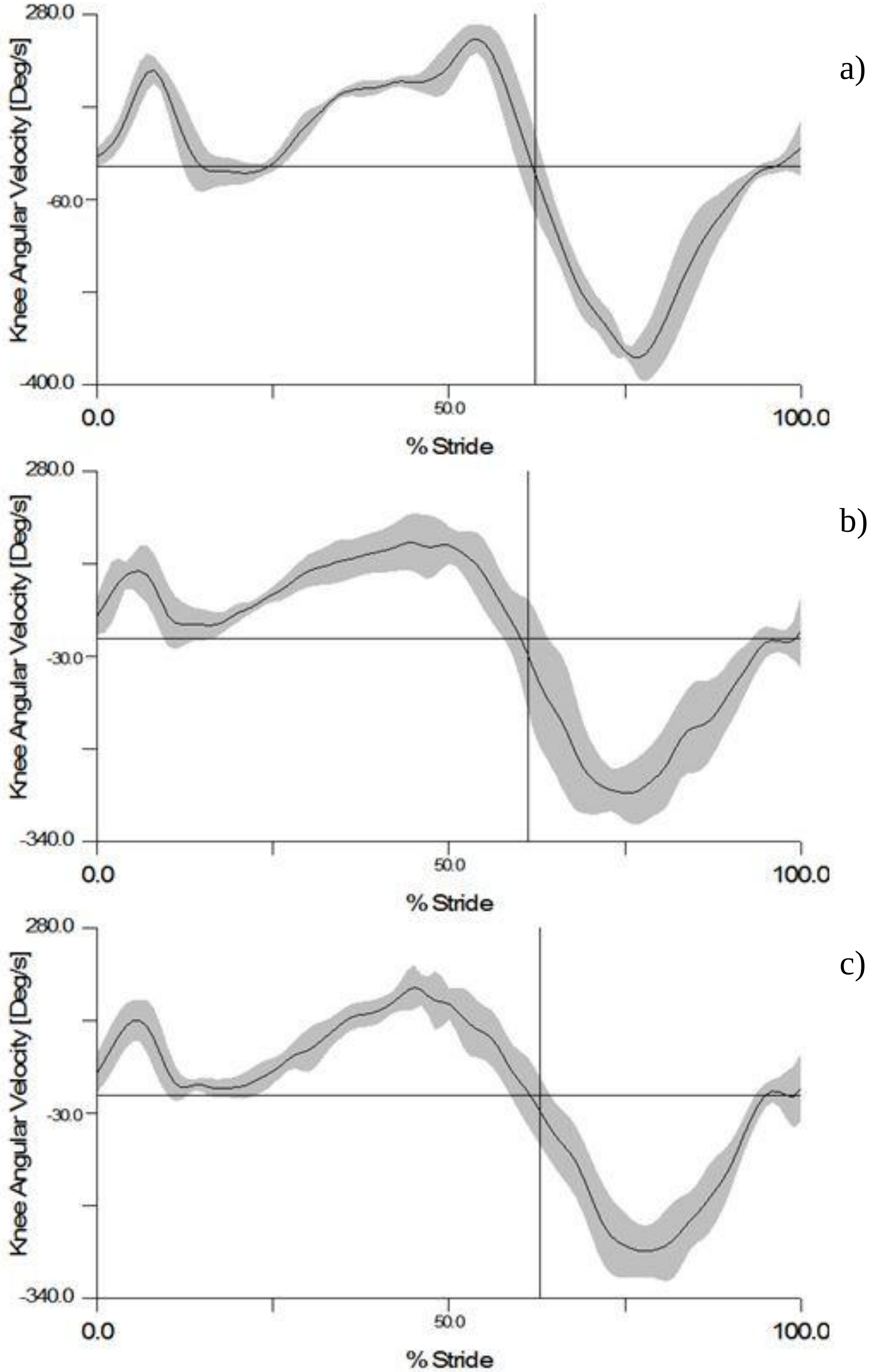


Figure C.4: Average sagittal knee angular velocity for stair descent using a) setting 1 (open), b) setting 8, c) setting 10. The vertical line represents average toe-off. Left of the line is stance phase and right of the line is swing phase. Knee flexion angular velocity is positive.

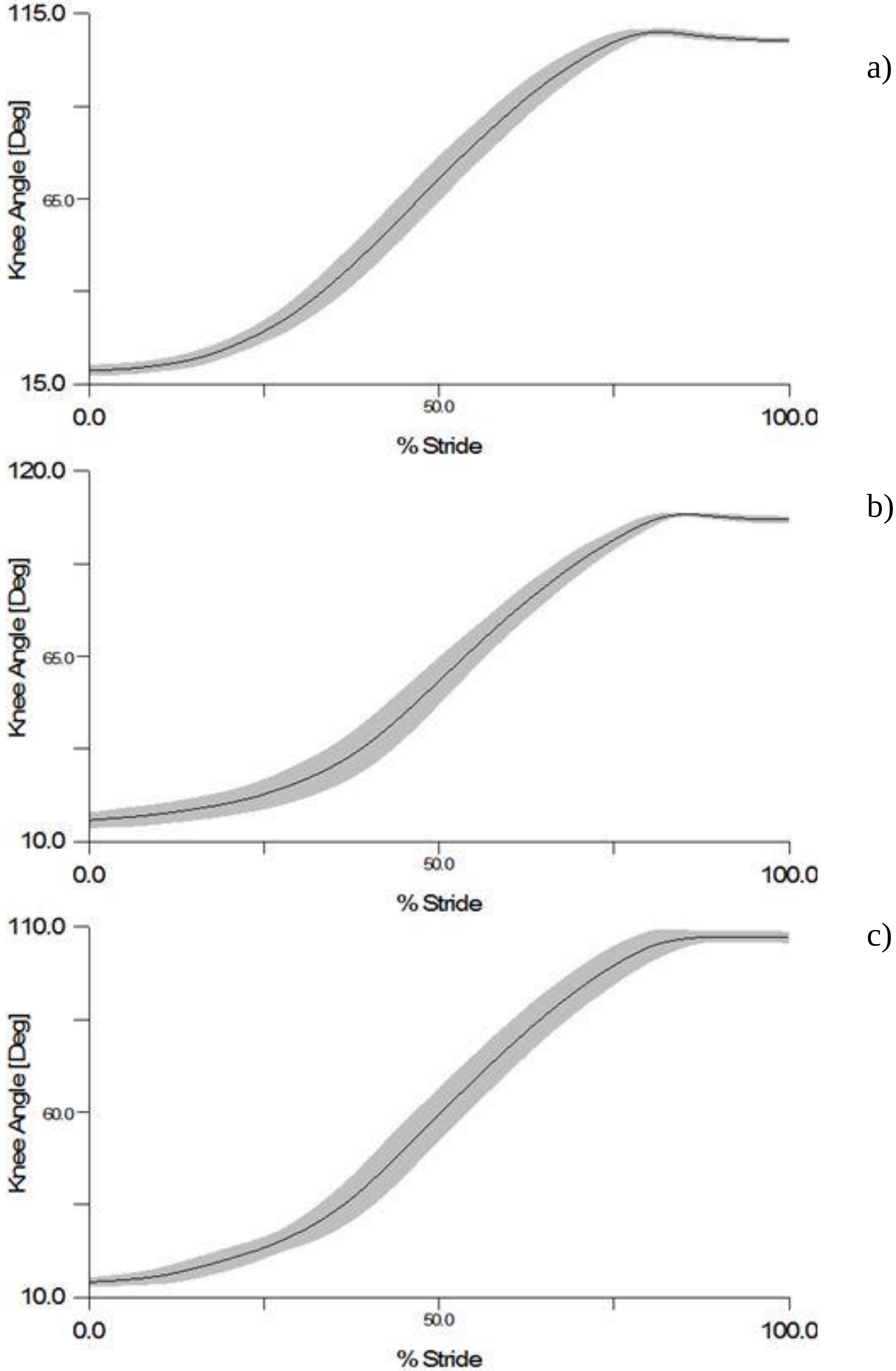


Figure C.5: Average sagittal knee angles for stand-to-sit trials using a) setting 1 (open), b) setting 8, c) setting 10. Knee flexion is positive.

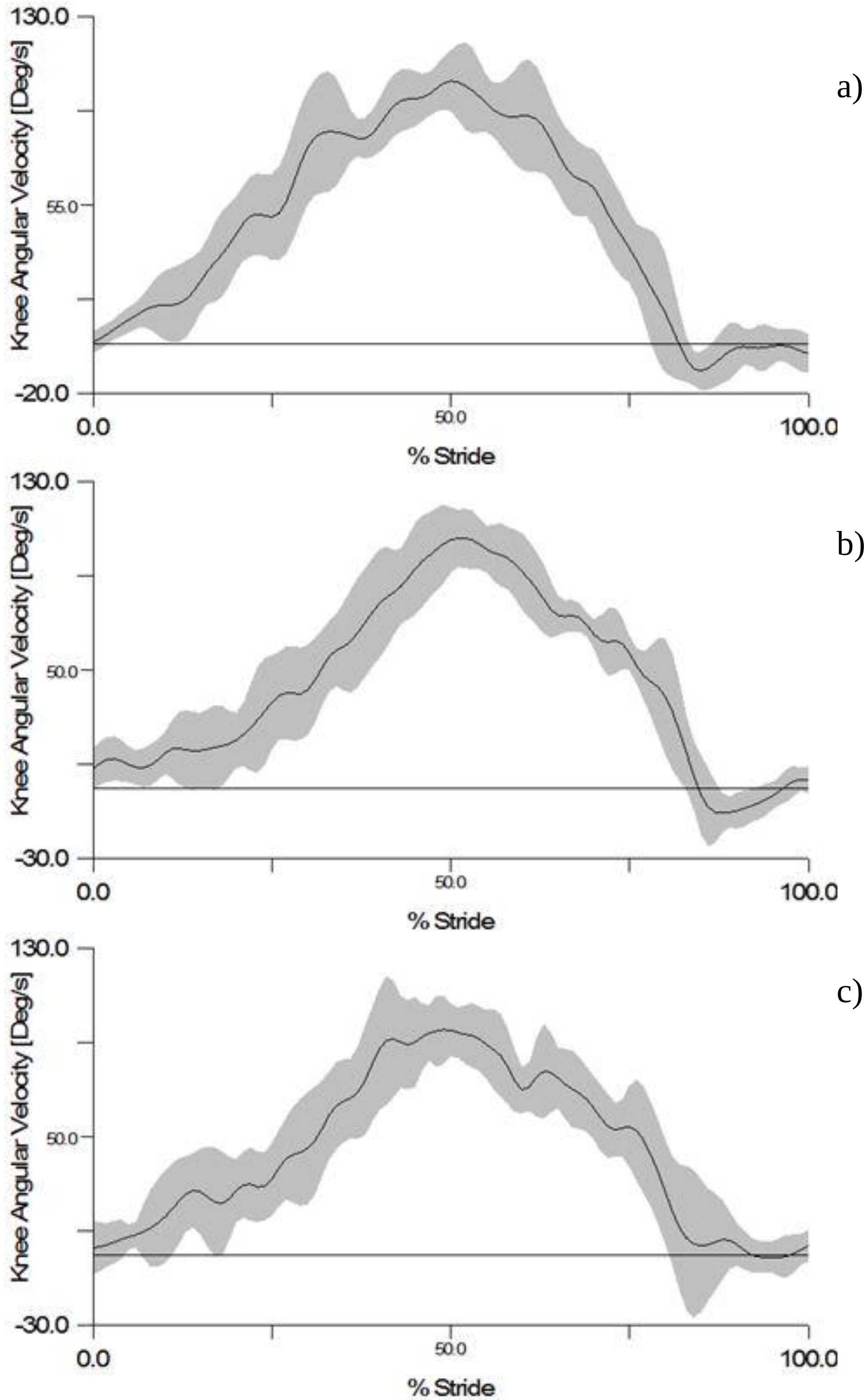


Figure C.6: Average sagittal knee angular velocity for stand-to-sit trials using a) setting 1 (open), b) setting 8, c) setting 10. Knee flexion angular velocity is positive.

# Appendix D: Biomechanical Testing Kinetic Data

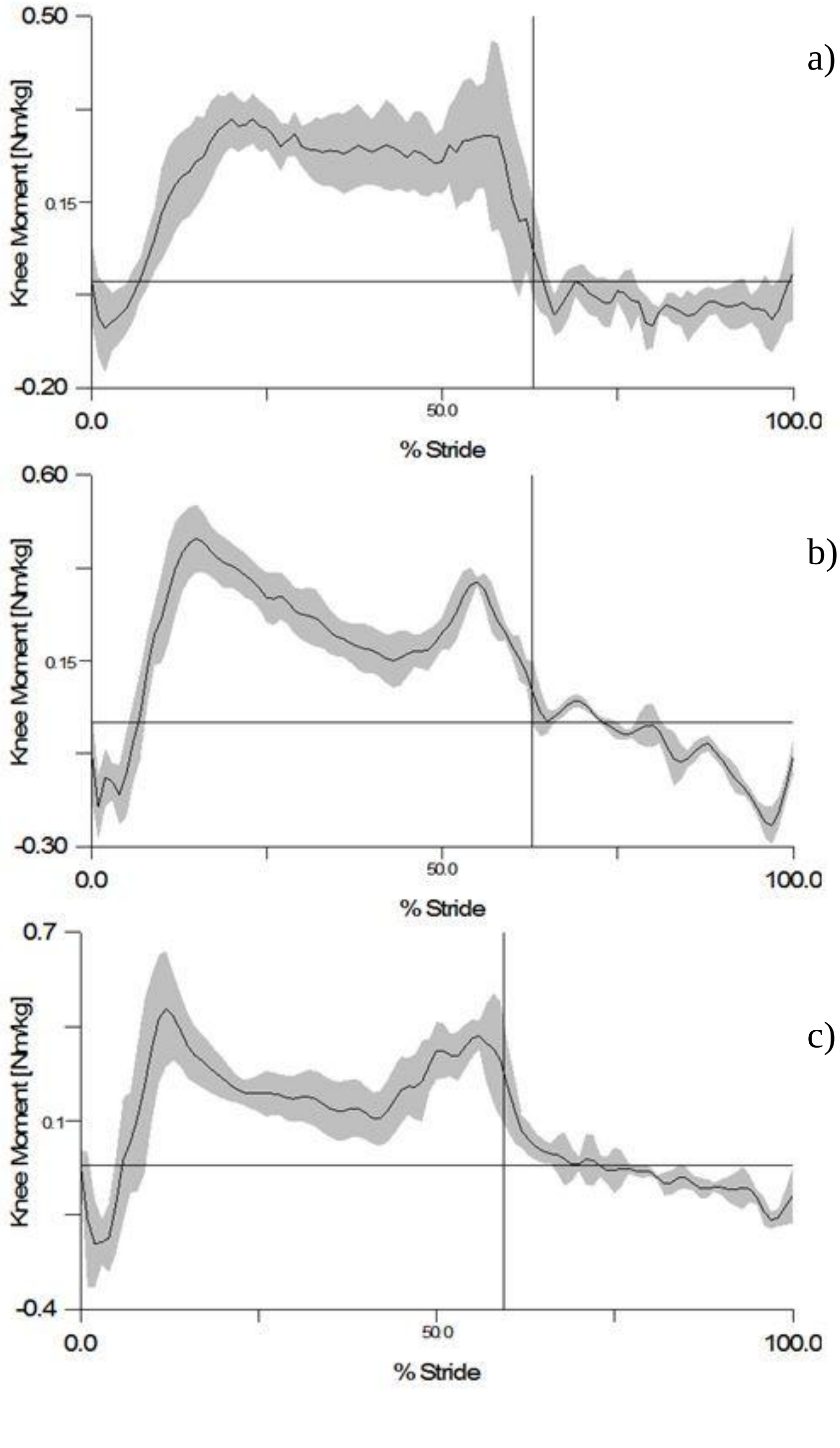


Figure D.1: Average sagittal knee moment for a) stance-control walking, b) open joint walking, and, c) locked-joint walking.The vertical line represents average toe-off. Left of the line is stance phase and right of the line is swing phase. Extension moment is positive.

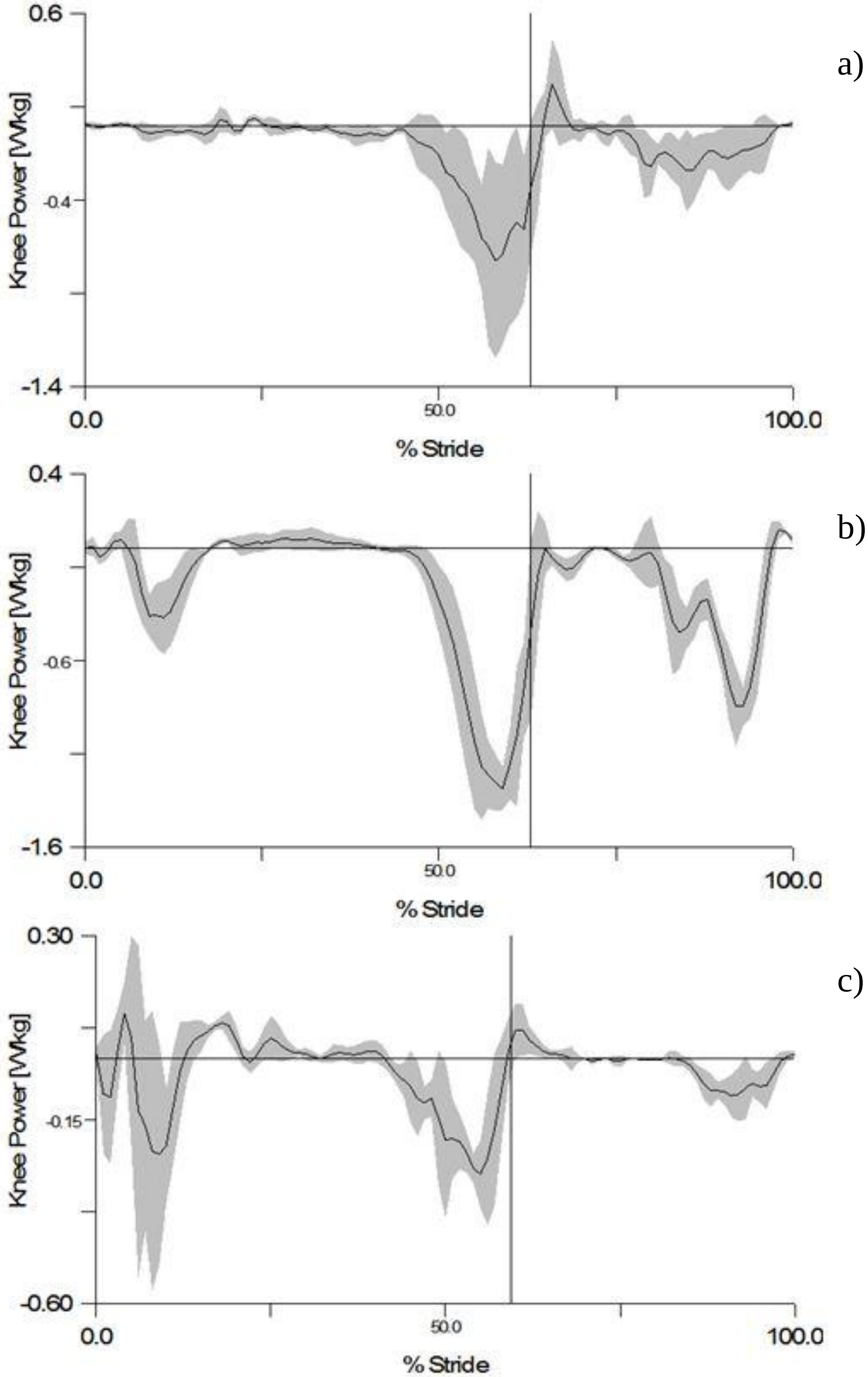


Figure D.2: Average sagittal knee joint power for a) stance-control walking, b) open joint walking (setting 1), and c) locked-joint walking (setting 0). The vertical line represents average toe-off. Left of the line is stance phase and right of the line is swing phase. Positive powers indicate concentric contractions and negative powers indicate eccentric contractions.

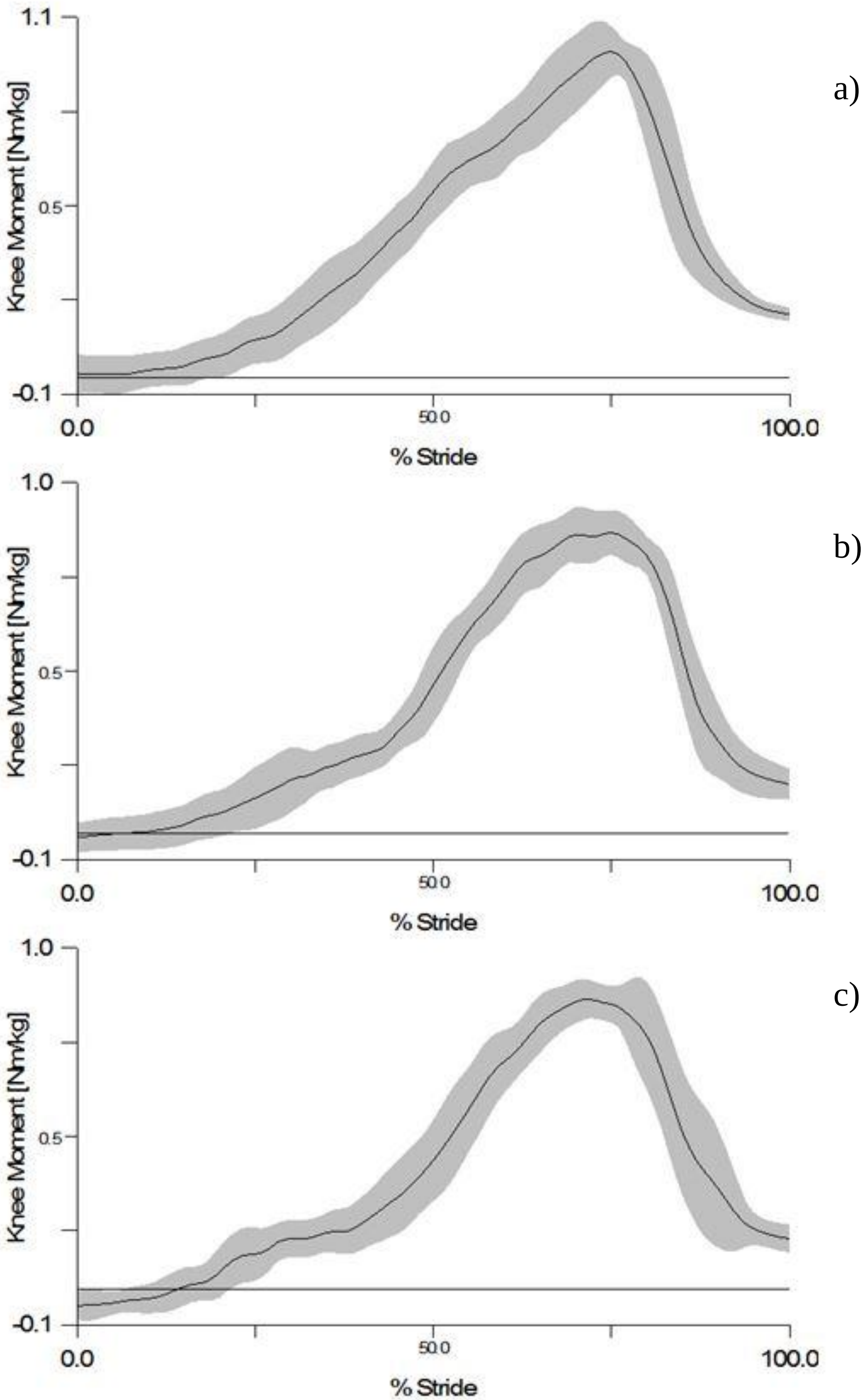


Figure D.3: Average sagittal knee moment for stand-to-sit trials using a) setting 1 (open), b) setting 8, c) setting 10. Extension moment is positive.

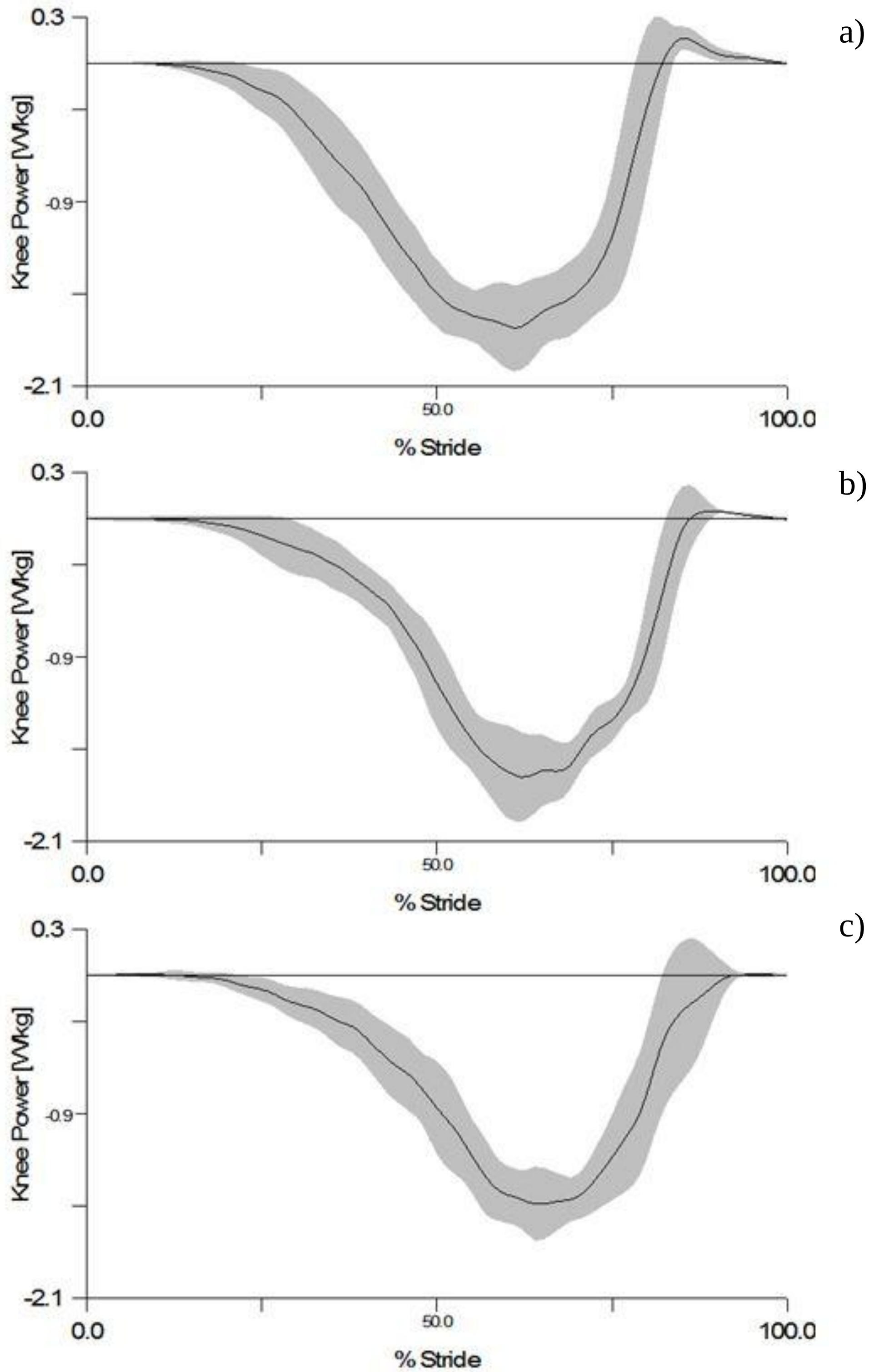


Figure D.4: Average sagittal knee joint power for stand-to-sit trials using a) setting 1 (open), b) setting 8, c) setting 10. Positive powers indicate concentric contractions and negative powers indicate eccentric contractions.

# Appendix E: Ottawa Health Science Network Research Ethics Board Approval

Ottawa Hospital Research Institute
Institut de recherche de l'Hôpital d'Ottawa

uOttawa

UNIVERSITY OF OTTAWA HEART INSTITUTE
INSTITUT DE CARDIOLOGIE DE L'UNIVERSITÉ D'OTTAWA

***Ottawa Health Science Network Research Ethics Board/ Conseil d'éthique de la recherche du Réseau de science de la santé d'Ottawa***

Civic Box 411 725 Parkdale Avenue, Ottawa, Ontario K1Y 4E9 613-798-5555 ext. 14902 Fax : 613-761-4311
http://www.ohri.ca/ohsn-reb

December 10, 2014

Dr. Edward Lemaire
[redacted]

Dear Dr. Lemaire:

**Re: Protocol # 20140825-01H** **Pilot Analysis of a Hydraulic Variable Resistance Orthotic Knee Joint**

**Protocol approval valid until - December 9, 2015**

I am pleased to inform you that this protocol underwent expedited review by the Ottawa Health Science Network Research Ethics Board (OHSN-REB) and is approved to only recruit English-speaking participants. No changes, amendments or addenda may be made to the protocol or the consent form without the OHSN-REB's review and approval.

Your request for French exemption was reviewed and is approved. Therefore, you will only recruit English-speaking participants in this study.

Approval is for the following documents:
- Protocol dated received October 23, 2014
- English Recruitment Notice dated December 8, 2014
- English Participant Informed Consent Form dated December 8, 2014

If the study is to continue beyond the expiry date noted above, a Renewal Form should be submitted to the REB approximately six weeks prior to the current expiry date. If the study has been completed by this date, a Termination Report should be submitted.

The Ottawa Health Science Network Research Ethics Board (OHSN-REB) was created by the merger of both the Ottawa Hospital Research Ethics Board (OHREB) and the Human Research Ethics Board (HREB) for meetings held at the University of Ottawa Heart Institute.

OHSN-REB complies with the membership requirements and operates in compliance with the Tri-Council Policy Statement: Ethical Conduct for Research Involving Humans; the International Conference on Harmonization - Good Clinical Practice: Consolidated Guideline; the provisions of the Personal Health Information Protection Act 2004.

Yours sincerely,

[redacted]

Raphael Saginur, M.D.
Chairperson
Ottawa Health Science Network Research Ethics Board

/cb

# Appendix F: The University of Ottawa Health Sciences and Science Research Ethics Board Approval

Université d'Ottawa University of Ottawa

Bureau d'éthique et d'intégrité de la recherche Office of Research Ethics and Integrity

December 16th, 2014

Andrew Herbert-Copley
Masters Student
Biomedical Engineering
University of Ottawa
[redacted]

Edward Lemaire
Supervisor
Faculty of Medicine
University of Ottawa/Ottawa Hospital
[redacted]

**Re: U of O Ethics file no. A12-14-02 – "Pilot Analysis of a Hydraulic Variable Resistance Orthotic Knee Joint"**

Dear Mr. Herbert-Copley and Dr. Lemaire,

Thank you for the protocol documents and Certificate of Approval from the OHSN-REB (# 20140825-01H) for your project named above.

This is to confirm that, in accordance with the agreement between the University of Ottawa and the OHSN-REB, the University of Ottawa has authorized this board to act as Board of Record for the review and oversight of research involving human subjects conducted at or through the hospital.

We remind you of your obligation to:

- Follow all procedures of the OHSN-REB including reporting and renewal procedures;
- Submit to the authority of the OHSN-REB and that you are subject to OHSN-REB requirements, including, without limitation, the requirement to modify or stop the research on demand of the OHSN-REB.

If you have any questions, please contact our ethics office at [redacted].

Sincerely yours,

[redacted]

Catherine Paquet
Director
Office of Research Ethics and Integrity

550, rue Cumberland
Ottawa (Ontario) K1N 6N5 Canada

550 Cumberland Street
Ottawa, Ontario K1N 6N5 Canada

(613) 562-5387 • Téléc./Fax (613) 562-5338
http://www.recherche.uottawa.ca/deontologie/
http://www.research.uottawa.ca/ethics/

# Appendix G: Recruitment Notice

The Ottawa Hospital | L'Hôpital d'Ottawa

**Recruitment Notice – Pilot Analysis of a Hydraulic Variable Resistance Orthotic Knee Joint**

The Ottawa Hospital Rehabilitation Centre (TOHRC) is designing a new variable resistance orthotic knee joint to be used with knee-ankle-foot orthoses (KAFO). This new knee joint improves upon current orthosis designs that are used by people with lower limb weakness, by allowing the person to slowly flex their knee when going down stairs and sitting, have free knee motion when swinging their leg during walking, and supporting the body during a stumble. This research study will assess the prototype KAFO to ensure that it works appropriately. The following healthy, able-bodied individuals are being asked to participate in this pilot test: employees of the Ottawa Hospital Rehabilitation Centre or students from the University of Ottawa working in the Ottawa Hospital Rehabilitation Centre, employees from Engineering Rehabilitation, Prosthetics and Orthotics, and Physiotherapy, and University of Ottawa graduate students working with Dr. Lemaire or Dr. Baddour.

If you choose to enroll in this study, you will be asked to complete one testing session in the TOHRC Rehabilitation Technology Lab. After completing a consent form and providing height, weight, and age, reflective markers will be attached to your body so that we can track how your limbs move. While we measure your movements, you will be asked to walk five times, at your comfortable pace, along an 8 meter walkway. You will then be asked to climb and descend a 4-step staircase, five times. The final activity is to perform 5 sit-stand-sit actions. The test session will take about an hour to complete.

To participate in this study, you must be over 18 years of age and must have the leg dimensions to fit our test KAFO. You must also be in good physical condition to perform multiple stair ascents, descents, walk continuously for 10 min, and sit to stand 5 times. You will be given opportunities to rest at any time. You are asked to wear shorts and a well-fitted shirt to testing sessions for the purpose of applying the reflective markers.

Participation is on a volunteer basis; you are not obligated to participate. If you decide to participate, you will be free to withdraw from the study at any time without suffering any negative consequences and without it affecting any of your present or future relationships with TOHRC. All testing will take place in the TOHRC Rehabilitation Technology Lab. If needed, parking expenses will be reimbursed by the research team.

Please reply to this email if you are interested in participating, if you have any questions, or if you would like more information to assist you in making your decision.

Thank you for your time,

Andrew Herbert-Copley, MASc Candidate (University of Ottawa)

Version Date: December 8, 2014

*Civic Campus Civic*
1053 av. Carling Avenue
Ottawa, Ontario K1Y 4E9

*General Campus Général*
501 chemin Smyth Road
Ottawa, Ontario K1H 8L6

*Riverside Campus Riverside*
1967 prom. Riverside Drive
Ottawa, Ontario K1H 7W9

# Appendix H: Information Form

**PARTICIPANT INFORMED CONSENT FORM**

**Title of Study: Pilot Analysis of a Hydraulic Variable Resistance Orthotic Knee Joint**

**Local Site Principal Investigator (PI): Dr. Edward Lemaire,** [redacted]

**Funding Agency**: Natural Sciences and Engineering Research Council (NSERC)

Participation in this study is voluntary. Please read this Participant Informed Consent Form carefully before you decide if you would like to participate. Ask the investigators as many questions as you like. We encourage you to discuss your options with family, friends or your healthcare team. This study is part of a master's thesis.

**Why am I being given this form?**

You are being asked to participate in this research study to evaluate a new hydraulic variable resistance orthotic knee joint prototype. The following healthy, able-bodied individuals are being asked to participate in this pilot test: employees of the Ottawa Hospital Rehabilitation Centre or students from the University of Ottawa working in the Ottawa Hospital Rehabilitation Centre, employees from Engineering Rehabilitation, Prosthetics and Orthotics, and Physiotherapy, and University of Ottawa graduate students working with Dr. Lemaire or Dr Baddour.

**Why is this study being done?**

We have designed an orthotic joint that will allow you to walk with a locked knee when standing or weight bearing and a freely moving knee when the leg is off the ground. The new knee joint will also allow you to slowly flex your leg when descending stair and the joint will engage to stop your leg from collapsing during a stumble. This pilot test is our first functional evaluation of the prototype.

**How is the study designed?**

A carbon-fibre knee-ankle-foot orthosis (KAFO) will be fitted to you by a certified orthotist at the Ottawa Hospital Rehabilitation Centre's (TOHRC) Prosthetics and Orthotics Service. The medial joint will be a standard orthotic single axis knee joint and the lateral joint will be the variable resistance prototype. You will be given the time needed to become comfortable with the KAFO while walking on level ground and stairs. During this time one of the investigators will walk with you acting as a spotter, until you feel confident on both terrain types.

In one test session, you will be asked to walk across a room 5 times, descend 4 steps (5 times), and complete 5 stand-to-sit and sit-to-stand movements. These tests will be performed in the TOHRC Rehabilitation Technology Lab.

**What is expected of me?**

Reflective markers will be attached to you using two sided tape, placed at the pelvis, thighs, lower legs, and feet. These markers allow us to track and analyze how you move during the study.
For level ground, you will be asked to walk along an 8 meter walkway at your comfortable pace. Data on five trials will be collected.

Before performing the stair descent trials, you will try different knee flexion resistance settings and then select the "most comfortable" setting. You will then be asked to perform stair descents with the brace set to the selected resistance setting. Data on five trials will be collected.

The same knee joint resistance setting will be used for the first sitting trial. You may request to change the setting for the remaining sitting trials.

**How long will I be involved in the study?**

Your participation in the study will last approximately one hour. Over this time, you will be required to visit the TOHRC Rehabilitation Technology Lab once.

Your participation in the study may be stopped for any of the following reasons:

- The primary or co-investigator feels it is in your best interest.
- You do not follow the study staff's instructions.

**What are the potential risks I may experience?**

This research has minimal risk (i.e., same risk as walking, descending stairs, and sitting). During the time you are given to become accustomed with the KAFO, an investigator will walk with you and act as a spotter until you feel confident with level ground walking and stair descents.

**Can I expect to benefit from participating in this research study?**

You will not receive any direct benefit from your participation in this study. Your participation will allow the researchers to evaluate the variable resistance orthotic knee joint. This may benefit future KAFO users.

**Do I have to participate? What alternatives do I have? If I agree now, can I change my mind and withdraw later?**

Your participation in this study is voluntary. The alternative to this study is not to participate.

You may decide not to be in this study, or to be in the study now, and then change your mind later without affecting the education/employment or other services to which you are entitled or are presently receiving at this institution.

If you withdraw your consent, the study team will no longer collect your personal identifying information for research purposes.

**What compensation will I receive if I am injured or become ill in this study?**

In the event of a study-related injury or illness, you will be provided with appropriate medical treatment and care. Financial compensation for lost wages, disability or discomfort due to an injury or illness is not generally available. You are not waiving any of your legal rights by agreeing to participate in this study. The study doctor and the Ottawa Hospital Rehabilitation Centre still has their legal and professional responsibilities.

**How is my personal information being protected?**

- All information collected during your participation in this study will be identified with a unique study number, and will not contain information that identifies you, such as your name, address, etc.
- The link between your unique study number and your name and contact information will be stored securely and separate from your study records, and will not leave this site.
- Any documents or samples leaving the Ottawa Hospital Rehabilitation Centre will contain only your unique study number. This includes publications or presentations resulting from this study.
- Information that identifies you will be released only if it is required by law.
- For audit purposes only, your original study records may be reviewed under the supervision of Dr. E. Lemaire's staff by representatives from:
    - the Ottawa Health Science Network Research Ethics Board (OHSN-REB),
    - the Ottawa Hospital Research Institute
    - University of Ottawa Research Ethics Board.
- Research records will be kept for 10 years, after this time they will be destroyed.

**Do the investigators have any conflicts of interest?**

There are no conflicts of interest to declare related to this study.

**What are my responsibilities as a study participant?**

It is important to remember the following things during this study:

- Ask the primary or co-investigator if you have any questions or concerns.
- Tell the primary or co-investigator if anything about your health has changed.

**Will I be informed about any new information that might affect my decision to continue participating?**

You will be told in a timely fashion of any new findings that could affect your willingness to participate in the study (i.e., only one test session).

**Who do I contact if I have any further questions?**

If you have any questions about this study, or if you feel that you have experienced a study-related injury or illness, please contact Dr. Lemaire at [redacted] or the research assistant (Andrew Herbert-Copley) at [redacted]

The Ottawa Health Science Network Research Ethics Board (OHSN-REB) and the University of Ottawa Health Sciences and Science Research Ethics Board has reviewed this protocol. The Board considers the ethical aspects of all research studies involving human participants at the TOHRC. If you have any questions about your rights as a study participant, you may contact the Chairperson at [redacted].



:

# Appendix I: Consent Form

Ottawa Hospital Research Institute
Institut de recherche de l'Hôpital d'Ottawa

uOttawa

University of Ottawa Heart Institute
Institut de cardiologie de l'Université d'Ottawa

**<u>Consent to Participate in Research</u>**

- I understand that I am being asked to participate in a research study about the development of a variable resistance orthotic knee joint.
- This study was explained to me by ___________________________.
- I have read, or have had it read to me, each page of this Participant Informed Consent Form.
- All of my questions have been answered to my satisfaction.
- If I decide later that I would like to withdraw my participation and/or consent from the study, I can do so at any time.
- I voluntarily agree to participate in this study.
- I will be given a copy of this signed Participant Informed Consent Form.

| ____________________________ | ____________________________ | ________________ |
|---|---|---|
| Participant's Printed Name | Participant's Signature | Date |

**<u>Investigator or Delegate Statement</u>**

I have carefully explained the study to the study participant. To the best of my knowledge, the participant understands the nature, demands, risks and benefits involved in taking part in this study.

| ____________________________ | ____________________________ | ________________ |
|---|---|---|
| Investigator/Delegate's Printed Name | Investigator/Delegate's Signature | Date |